

UNCLASSIFIED

AD 274 006

*Reproduced
by the*

**ARMED SERVICES TECHNICAL INFORMATION AGENCY
ARLINGTON HALL STATION
ARLINGTON 12, VIRGINIA**



UNCLASSIFIED

NOTICE: When government or other drawings, specifications or other data are used for any purpose other than in connection with a definitely related government procurement operation, the U. S. Government thereby incurs no responsibility, nor any obligation whatsoever; and the fact that the Government may have formulated, furnished, or in any way supplied the said drawings, specifications, or other data is not to be regarded by implication or otherwise as in any manner licensing the holder or any other person or corporation, or conveying any rights or permission to manufacture, use or sell any patented invention that may in any way be related thereto.

274 006

TECHNICAL REPORT

62-3-1

Third Interim Engineering Report
and
Final Report

HIGH FREQUENCY TRANSISTOR STUDY

Contract No. NObsr - 85296

United States Navy
Bureau of Ships

March 16, 1962

Best Available Copy



THIRD INTERIM ENGINEERING REPORT
AND
FINAL REPORT
FOR
HIGH FREQUENCY TRANSISTOR STUDY

This report covers the period 1 October, 1961 through 28 February, 1962

Development Laboratory
HUGHES AIRCRAFT COMPANY
Semiconductor Division
Newport Beach, California.

NAVY DEPARTMENT BUREAU OF SHIPS ELECTRONICS DIVISIONS

Contract No. NObsr-85296, Index No. SR0080302, ST-9349

March 16, 1962

LIST OF CONTENTS

	<u>Page</u>
ABSTRACT	i
LIST OF ILLUSTRATIONS	ii
 <u>PART I</u> Hughes Aircraft Company, Semiconductor Division Report	
GENERAL FACTUAL DATA	
References	iii
Identification of Technical Personnel	iv
 DETAIL FACTUAL DATA	
Introduction	1
1. Device Design and Fabrication	3
2. Coaxial Package	9
3. Electrical Evaluation of Package and Transistor	11
4. Parametric Mixer	19
5. Instrumentation	22
6. Nonlinear Elements in Transistors for Frequency Conversion	24
 APPENDIX I	 28
 <u>PART II</u> Lenkurt Electric Company Report	
Summary	37
Table of Contents	38
List of Illustrations	39
Final Engineering Report	40
 <u>PART III</u> Final Report, Hughes Aircraft Company, Semiconductor Division	
Introduction	58
1. Accomplishments	60
2. Conclusions	66

ABSTRACT

A 1 Gc, coaxially packaged, germanium PNP epitaxial mesa transistor has been developed and its electrical properties have been evaluated in the frequency range from 200 to 1500 MC. The Hughes (Design I) coaxial package has reduced the parasitic elements of the encapsulation to such an extent, that at frequencies up to 2.5 Gc, the required electrical properties of the particular transistor design are satisfactory for performance in suitable microwave circuitry.

The existence of the transit-time mode oscillation has been verified around 1.5 Gc in combination with a parametrically pumped down converter at a signal frequency of 750 MC. A coaxial mixer has been constructed which will accommodate these coaxially packaged transistors. The mixer arrangement requires oscillation in the transit-time mode and with proper termination without feedback can be adjusted over the range from 1.4 to 3 Gc. Simultaneously, the signal frequency can vary from 0.7 to 1.5 Gc. A stable conversion power gain of approximately 45 db at 750 MC signal and 2 MC intermediate frequency has been obtained. The approximate noise figure of 15 db has been calculated from a measured sensitivity of 2 μ V and a bandwidth of 500 KC. By reducing the extrinsic base resistance in the transistors used, improvement in respect to sensitivity and noise figure is expected.

The nonlinear elements in drift transistors, which can be used for frequency conversion, have been treated theoretically and verified experimentally. A variable, nonlinear reactance available at the emitter-to-base terminal of a drift transistor has been employed for reactive mixing in a parametrically excited mode. Conversion power gain in such circuits is experimentally verified and is much higher than in a conventional, resistive transistor mixer.

Although the transistor is intended for application in common base circuits, a measuring device has been constructed which will perform f_T measurements in the common emitter configuration from 200 to 800 MC fundamental frequency.

Prepared by Hans G. Dill
Hans G. Dill
Member of Technical Staff

R. Zuleeg
R. Zuleeg
Senior Staff Physicist

Approved by E. L. Steele
E. L. Steele, Manager
Development Laboratory

LIST OF ILLUSTRATIONS

- Figure 1 Measurement of Emitter Depletion Layer Capacitance C_E , and plot of $1/C_E^2$ vs. applied voltage for determination of impurity concentration adjacent to emitter junction.
- Figure 2 Base contact gold alloy showing discontinuities by balling up.
- Figure 3 Acceptable gold and aluminum alloy structure.
- Figure 4 Actual dimensions of transistor geometry.
- Figure 5 f_T measurements as a function of emitter current and plot of $1/f_T$ vs. $1/I_E$ to determine the emitter depletion layer capacitance, C_E and to show the influence upon two different transistors.
- Figure 6 10 KC small signal amplification factor (beta) vs. collector current, I_C , at $V_{CE} = -2$ volts of transistor R-30-4.
- Figure 7 Theoretical relation of transistor base width, W , in relation to cut-off frequencies, f_{ca} and f_T .
- Figure 8 Photograph of the two-part coaxial transistor package of Hughes Design I.
- Figure 9 Cross-sectional drawing of Hughes Design I coaxial package and dimensions.
- Figure 10 Illustration of transistor mounting and emitter and base thermocompression bonds to base diaphragm and auxiliary emitter post.
- Figure 11 Parasitic elements of Hughes Design I coaxial package excluding the transistor.
- Figure 12 Complex representation of intrinsic current amplification, α_i and the effect of $r_b' C_c$ upon its effective behavior.
- Figure 13 Complex representation of intrinsic current amplification, α_i and the effect of $L_b C_c$ upon its effective behavior.
- Figure 14 Actual and corrected measurement of the complex current amplification factor.

- Figure 15 Measurements of complex current amplification factor, α_{eff} , as function of emitter current.
- Figure 16 Theoretical evaluation of emitter cut-off frequency on the overall cut-off frequency, f_{ceff} .
- Figure 17 Theoretical input impedance of a drift transistor and the effect of emitter depletion layer capacitance upon its variation.
- Figure 18 Input impedance, h_{ib} , of a coaxial transistor at $V_c = 10$ V and $I_e = 3$ mA as a function of frequency.
- Figure 19 Real and imaginary part of input impedance, h_{ib} , as function of emitter current, I_e , for various fixed frequencies to demonstrate the nonlinear reactance.
- Figure 20 Measurement of f_T and its variation in the $V_c I_c$ plane.
- Figure 21 Mixer performance of unit HC-9 for various signal levels.
- Figure 22 Measuring set-up to determine the noise figure of the parametric mixer.
- Figure 23 Theoretical curves for determination of noise figure from sensitivity and bandwidth values.
- Figure 24 Equivalent circuit of the f_T jig.
- Figure 25 Mechanical drawing of the f_T jig.
- Figure 26 Photograph of the f_T jig.
- Figure 27 Normalized excess base charge distribution, p/p_0 , vs. normalized distance, x/x_0 , with reduced current density as parameter for a drift transistor.
- Figure 28 Normalized base charge capacitance, C_b/C_{b0} , vs. normalized emitter current, I_E/I_{E0} , for diffusion and drift transistor in the low level and high level injection state.
- Figure 29 Measurements of base-charge (=diffusion) capacitance as a function of emitter current
- A) for a diffusion transistor
- B) for a drift transistor

GENERAL FACTUAL DATA

REFERENCES

1. L. G. Cripps, "Transistor High Frequency Parameter f_T ".
Electronic and Radio Engineering, Sept. pp 341 - 346.
2. J. M. Rollett, "The Characteristic Frequencies of a Drift Transistor",
Journal of Electronics and Control, Vol. 7 No. 3, Sept. 1959
pp 193 - 213.
3. M. B. Das and A. R. Boothroyd, "Determination of Physical Parameters of Diffusion and Drift Transistors", IRE Transactions
on Electron Devices, Vol. ED-8, No. 1, Jan. 1961, pp 15 - 30.
4. J. Lindmayer and C. Y. Wrigley, "Beta Cut-off Frequencies of
Junction Transistors", Proceedings IRE, Vol. 50, No. 2, Feb.
1962, pp 184 - 198.
5. C. T. Kirk, (Private Communication, March 1961).
6. F. J. Hyde, "The Internal Current Gain of Drift Transistors", Proc.
IRE (Correspondence), Vol. 46, No. 12, Dec. 1958, pp. 1963-1964.
7. J. te Winkel, "Drift Transistors Simplified Electrical Characterization",
Electronic and Radio Engineering, Vol. 36, No. 8, pp 280 - 288,
Aug. 1959.
8. F. E. Terman, Radio Engineer's Handbook, McGraw-Hill Book Company,
Inc., New York and London 1943, p. 49.
9. J. F. Gibbons, "An Analysis of the Modes of Operation of a Simple
Transistor Oscillator", Proc. IRE, Vol. 49, No. 9, pp. 1383 - 1390,
Sept. 1961.
10. J. Zawels, "The Transistor as a Mixer", Proc. IRE, Vol. 42, No. 3.,
pp 542 - 548, March 1954.
11. R. Zuleeg, V. W. Vodicka, "Microwave Operation of Drift Transistors
in the Transit-Time Mode", IRE Transactions on Circuit Theory,
Vol. C T-8, No. 4. pp 426 - 433, Dec. 1961.
12. R. Zuleeg, V. W. Vodicka, "Parametric Amplification Properties in
Transistors", Proc. IRE, Vol. 48, No. 10, pp 1785 - 1786, Oct.
1960.
13. U. L. Rohde, "Parametric Amplification with Transistors", Wireless
World, Vol. 67, No. 10, pp 498 - 499, Oct. 1961.

14. J. Lindmayer, C. Wrigley, "On Parametric Amplification in Transistors", Proc. IRE, Vol. 49, No. 8, pp. 1335-1337 August, 1961.
15. J. Lindmayer, C. Wrigley, "The High-Injection Level Operation of Drift Transistors", Solid State Electronics, Vol. 2, Nos. 2, 3, pp. 79 - 84, March, 1961.
16. J. Lindmayer, C. Wrigley, "The Emitter Diffusion Capacitance of Drift Transistors", Proc. IRE, Vol. 48, No. 10, pp. 1777-1778, October, 1960 (Correspondence).
17. H. Kroemer, "Zur Theorie des Diffusions- und des Drift-Transistors, III", Dimensionierungsfragen, A.E.U. 8, pp. 499-504, 1954.
18. W. M. Webster, "On the Variation of Junction Transistor Current Amplification Factor with Emitter Current ", Proc. IRE Vol. 42, pp. 914, June, 1954.

GENERAL FACTUAL DATA

IDENTIFICATION OF PERSONNEL

	<u>Work Hours</u>
H. G. Dill, Member of Technical Staff	279
G. Dorosheski, Member of Technical Staff	.98
R. Zuleeg, Senior Staff Physicist	741
W. Waters, Head, Device Development Department	276
C. Fa, Member of Technical Staff	136
D. Thrasher, Member of Technical Staff	264
F. Rhoads, Associate Engineer	72
Research Assistants	1063
Lab Technicians	1472
Services	272
Other	136
Total - - - -	<u><u>4,810</u></u>

PART I

DETAIL FACTUAL DATA

INTRODUCTION

During the reporting period, the assembly of the 1 Kmc epitaxial germanium mesa transistor in the coaxial package was accomplished. The Hughes Design I coaxial package has been found satisfactory in its mechanical properties and the electrical evaluation indicated operational capabilities up to 2.5 Kmc which were accomplished by reducing the inductive parasitic elements.

The emitter alloy has been brought under control to a base diffusion depth of 0.5 to 0.7 μ and gives consistently good electrical yields. The gold alloy geometry of the base contact sometimes caused a high base resistance; this was traced to a discontinuous film. Up to the dicing operation good yields have been achieved. The major losses are now encountered in the thermocompression bonding operation and are due to physical damage to the structure. Presently, the existing equipment for this evaluation lacks the high degree of mechanical stability and tolerance for this precise operation. The skill of the operator is responsible for success in completing the coaxial transistor structures.

Epitaxial material with the required higher resistivity layers was available, but the impurity distribution (gradient) in the epitaxially grown layer needs some improvement in order to achieve the low collector depletion layer capacitances.

Thorough characterization of the coaxial transistors and the package have been carried out with the General Radio transfer function meter, but the corrected adjustments for the bridge short and open reference terminations have not been completed to our complete satisfaction.

The integrated coaxial parametric mixer incorporating the coaxial transistor operating in the transit time mode has functioned properly at 750, 1500, and 2250 Mc.

1. DEVICE DESIGN AND FABRICATION

A. Fabrication

During this period most effort has been devoted to establishing optimized evaporation and alloying cycles and conditions which produce consistent wetting and depth control of the aluminum and gold (plus antimony) alloy.

In this evaluation, the base diffusion has been kept constant with a sheet resistivity of $100\Omega/\square$ ($\pm 10\%$) and a junction depth of 0.7μ ($\pm 10\%$).

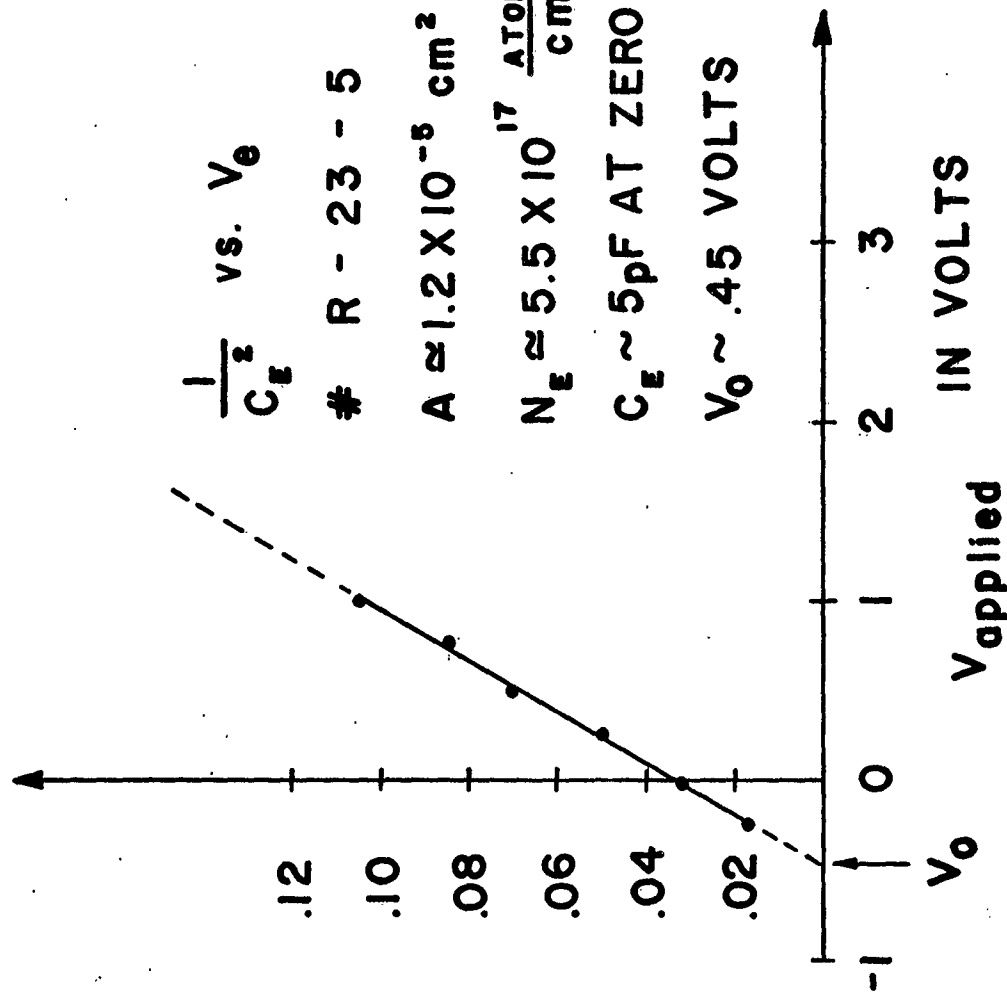
With an aluminum film thickness of about 2000 \AA , consistently good emitter junction formation has been obtained. The alloying depth is approximately 0.2μ . This depth corresponds to an impurity concentration of $3-5 \times 10^{17}$ atoms/cm³ in the impurity profile. The impurity concentration adjacent to the emitter junction has been evaluated by capacitance vs. voltage measurements.

For the capacitance evaluation it was assumed that a step junction is present, so that in a plot of $1/C^2$ vs. V , the slope is proportional to N_E , according to the relation

$$\frac{\Delta V}{\Delta(1/C_E^2)} = \frac{q \epsilon \epsilon_0 A_E^2 N_E}{2} \quad (1)$$

With the narrow depletion layer width at doping levels greater than 10^{17} atoms/cm³, the impurity concentration changes very little and the computed N_E , although an average, is very nearly the impurity concentration at the emitter junction. A typical evaluation is given in Figure 1.

$$\frac{1}{C_E^2} \times 10^{24} [F^{-2}]$$



$\frac{1}{C_E^2}$ vs. V_0

R - 23 - 5

$A \approx 1.2 \times 10^{-8} \text{ cm}^2$

$N_E \approx 5.5 \times 10^{17} \frac{\text{ATOMS}}{\text{cm}^3}$

$C_E \sim 5 \text{ pF AT ZERO BIAS}$

$V_0 \sim .45 \text{ VOLTS}$

FIGURE 1

MEASUREMENT OF EMITTER DEPLETION LAYER CAPACITANCE C_E , AND PLOT OF $1/C_E^2$ VS. APPLIED VOLTAGE FOR DETERMINATION OF IMPURITY CONCENTRATION ADJACENT TO EMITTER JUNCTION.

The gold film, about 1500 Å thick and containing 2% antimony, has been alloyed satisfactorily. However, on some occasions, bad wetting or abnormal surface tension causes a balling-up of the gold. A typical pattern is shown in Figure 2. This type of base alloying means that the gold layer is discontinuous and, as a consequence, the unit has a higher base spreading resistance. Two thermo compression bond leads, each at one end of the horse-shoe base contact, indicated an ohmic resistance varying from 30 to 100Ω for bad alloys and 3-5Ω for good alloys. A transistor structure with good gold and aluminum alloys is shown in a photograph of Figure 3. The nominal design dimensions of the structures are revealed in Figure 4.

B. Device Design

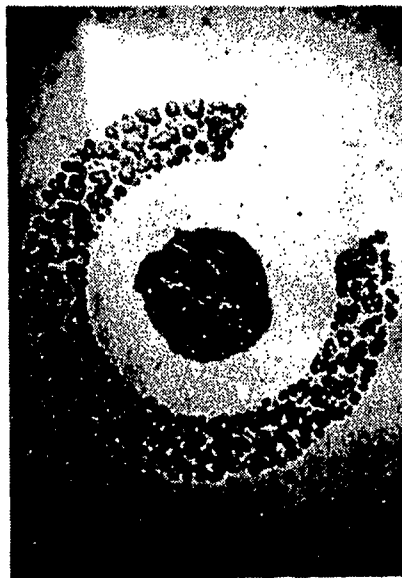
From the geometry of the device structure and the impurity concentration distribution in the base and collector material, the electrical parameters can be predicted.

The collector depletion layer capacitance, C_c , can be estimated from the relation

$$C_c \approx \left(\frac{q \epsilon \epsilon_0 A_c^2 N_c}{2 (V_c + V_o)} \right)^{\frac{1}{2}} \quad (2)$$

For a collector mesa of 7 mils in diameter and an applied voltage of 10 volts, assuming a resistivity of 2Ω cm material (e.g. $N_c \approx 1.5 \times 10^{15}$ atoms/cm³) in the epitaxial layer, we compute the value of capacitance as:

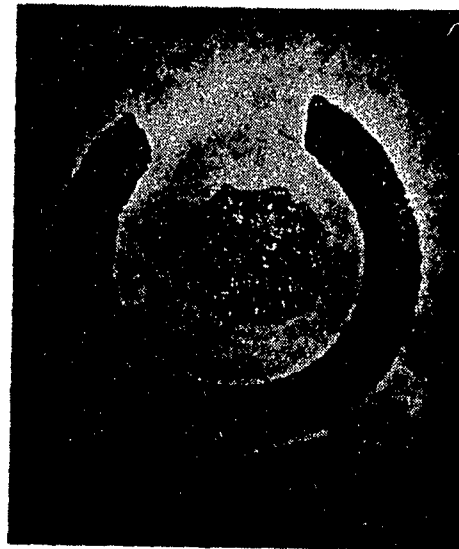
$$C_c \approx .8 \text{ pf}$$



Scale : 1cm. = .001"

FIGURE 2

BASE CONTACT GOLD ALLOY SHOWING DISCONTINUITIES
BY BALLING UP.



Scale: 1 cm. = .001"

FIGURE 3

ACCEPTABLE GOLD AND ALUMINUM ALLOY STRUCTURE

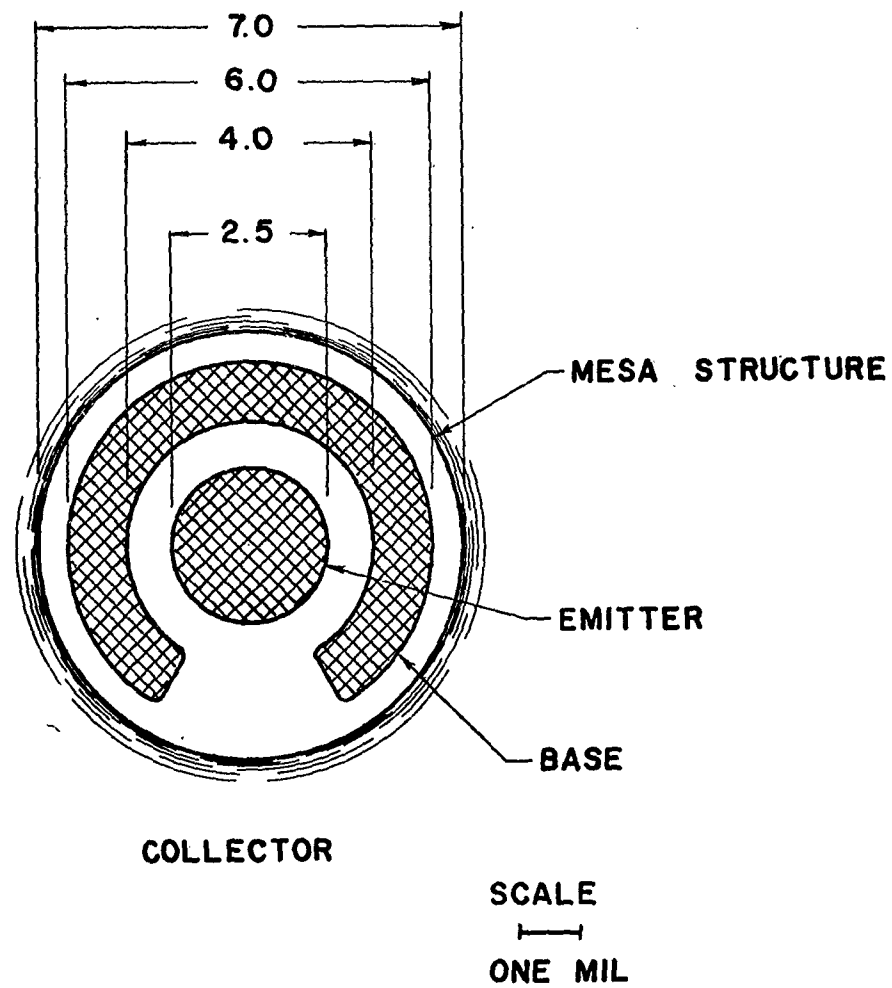


FIGURE 4 ACTUAL DIMENSIONS OF TRANSISTOR GEOMETRY

For a 20Ω cm epitaxial layer resistivity we would obtain:

$$C_c \simeq .25 \text{ pf}$$

Likewise for the zero bias capacitance of the emitter junction, one obtains by using equation (2) with $V_o = .4$ volts and $A_E \simeq 1.2 \times 10^{-5} \text{ cm}^2$ (diameter of 1.9 mils) and $N_E \simeq 5 \times 10^{17} \text{ atoms/cm}^3$

$$C_E \simeq 4.5 \text{ pf}$$

This capacitance can also be deduced conveniently from a measurement of f_t vs. I_E with a constant collector voltage by plotting $1/f_t$ vs. $1/I_E$.

The slope of the straight line portion at low current densities is proportional to C_E if $C_c \ll C_E$ and is given by

$$C_E \simeq \frac{q}{2\pi kT} \left[\frac{\Delta(1/f_T)}{\Delta(1/I_E)} \right] \quad (3)$$

Equation (3) has been obtained from the relation^{(1) (2)}

$$1/f_T = 1/f_b + \frac{2\pi kT C_E}{q I_E} \quad (4)$$

The interception of $1/f_T$ at $1/I_E$ approaching zero, e.g. very large emitter currents, will yield the base transit time $\tau_b = 1/2\pi f_b$ of the intrinsic transistor which is proportional to the reciprocal of the base

cut-off frequency. A measurement is presented in Figure 5. The effects of the emitter depletion layer capacitance upon the relation of the $1/f_T$ vs $1/I_E$ are emphasized. Two transistors with approximately the same effective base width, but with different emitter areas are characterized. A difference in emitter zero bias capacitance is the result. Unit No. R-23-3 shows a marked deviation from a straight line at low currents, which is attributed to the mild logarithmic dependence of the depletion layer capacitance on emitter current.

The deviation from a straight line at higher currents in unit No. R-23-3 can be due to drift field reduction^{(3) (4)} and two-dimensional current flow (=crowding) in the base region of the transistor or a space charge limited current condition in the collector depletion region which will move the space charge edge⁽⁵⁾. These effects tend to increase the base transit time τ_b and constitute an apparent widening of the base. It should be further noticed, that a critical current density to cause deviation from the linear behavior of $1/f_T$ vs i/I_E , under the assumption of identical doping in the base, is evidenced in unit R-23-3 at 5 mA and is in the order of 250 A/cm^2 . Unit R-30-4 does not show any deviation effects within the current range of the measurement.

The "focussing" action of the high drift field surrounding the emitter junction upon the minority carrier flow up to 200 mA currents is reflected in the dependence of grounded emitter small signal amplification factor, β , vs. collector current, I_C . Figure 6 gives a display of β vs I_C at signal frequency of 10 KC and a constant collector voltage of -2 volts of unit R-30-4.

An independent method of determining the base transit time, τ_b ,⁽³⁾ has also been employed and results will be reported in another section.

The extrinsic base resistance, r_b' of the device can be approximated by

$$r_b' \simeq \frac{R_s}{2\pi} \ln \left[\frac{D_B}{D_E} \right] \quad (5)$$

x # R-23-3
 o # R-30-4
 $V_{CE} = -10 \text{ VOLTS}$

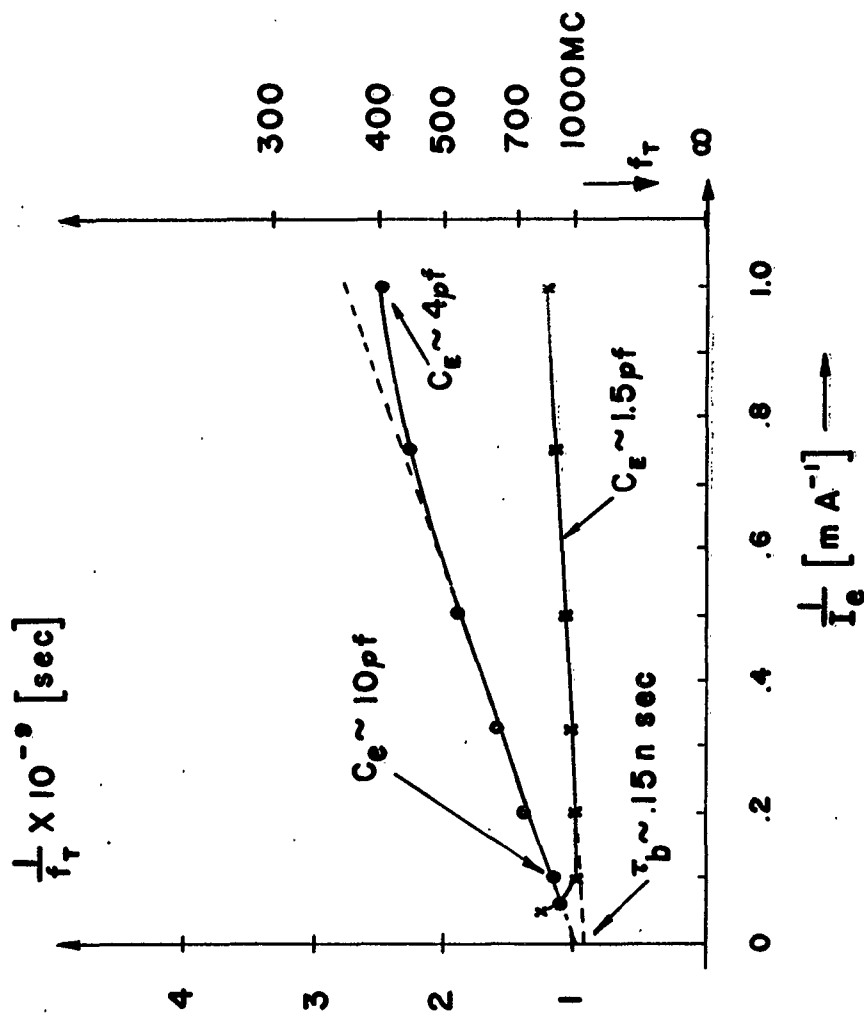
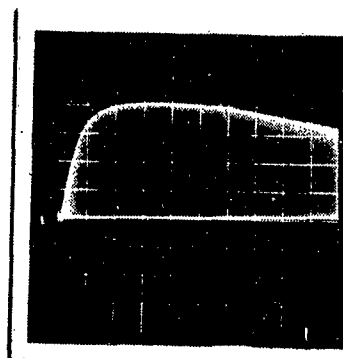


FIGURE 5. f_T MEASUREMENTS AS A FUNCTION OF EMITTER CURRENT AND PLOT OF $1/f_T$ VS. $1/I_E$ TO DETERMINE THE EMITTER DEPLETION LAYER CAPACITANCE, C_E AND TO SHOW THE INFLUENCE UPON TWO DIFFERENT TRANSISTORS.

β
20/Division



I_c 20mA/Division

FIGURE 6.

10 KC SMALL SIGNAL AMPLIFICATION FACTOR (BETA) VS.
COLLECTOR CURRENT, I_c , AT $V_{cE} = -2$ volts OF TRANSISTOR
R-30-4.

For a sheet resistivity $R_s = 100 \Omega/\square$ and an inner diameter of the base ring, D_B , of 4 mils and an emitter junction diameter, D_E , of 2 mils

$$r_b' \approx 11 \Omega$$

The frequency dependent parameter, f_T , and f_{ca} , which are inter-related with each other by the amount of drift field present in the base⁽⁶⁾ are difficult to calculate exactly since an average diffusion constant has to be used and fringing effects on the current flow have to be taken into consideration.

We have used an average hole diffusion constant of $D_p = 11 \text{ cm}^2/\text{sec}$ and a fringing factor K of 0.5 and plotted the function f_T and f_{ca} vs. W in Figure 7 from the relation

$$f_T = K' \frac{D_p}{\pi W^2} \quad (6)$$

$$\text{where } K' = K \left(\frac{1/2 A^2}{A - 1 + e^{-A}} \right) \quad (7)$$

$$\text{and } A = \ln \left(\frac{N_E}{N_C} \right) \quad (8)$$

$$\text{Furthermore } f_{ca} = F \left(\frac{N_E}{N_C} \right) f_T \quad (9)$$

f_{ca} vs. W in Ge PNP transistors

$D_{eff} = 11 \frac{cm^2}{sec}$

$\Delta V = 8 \frac{KT}{q}$

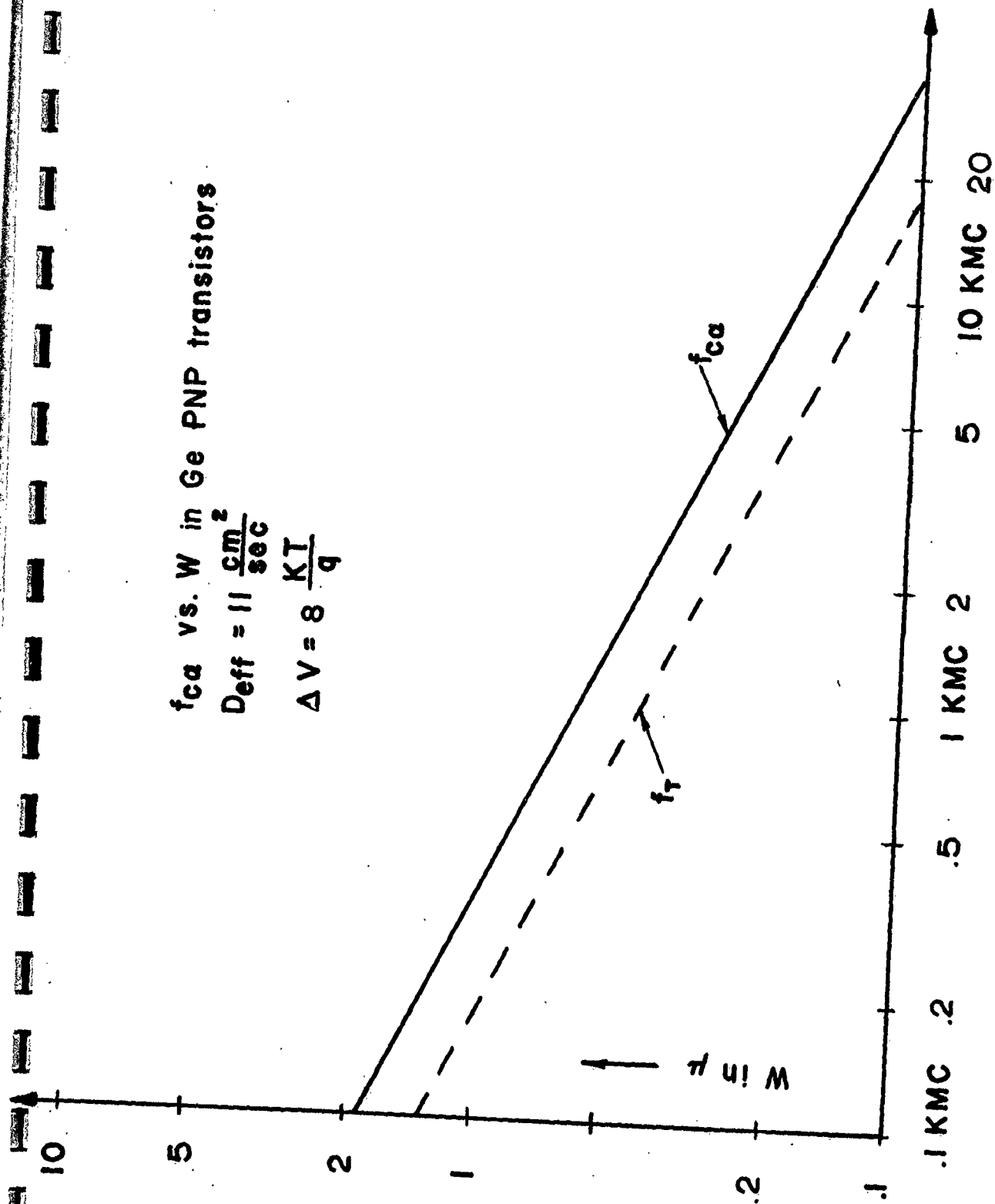


FIGURE 7 THEORETICAL RELATION OF TRANSISTOR BASE WIDTH, W , IN RELATION TO CUT-OFF FREQUENCIES, f_{ca} AND f_T .

and reference (6) gives the function $F\left(\frac{N_E}{N_C}\right) = \frac{f_{ca}}{f_T}$ vs. drift field factor $\Delta V/kT = \ln\left(\frac{N_E}{N_C}\right) = A$

For an effective base width of 0.5μ we find $f_T \sim 700$ Mc and $f_{ca} \sim 850-1400$ Mc depending upon the drift field. On the other hand, for a base width of $.3\mu$ we would expect $f_T \sim 2000$ Mc and $f_{ca} \sim 2440 - 4000$ Mc. The base width relation to f_T and f_{ca} has been empirically confirmed with transistors of the same structure and base widths of $1.5, 1.0, .7, .5\mu$.

The maximum frequency of oscillation, f_{max} , is determined from (2)

$$f_{max} = \left(\frac{a_o f_T}{8\pi r_b' C_c} \right)^{\frac{1}{2}} \quad (10)$$

and assuming $a_o \simeq 1$, we compute for the design with $f_T = 700$ Mc and $r_b' = 11\Omega$ and $C_c = .8$ pf.

$$f_{max} \simeq 1800 \text{ Mc.}$$

which would predict a power gain of about 6 db at 900 Mc.

Correspondingly, for a $f_T = 1000$ Mc and $r_b' = 10\Omega$ and $C_c = .25$ pf equation (10) yields

$$f_{max} \simeq 4000 \text{ Mc}$$

which in turn implies a power gain of 6 db at 2 Kmc and 12 db at 1 Kmc.

2. COAXIAL PACKAGE

The Hughes coaxial package is shown in a photograph, Figure 8. The details of the package are shown in Figure 9. The package is designed to be used with 50 ohm coaxial lines and type N connectors.

The germanium die is mounted on the collector post. 1 mil gold wires compression bonded to the base ring and emitter are welded to the base diaphragm and the auxiliary emitter post.

The 1 mil gold wires contribute most of the inductance of the package. They should be as short as possible. The detail drawing, Figure 10, shows the mounting technique to reduce the 1 mil wire length as much as possible.

Figure 11 shows the equivalent circuit of the package. The parasitic inductances and capacitances are measured at 1000Mc if not indicated otherwise. C_{EB} and C_{CB} are present because of an impedance mismatch where the center post is fixed in the glass. The impedance there is about 30 ohm instead of 50 ohm. The inductances are mainly produced by the 1 mil gold wire connecting emitter and base to the package. These wires are about 50 mils long and contribute at least 1 nH each. The inductance can be approximately calculated from the relation ⁽⁸⁾:

$$L \simeq 5.08 \times 10^{-3} \, l \left[2.303 \log_{10} \frac{4l}{d} - 1 \right] \mu\text{H} \quad (11)$$

where

l = length of wire

d = diameter of wire

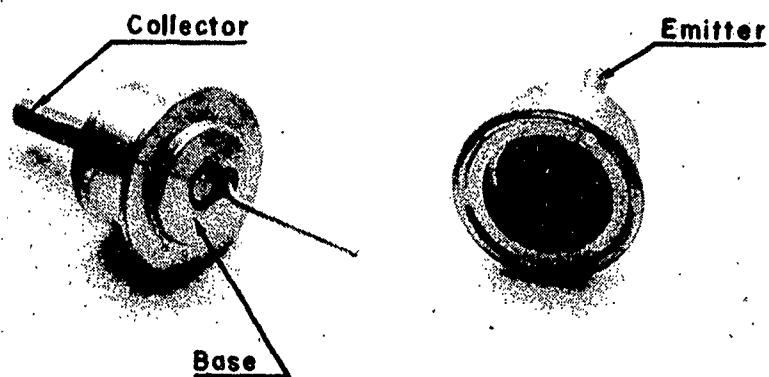


FIGURE 8

PHOTOGRAPH OF THE TWO-PART COAXIAL TRANSISTOR
PACKAGE OF HUGHES DESIGN 1.

ALL KOVAR PARTS
PLATED WITH
HIGH TEMPERATURE
GOLD.

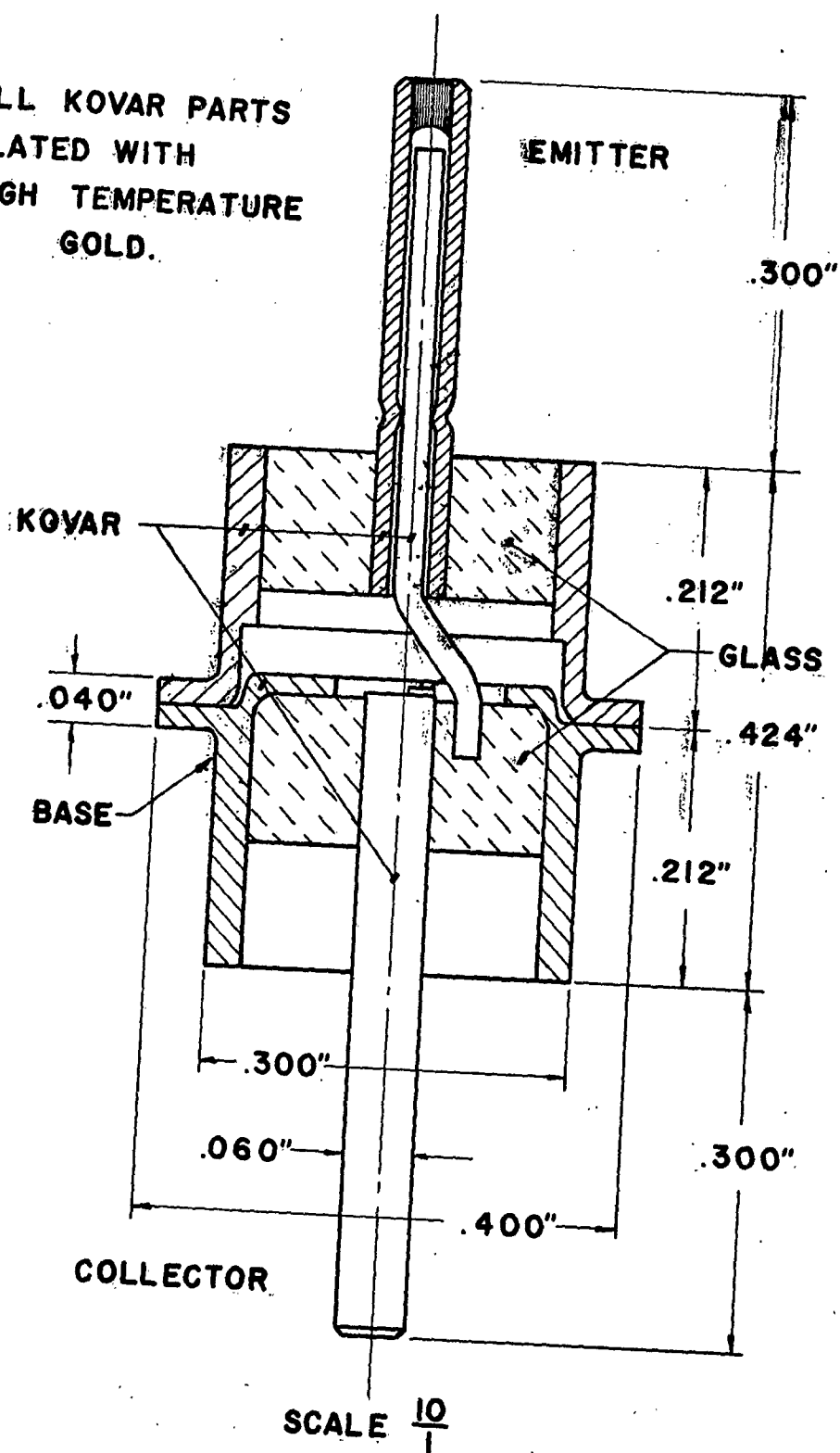
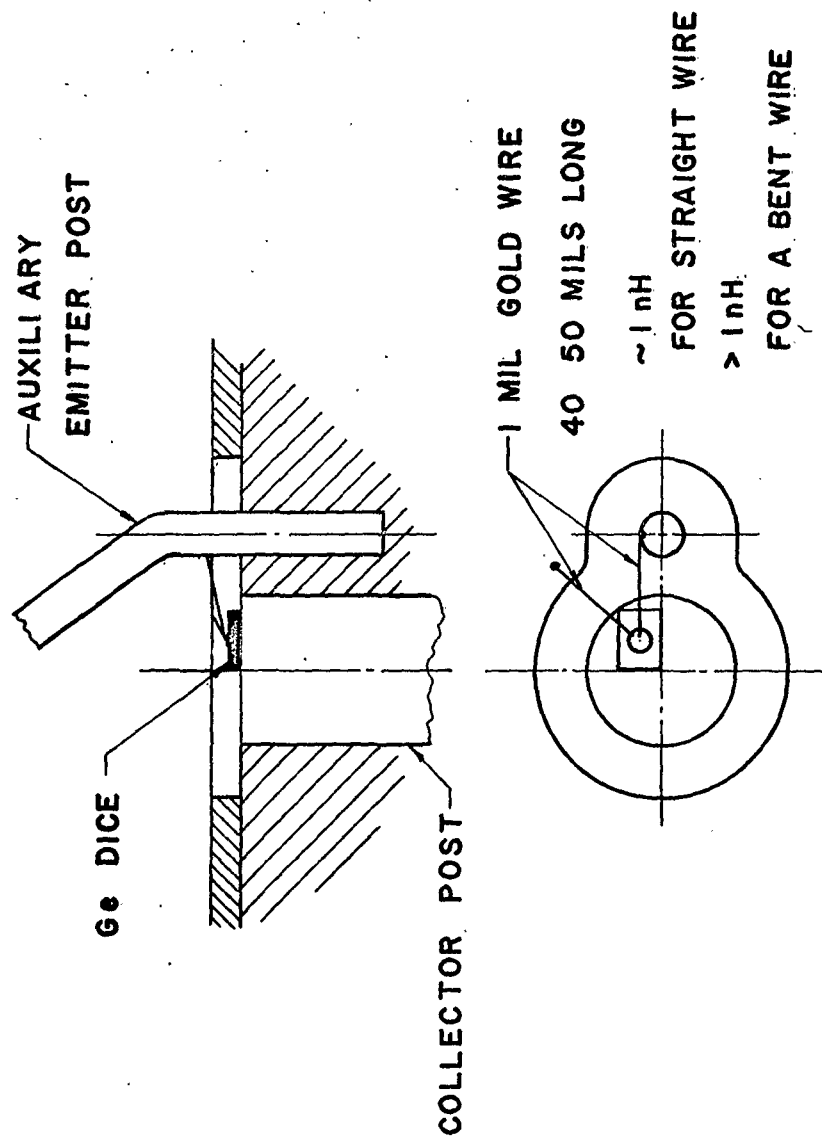


FIGURE 9. CROSS-SECTIONAL DRAWING OF HUGHES DESIGN I
COAXIAL PACKAGE AND DIMENSIONS.



SCALE $\frac{20}{1}$

FIGURE 10 ILLUSTRATION OF TRANSISTOR MOUNTING AND EMITTER
AND BASE THERMOCOMPRESSION BONDS TO BASE
DIAPHRAGM AND AUXILIARY EMITTER POST.

The capacitance C_{EC} between emitter and collector is introduced by the auxiliary emitter post. The coaxial transistor is generally used in a grounded base configuration. In this case, the base membrane acts as a shield between input and output. There is also a possibility of connecting the emitter to the main body and the base to the emitter post. This arrangement may be used for special circuit arrangements like the transit time oscillator by Gibbons⁽⁹⁾.

The lowest self resonance of the coaxial package determines the frequency limitation. The values in the equivalent circuit Figure 11 indicate that the package is useful up to 3 Kmc.

The capacitance, C_{EB} and C_{CB} are always included in the input and output resonance circuit and do, therefore, not load the circuit below the resonance frequency of the package.

The capacitance C_{EC} may produce undesirable feedback action between input and output but with the value given in Figure 11 this capacitance has little influence at 2 Kmc and below.

Plans for a more advanced package useful up to 5 Kmc include the following changes:

- a) Ceramic instead of glass will be used to keep the losses down.
- b) Better matching to 50 ohm impedance will reduce the input and output capacitance considerably.
- c) Elimination of the auxiliary emitter post reduces C_{EC} to a negligible value up to 5 Kmc.
- d) Reduction of the base and emitter inductance to less than 1 nH.

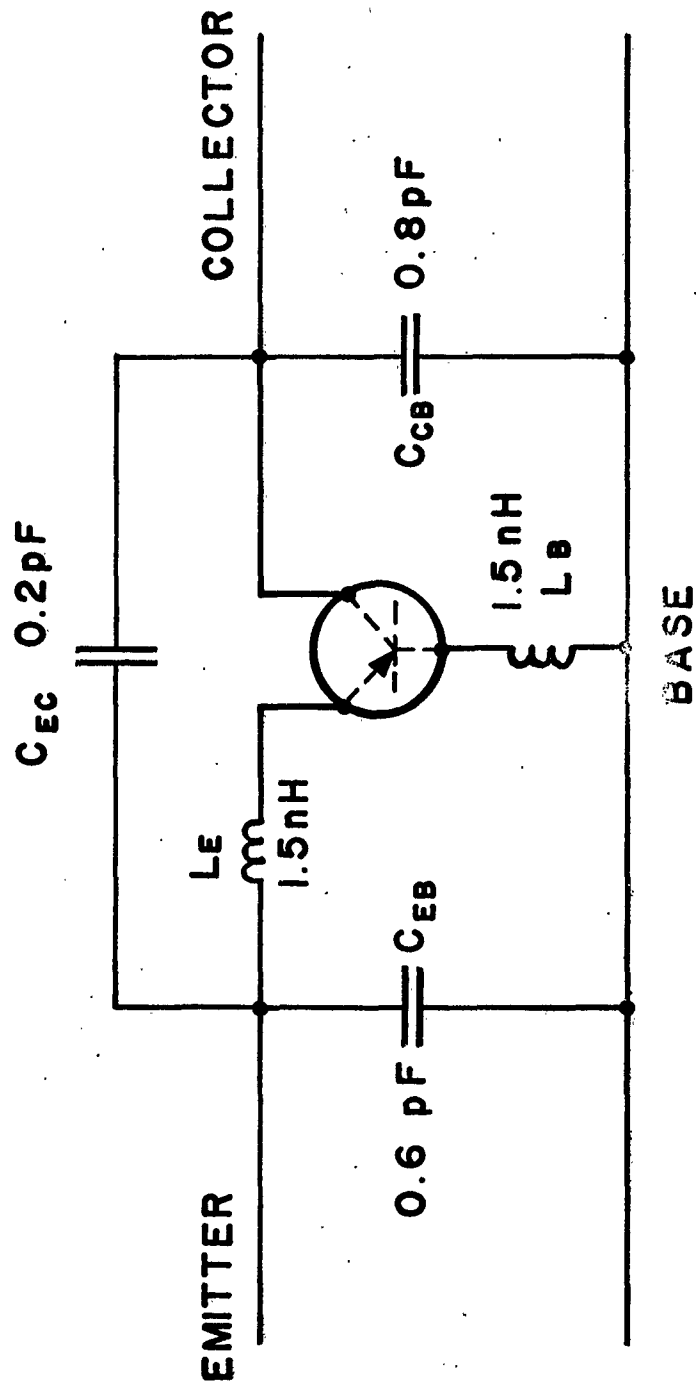


FIGURE 11 PARASITIC ELEMENTS OF HUGHES DESIGN I COAXIAL PACKAGE, EXCLUDING THE TRANSISTOR.

3. ELECTRICAL EVALUATION OF PACKAGE AND TRANSISTOR

The evaluation of Hughes Design I coaxial package indicates interference free operation up to 2.5 Kmc. In actual circuitry the input and output capacitance of the package can be part of the coaxial line connection to the transistor and thus can be tuned out. The remaining parasitic elements of the package are

- a) a feedback capacitance between input and output C_{EC} (0.2 - 0.3 pf).
- b) the base and emitter lead inductance of the thermo compression bonds to the package elements.

The intrinsic transistor, which is characterized by an alpha transfer characteristic of

$$a_i = a_o \left[\frac{\exp(-j m \omega / \omega_c)}{1 + j \omega / \omega_c} \right] \quad (12)$$

is mainly affected by the extrinsic elements of the transistor design, namely the base resistance r_b , the collector capacitance C_c , and the extrinsic base lead inductance L_b .

The effective transfer characteristic including r_b , C_c , L_b , is

$$a_{eff} = \frac{a_i + j \omega r_b C_c - \omega^2 L_b C_c}{1 + j \omega r_b C_c - \omega^2 L_b C_c} \quad (13)$$

Considering the effect of $r_b' C_c$ and $L_b C_c$ independent of each other we get for the $r_b' C_c$ losses

$$a_{eff1} = \frac{a_i + j \omega r_b' C_c}{1 + j \omega r_b' C_c} \quad (14)$$

and for the $L_b C_c$ disturbance

$$a_{eff2} = \frac{a_i - \omega^2 L_b C_c}{1 - \omega^2 L_b C_c} \quad (15)$$

The influence of various $r_b' C_c$ and $L_b C_c$ parameters has been computed numerically for our present transistor design with $f_b = 1200$ Mc and $m = 1$ [drift field of $8 \text{ kT}/q$]

Figure 12 represents the data for equation 14 with $r_b' C_c$ equal to 0, 5, 10, 20, 40×10^{-12} sec. Figure 13 represents the data for equation 15 with $L_b C_c$ equal to 0, 5, 1, 2, 5×10^{-21} sec.².

With our present transistor structure and the package, the disturbing effects of $r_b' C_c$ are negligible at 1 Kmc, if their product is smaller than 10×10^{-12} sec, (e.g. $r_b' = 10 \Omega$, $C_c = 1 \text{ pf}$), and of $L_b C_c$, if their product is smaller than 1×10^{-21} sec.² (e.g. $L_b = 1 \text{ nH}$, $C_c = 1 \text{ pf}$).

Our present coaxial transistor has $L_b \approx 1 - 1.5 \text{ nH}$, $C_c \leq 1 \text{ pf}$ which allows us to neglect the influence of $L_b C_c$.

Figure 14 gives the measurement of a_{eff} of a coaxial transistor with the GR transfer function bridge. On the same graph a_i has been found by

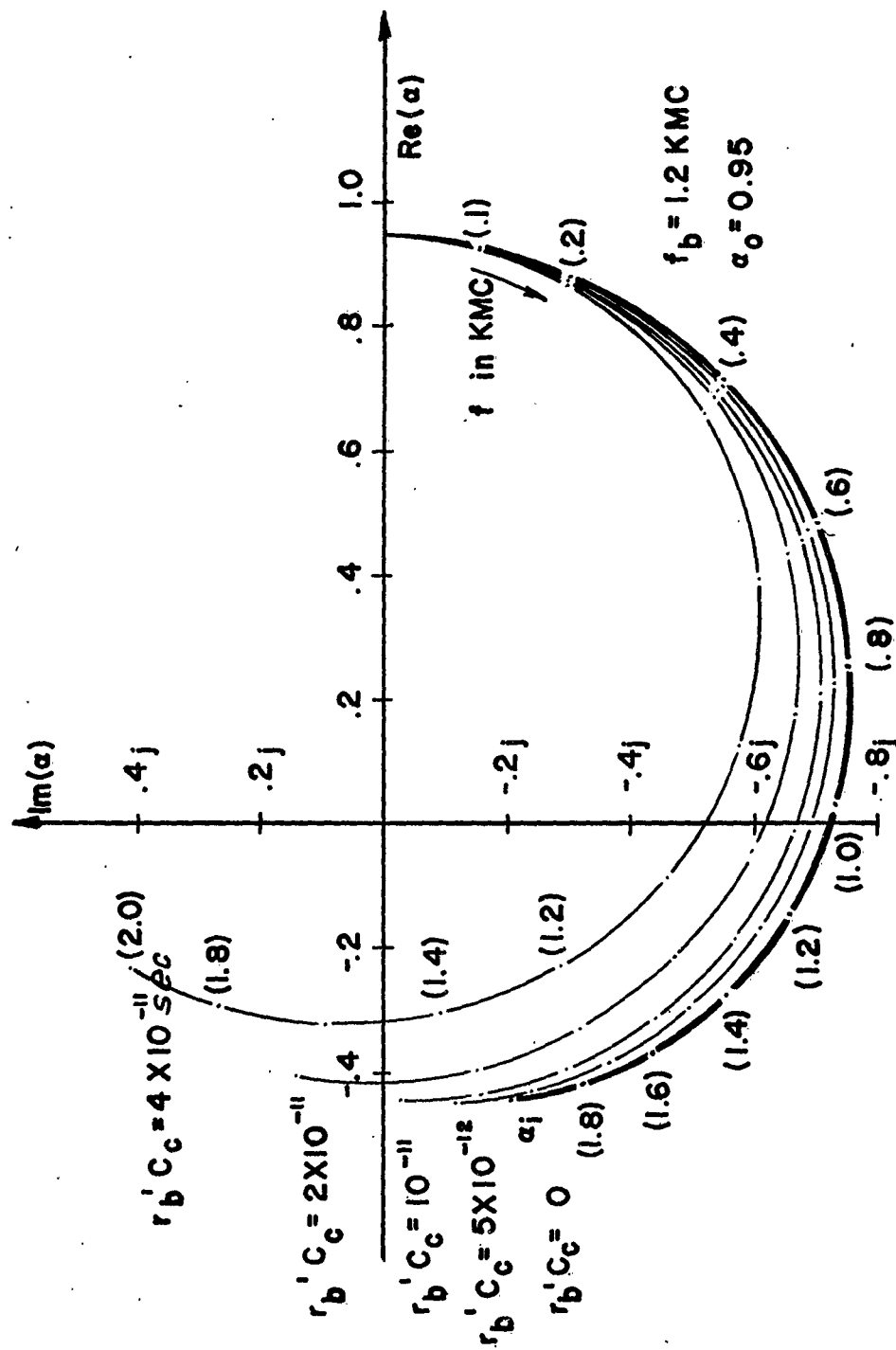


FIGURE 12 COMPLEX REPRESENTATION OF INTRINSIC CURRENT AMPLIFICATION, α AND THE EFFECT OF $r_b' C_c$ UPON ITS EFFECTIVE BEHAVIOR.

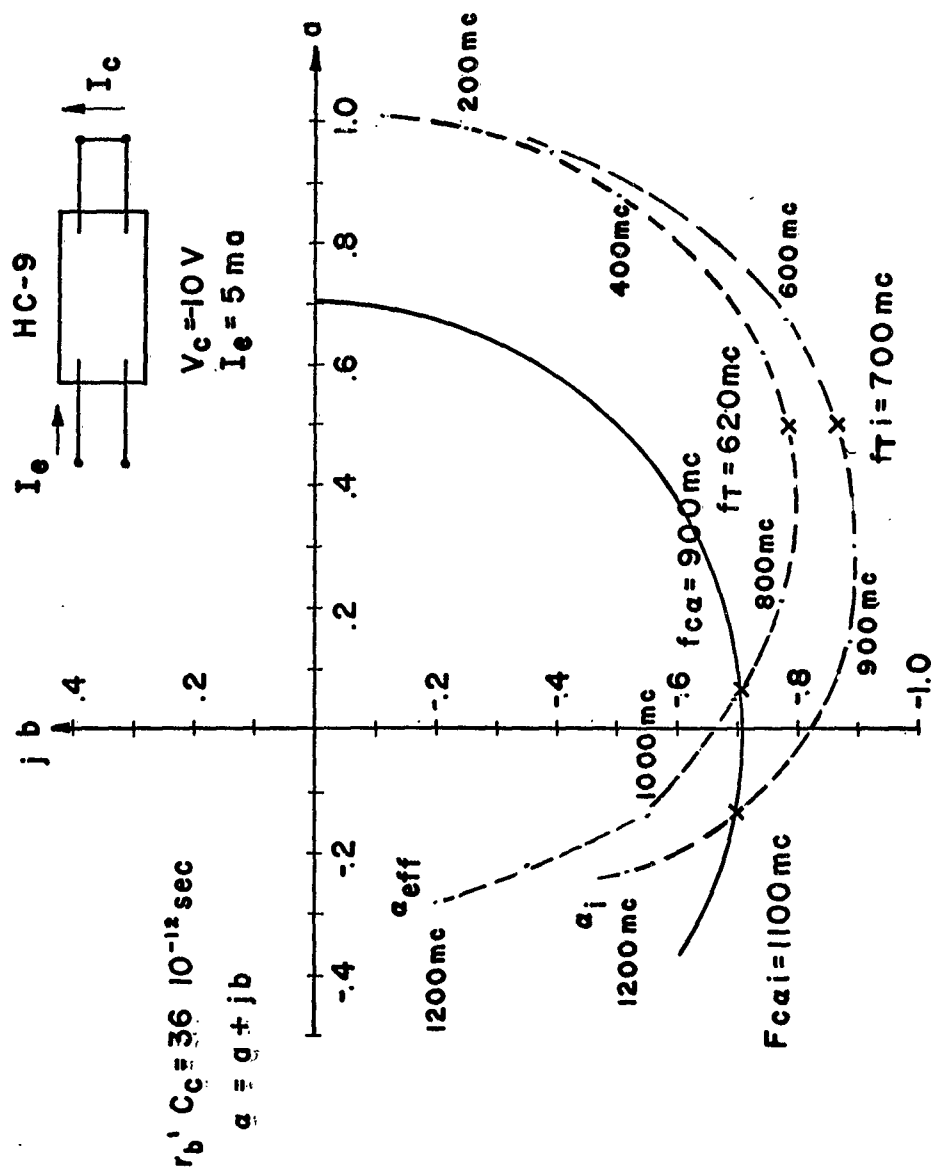


FIGURE 14 ACTUAL AND CORRECTED MEASUREMENT OF THE COMPLEX CURRENT AMPLIFICATION FACTOR.

correcting for the $r_b' C_c$ influence. The correcting formulas are derived from equation 14.

$$a_i = a_{eff} - b_{eff} \omega r_b' C_c \quad (16)$$

$$b_i = b_{eff} - \omega r_b' C_c \left[1 - a_{eff} \right] \quad (17)$$

where

$$a_i = a_i + j b_i \quad a_{eff} = a_{eff} + j b_{eff}$$

The characteristic values for the experimental Hughes HC-9 coaxial transistor are

β	=	20	
r_b'	\approx	60 Ω	
C_c	=	0.6 pF	
$r_b' C_c$	=	36×10^{-12} sec.	
f_{ca}	=	900 Mc	uncorrected for $r_b' C_c$
f_T	=	620 Mc	
f_{cai}	=	1100 Mc	corrected for $r_b' C_c$
f_{Ti}	=	700 Mc	
L_b	=	$L_e = 1.5$ nH	
$L_b C_c$	=	1×10^{-21} sec. ²	

Figure 15 shows the influence of the emitter current I_e on a_{eff} . Three curves at $I_e = 1, 2, 4$ mA are given. This effect results from the influence of the emitter cut-off on a and the diminution of the base-drift field in the high forward current region.

The influence of the emitter cut-off at low I_e changes a_{eff} according to

$$a_{eff} = \frac{a_i}{1 + j\omega r_e C_e} \quad (18)$$

A plot which shows the influence of the emitter cut-off is shown in Figure 16.

The resulting cut-off frequency, $f_{c_{eff}}$, from the emitter and collector cut-off frequency can be derived with the following formula⁽²⁾

$$\frac{1}{f_{c_{eff}}^2} = \frac{1}{f_c^2} + \frac{1}{f_e^2} \quad (19)$$

The input impedance h_{ib} for shorted output is given by

$$h_{ib} = r_e + r_b' (1 - a_i) = r_e + r_b' (1 - a_i) - j b_i r_b' \quad (20)$$

$$a_i = a_i + j b_i$$

The influence of L_E , the inductance of the emitter lead and C_E , the emitter depletion layer capacitance are very degenerating upon the input impedance h_{ib} of the transistor.

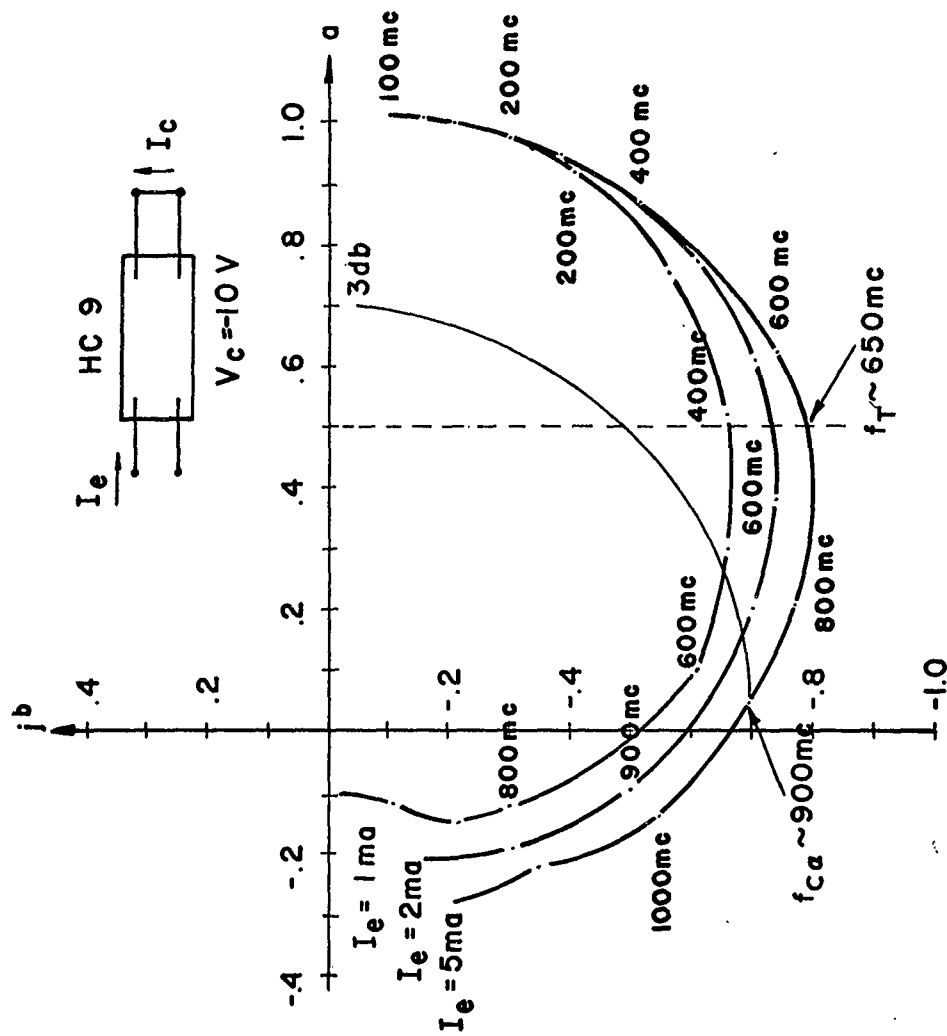
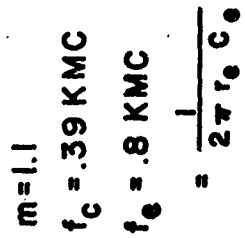


FIGURE 15 MEASUREMENTS OF COMPLEX CURRENT AMPLIFICATION FACTOR, a_{eff} , AS FUNCTION OF EMITTER CURRENT.

 $f_{c\text{off}}$

$$h_{ib} = \frac{r_e}{1 + (\omega r_e C_E)^2} + r_b' (1 - a_{eff}) \quad (21)$$

$$+ j \left\{ \omega L_E - r_b' b_{eff} - \frac{\omega r_e^2 C_E}{1 + (\omega r_e C_E)^2} \right\}$$

where

$$a_{eff} = a_{eff} + j b_{eff}$$

Figure 17 sketches the function of equation (21).

Considering the frequency dependence of the imaginary part one can show that for the intrinsic transistor the input impedance looks inductive for an alpha phase shift of less than 180° ; it is real for an alpha phase shift of exactly 180° and turns capacitive for a phase shift larger than 180° . The modified input impedance of equation (21) however, experiences a considerable change in the inductive part, $j b_{eff} r_b'$, by the third term of the imaginary part, which is a capacitive reactance. The point where h_{ib} is real will occur at a frequency lower than the frequency where a_{eff} has a phase shift of 180° . At the higher frequencies the first term will cause another cross-over point from the capacitive to inductive reactance, since the third term will vanish as it has a $1/\omega$ dependence, whereas the first term is proportional to ω and will be dominating. The actual measurement for transistor No. HC-9 is given in Figure 18.

From Figure 18 we concluded that mixing takes place at $I \approx 3$ mA and 700 mc where h_{11} is purely resistive if the input current is tuned to that

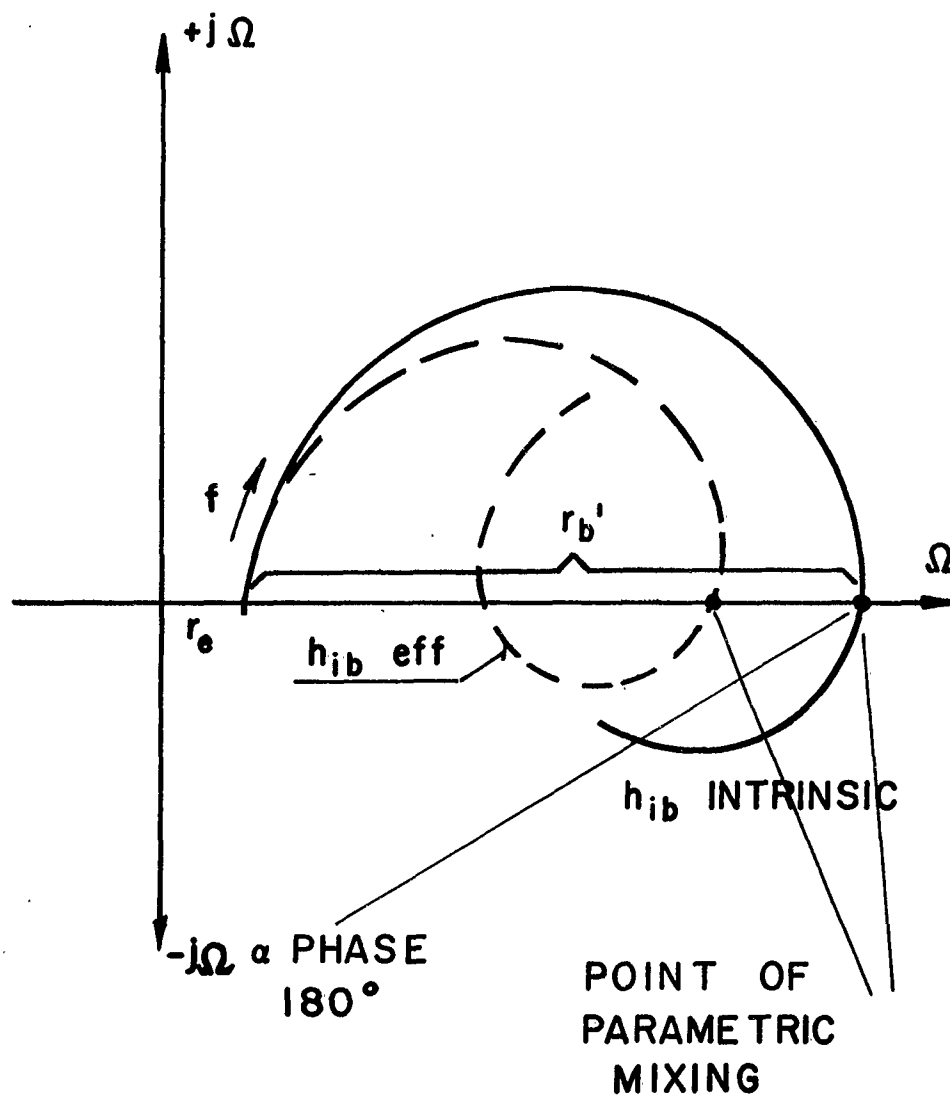


FIGURE 17

THEORETICAL INPUT IMPEDANCE OF A DRIFT TRANSISTOR
 AND THE EFFECT OF EMITTER DEPLETION LAYER
 CAPACITANCE UPON ITS VARIATION.

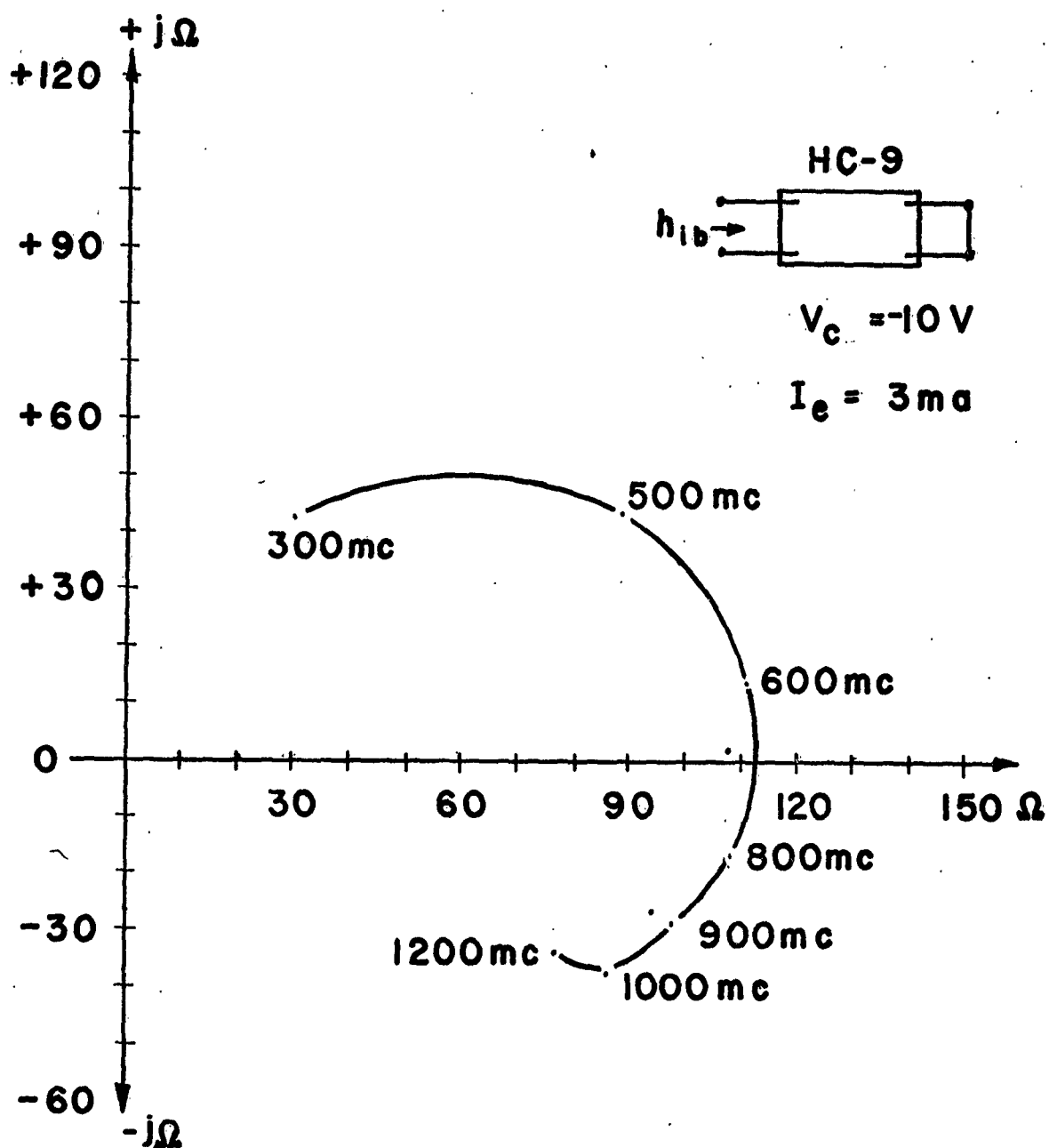


FIGURE 18

INPUT IMPEDANCE, h_{ib} , OF A COAXIAL TRANSISTOR AT $V_c = -10V$ AND $I_e = 3mA$ AS A FUNCTION OF FREQUENCY.

frequency. Figure 19 shows a plot of the real and imaginary part of h_{11} in function of the emitter current at 650, 700 and 800 Mc. It is easy to see that the nonlinear reactance is responsible for mixing. The best operating point is at 700 Mc and 2.8 mA. There is another region at 1 mA where mixing could occur but at that bias no transit time oscillations occur because the higher r_e dampens the circuit too much.

Since a power gain measuring set-up is not available at the time of writing this report, an indirect method has been executed to determine this parameter. A set of the four h-parameters have been measured at 1 Kmc and a bias of $I_e = 3\text{mA}$ and $V_C = -10\text{V}$. The power gain, G_p can then be calculated from the relation

$$G_p = \frac{|h_{21}|^2}{R_e(h_{11}) R_e(h_{22}) [(1+x)^2 + Y^2]} \quad (22)$$

where $x = \frac{m_{12} n_{12} + m_{21} n_{21}}{2 m_{11} m_{22}}$

$$Y = \sqrt{1 - A - x^2}$$

and $A = \frac{m_{12} m_{21} - n_{12} n_{21}}{m_{11} m_{22}}$

with $h_{ij} = m_{ij} + j n_{ij}$

HC-9

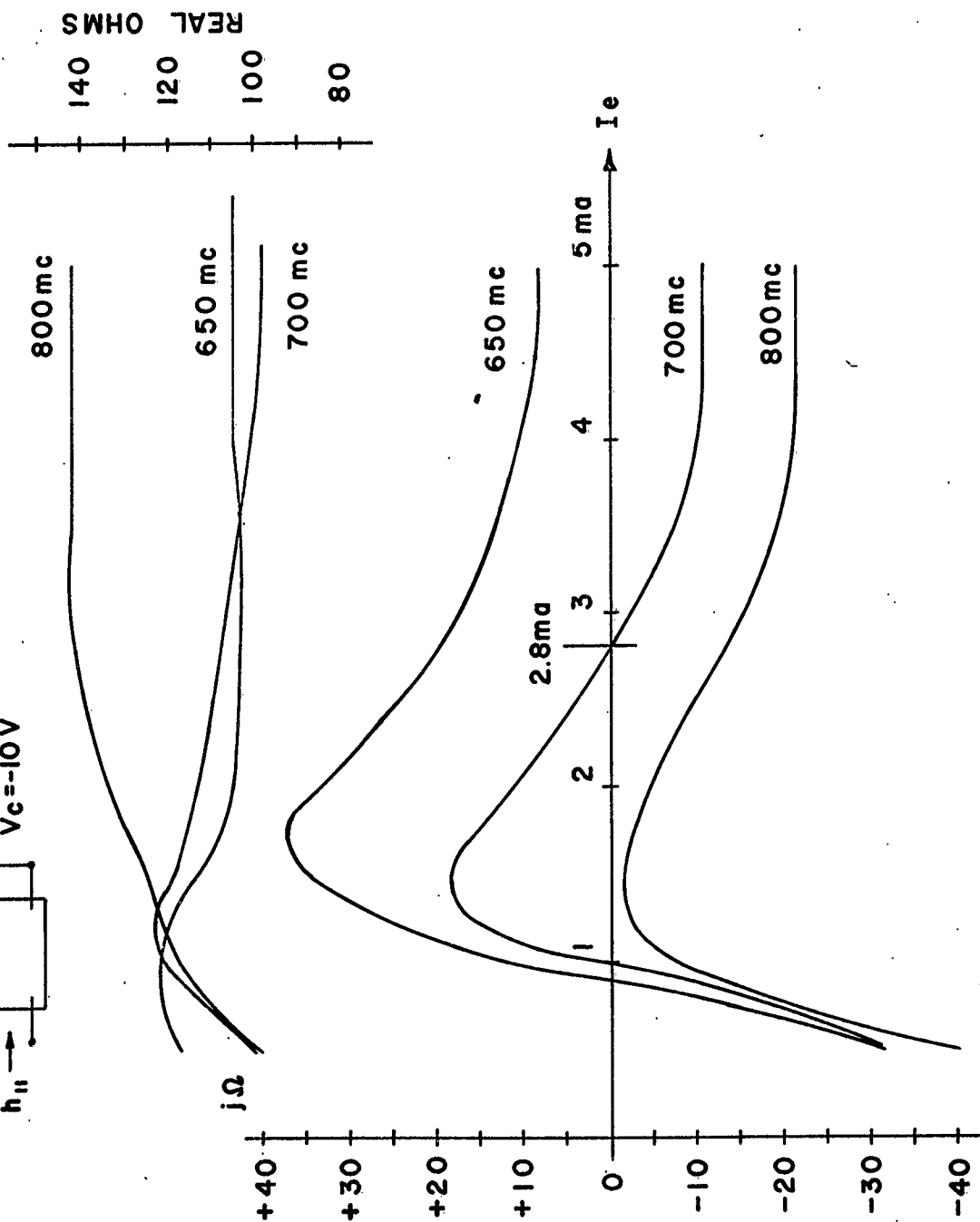
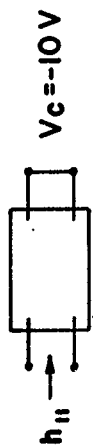


FIGURE 19 REAL AND IMAGINARY PART OF INPUT IMPEDANCE, h_{ib} , AS FUNCTION OF EMITTER CURRENT, I_e , FOR VARIOUS FIXED FREQUENCIES TO DEMONSTRATE THE NONLINEAR REACTANCE.

In case of zero feedback $h_{12} = 0$ we get:

$$G_P = \frac{|h_{12}|^2}{2 \operatorname{Re}(h_{11}) \operatorname{Re}(h_{22})} \quad (23)$$

$$P_G = 10 \lg_1 (G_P) \text{ in db} \quad (24)$$

The following table shows the measured h parameters and the calculated power gain for a typical transistor at 1000 Mc.

<u>Transistor</u>	<u>HC - 16R</u>
V_c	- 10V
I_e	3 mA
h_{11}	(70 + j 22) ohm
h_{22}	(1 + j 3.2) m mho
h_{21}	(-0.7 + j 0)
h_{12}	~ 0
P_G	5.5 db
f_{\max}	~ 2000 Mc (from P_G)

The low power gain is due to a high r_b and C_c . Better epitaxial material available now will reduce C_c . High r_b has been traced to

a discontinuous gold film on the base ring and in part to bad alloying of the germanium die to collector post.

Some of our experimental transistors mounted in a TO5 package have been tested in a high speed switching circuit. The results in Table 2 were very encouraging if one considers that this transistor has been designed for oscillators and amplifiers.

Switching Performance of Unit

R-30-2

$$t_{\text{on}} = 6 \text{ n sec}$$

$$\beta = 36$$

$$t_{\text{off}} = 6 \text{ n sec}$$

$$f_T = 960 \text{ Mc at } V_{\text{cc}} = -7\text{V},$$

$$I_c = 10 \text{ mA}$$

$$t_{\text{storage}} = 10 \text{ n sec}$$

Also see figure 20

Saturated switching
circuit

TABLE 2

The minority carrier storage could be reduced substantially by reducing the high resistivity epitaxial layer from 10 to 3μ . A reduction of the collector breakdown voltage to about 15V would be acceptable for most circuit applications. Figure 20 shows f_T in function of V_c and I .

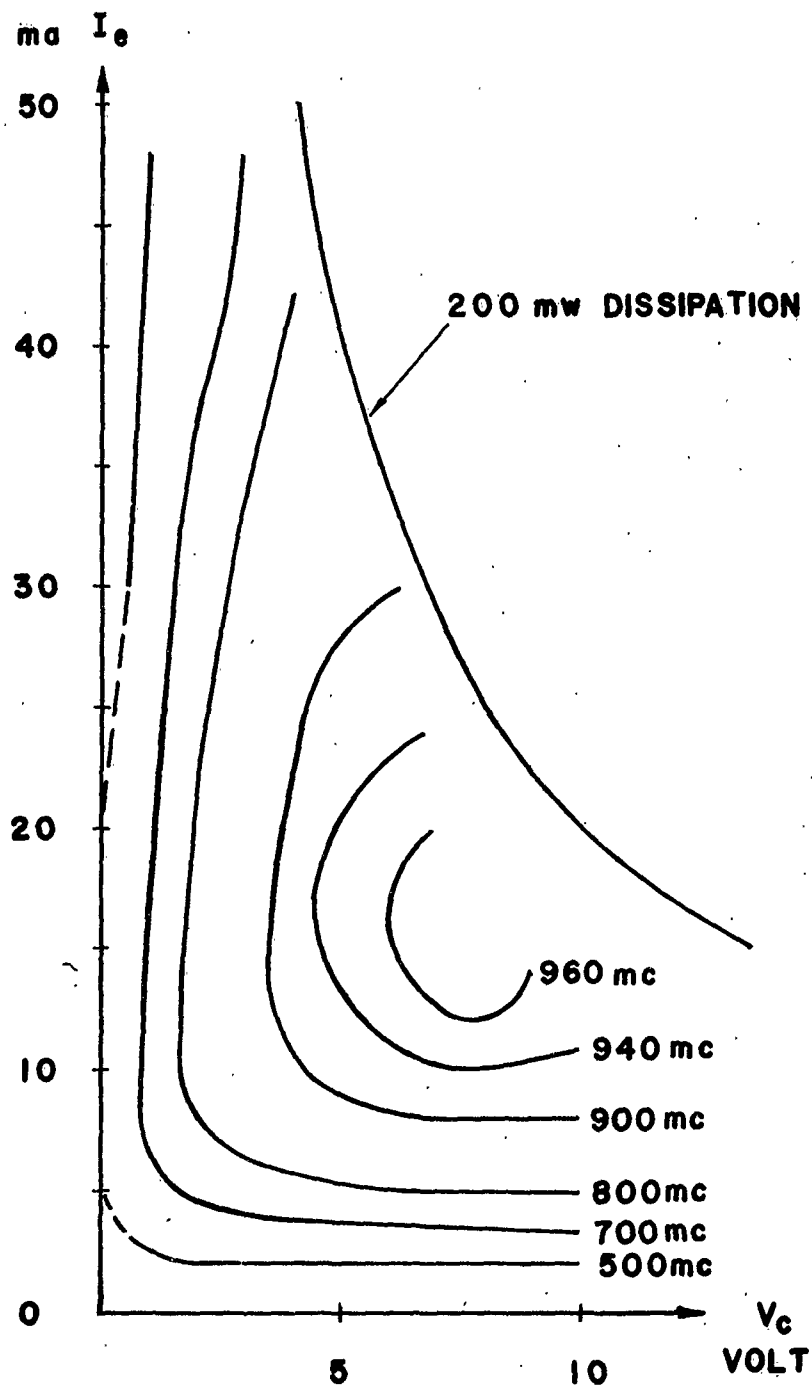


FIGURE 20 MEASUREMENT OF f_T AND ITS VARIATION IN THE $V_c I_c$ - PLANE.

4. PARAMETRIC MIXER

The principle of parametric mixing has been explained in the previous section of this report and in our Second Interim Engineering Report. Extensive power gain and noise measurements with our coaxial mixer have been performed. Figure 21 shows the output signal level and the power gain of the mixer in function of the input signal level.

The noise figure has been measured in a set-up shown in Figure 22. The noise figure F is defined by

$$F = \frac{GN_G + N_m}{GN_G} \quad (25)$$

where G = gain of amplifier
 N_G = noise of generator
 N_m = noise of amplifier

If the sensitivity of the mixer and the IF bandwidth are known, F can be calculated. The sensitivity of a mixer is equal to that particular input signal where the output signal power and output noise power are equal. This leads to the relation

$$GN_G + N_m = S_G G \quad (26)$$

If we combine equation (25) and (26) we get

$$F = \frac{S_G}{N_G} = \frac{U_G^2}{R_m KTB} \quad (27)$$

where S_G = input signal level

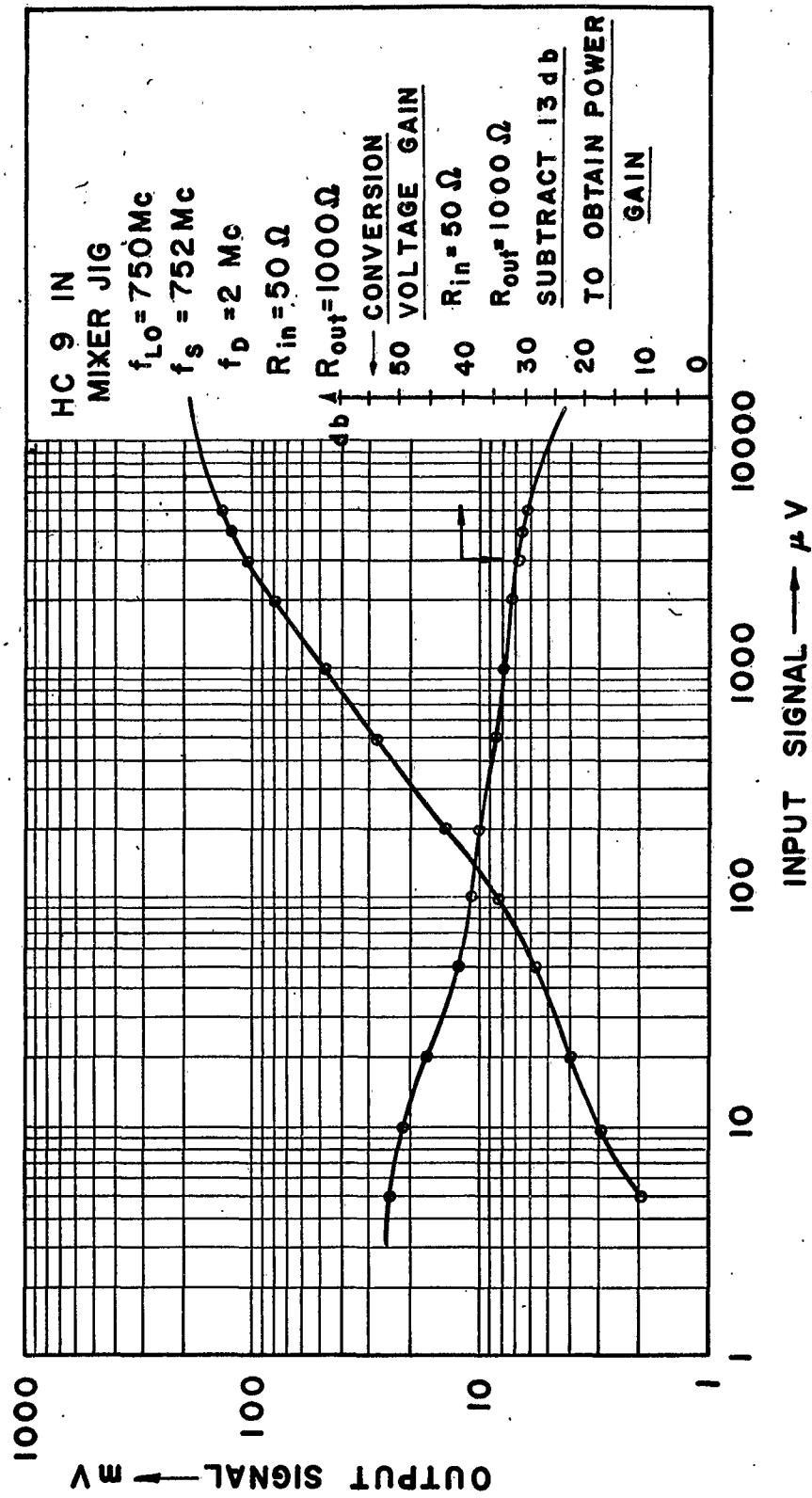


FIGURE 21 MIXER PERFORMANCE OF UNIT HC-9 FOR VARIOUS SIGNAL LEVELS.

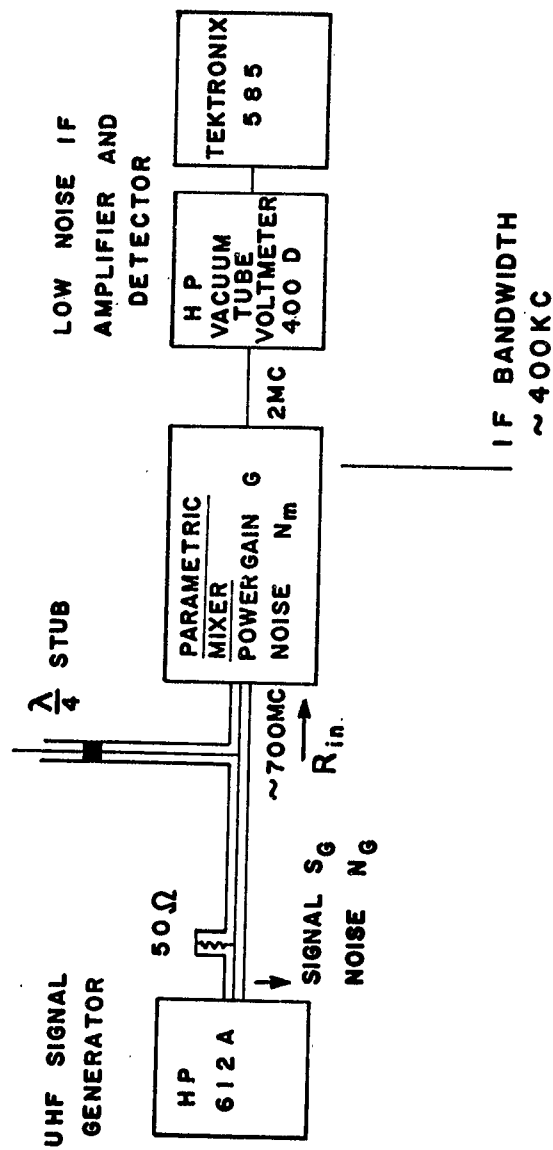


FIGURE 22 MEASURING SET-UP TO DETERMINE THE NOISE FIGURE OF THE PARAMETRIC MIXER.

U_G = input signal voltage
 R_m = input impedance of amplifier
 B = IF bandwidth of the amplifier

The relation of equation (27) is plotted in Figure 23.

With our first coaxial transistors, a sensitivity of $2\mu V$ has been measured. The IF bandwidth is about 400 Kc. This gives us a noise figure of 15 db.

This relative high noise figure can be improved considerably by the following methods:

- a) The matching from the generator to the mixer is far from ideal. To be on the safe side we have terminated the generator with 50 ohm which reduces our sensitivity. The $\frac{\lambda}{4}$ stub is used to tune out any reactances.
- b) Present transistors have a base resistance of 50 to 100 ohm. This is about 3 to 4 times the theoretical value predicted in Section 1. The reason has been found to be a discontinuous gold film of the base ring and bad wetting of the die in the mounting operation to the center collector post.

Mixing at the second and third harmonic has also been investigated. The results are given below.

f	<u>Overall Power Gain</u>
2nd harmonic 1400 Mc	5 db
3rd harmonic 2100 Mc	1 db

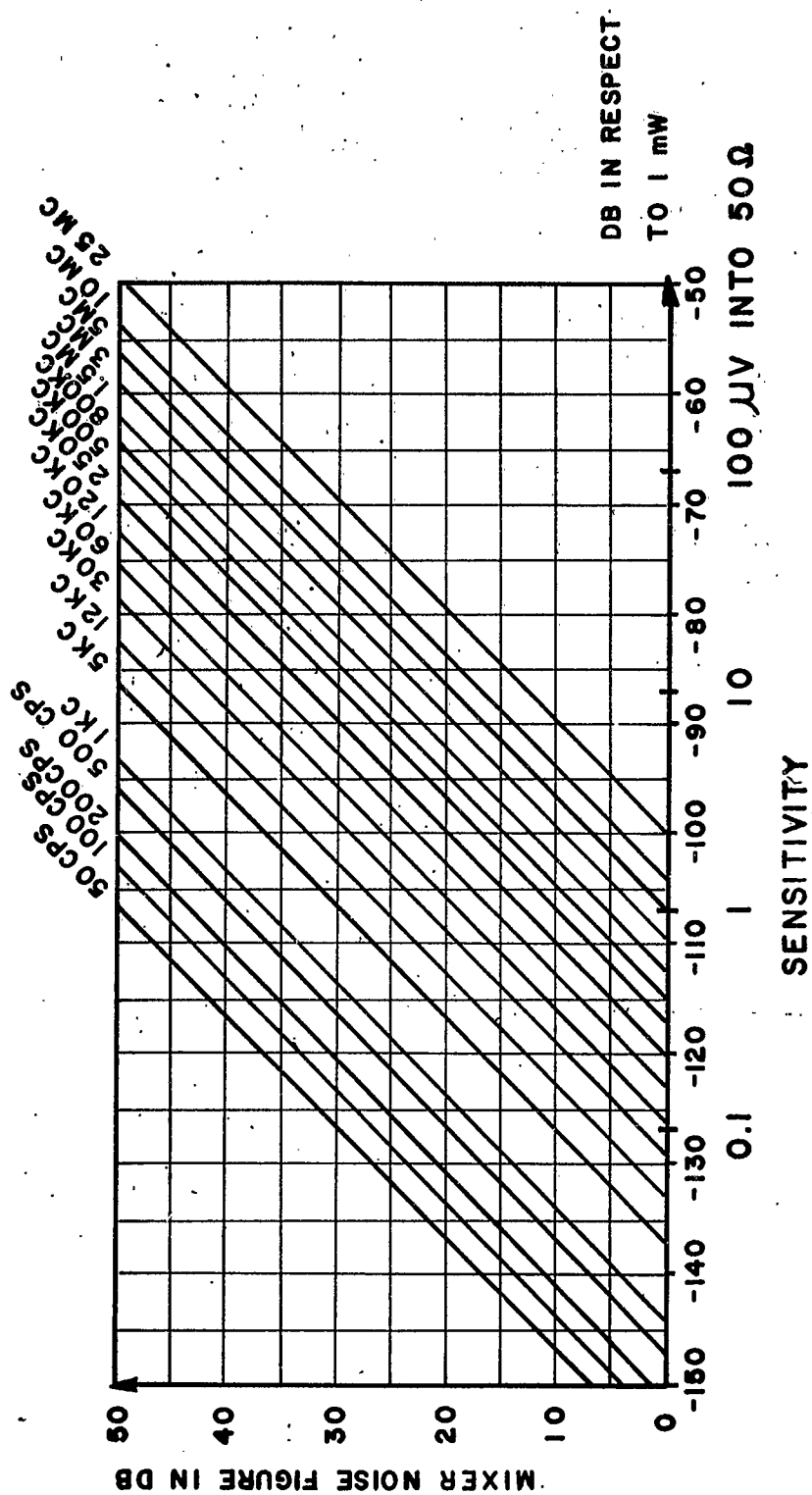


FIGURE 23 THEORETICAL CURVES FOR DETERMINATION OF NOISE
FIGURE FROM SENSITIVITY AND BANDWIDTH VALUES.

It is to be expected that the gain is low at 1400 Mc because the tuned $\frac{\lambda}{2}$ emitter line shorts the input signal. The results should be better at 2100 Mc but increased losses may account for the low gain.

5. INSTRUMENTATION

Due to its particular shape all test jigs had to be redesigned for the coaxial package. This includes

- a) Holder for the Tektronix Curve Tracer
- b) Jig for the GR Transfer Bridge
- c) $r_b' C_c$ jig
- d) f_T jig

The f_T measuring gear will be described for its merit to high frequency transistor evaluation.

f_T Test Equipment

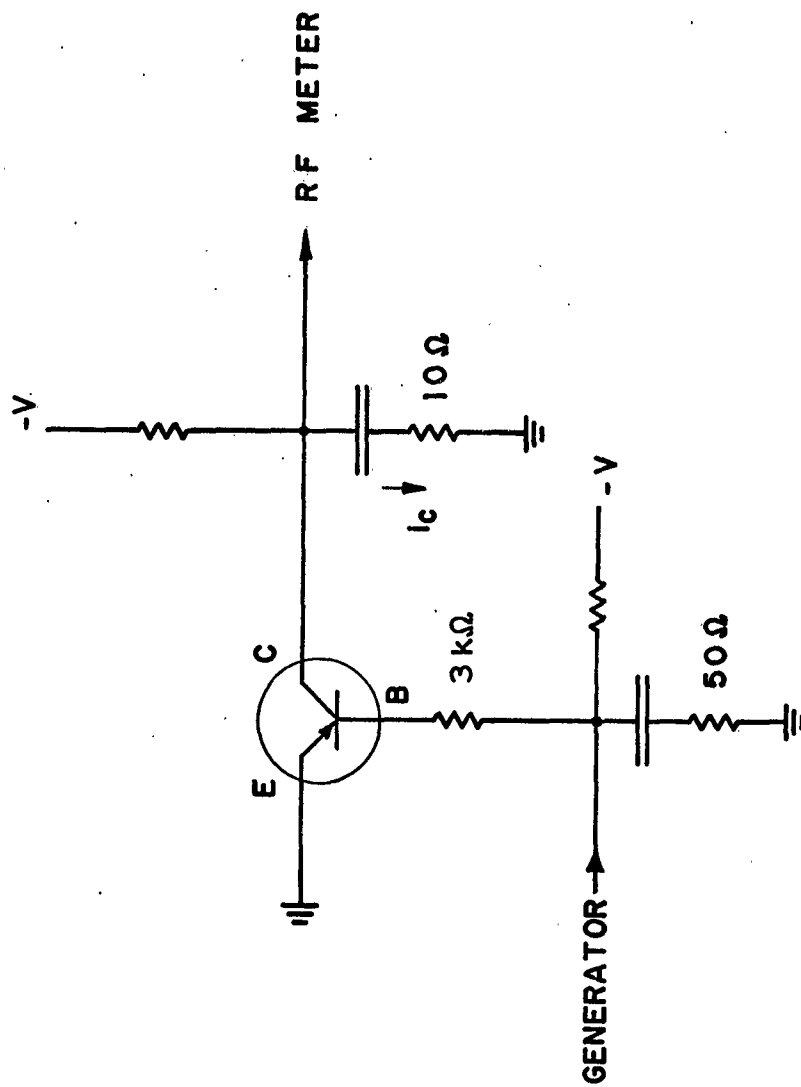
f_T is the frequency where the current gain β in the grounded emitter configuration is equal to 1. The equivalent circuit is shown in Figure 24. A dummy transistor with a collector to base short and emitter open is used to establish the collector current i_c according to a β of 1.

Assume we get a reading of A db with the RF meter. With the transistor inserted, the RF meter shows B db. If we assume that β falls off 6 db per octave with increasing frequency, we get for f_T

$$\underline{f_T = f_{\text{measure}} \cdot 10^{\left(\frac{B-A}{20}\right)}} \quad (28)$$

The jig has been tested up to 800 mc with very good frequency linearity.

Figure 25 shows the construction of the jig. A problem arose because of the difficulty of using the coaxial package in grounded



MEASUREMENT PROCEDURE

1. Choose measurement frequency f : 100 - 600 MC.
2. Insert dummy transistor with C-B short and E open.
RF meter indicates A db.
3. Insert transistor to be measured.
RF meter indicates B db.
4. $f_T = f 10^{\frac{B-A}{20}}$

FIGURE 24 EQUIVALENT CIRCUIT OF THE f_T JIG

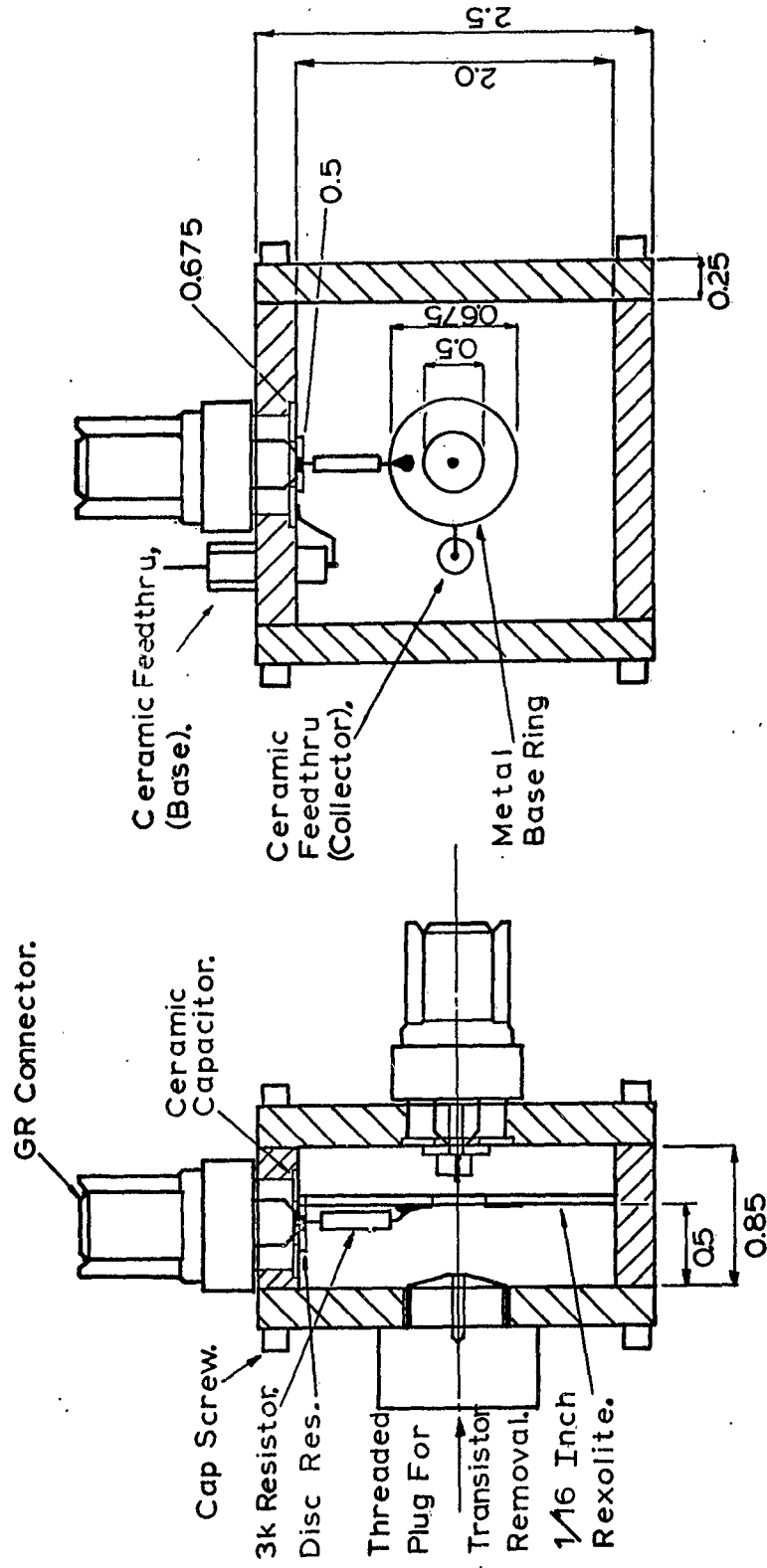


FIGURE 25 MECHANICAL DRAWING OF THE f_T JIG

emitter configuration. An RF current source to the base is difficult to establish. The problem has been solved by using an isolating membrane to hold the base and connect it with an RF resistor to the generator. Low bypass capacitance has been achieved with this design. The generator terminating resistor and the collector resistor are of a coaxial type soldered inside of a coaxial dc blocking capacitor. This arrangement gives an excellent impedance behavior up to 1000Mc. A photograph of the jig is shown in Figure 26.

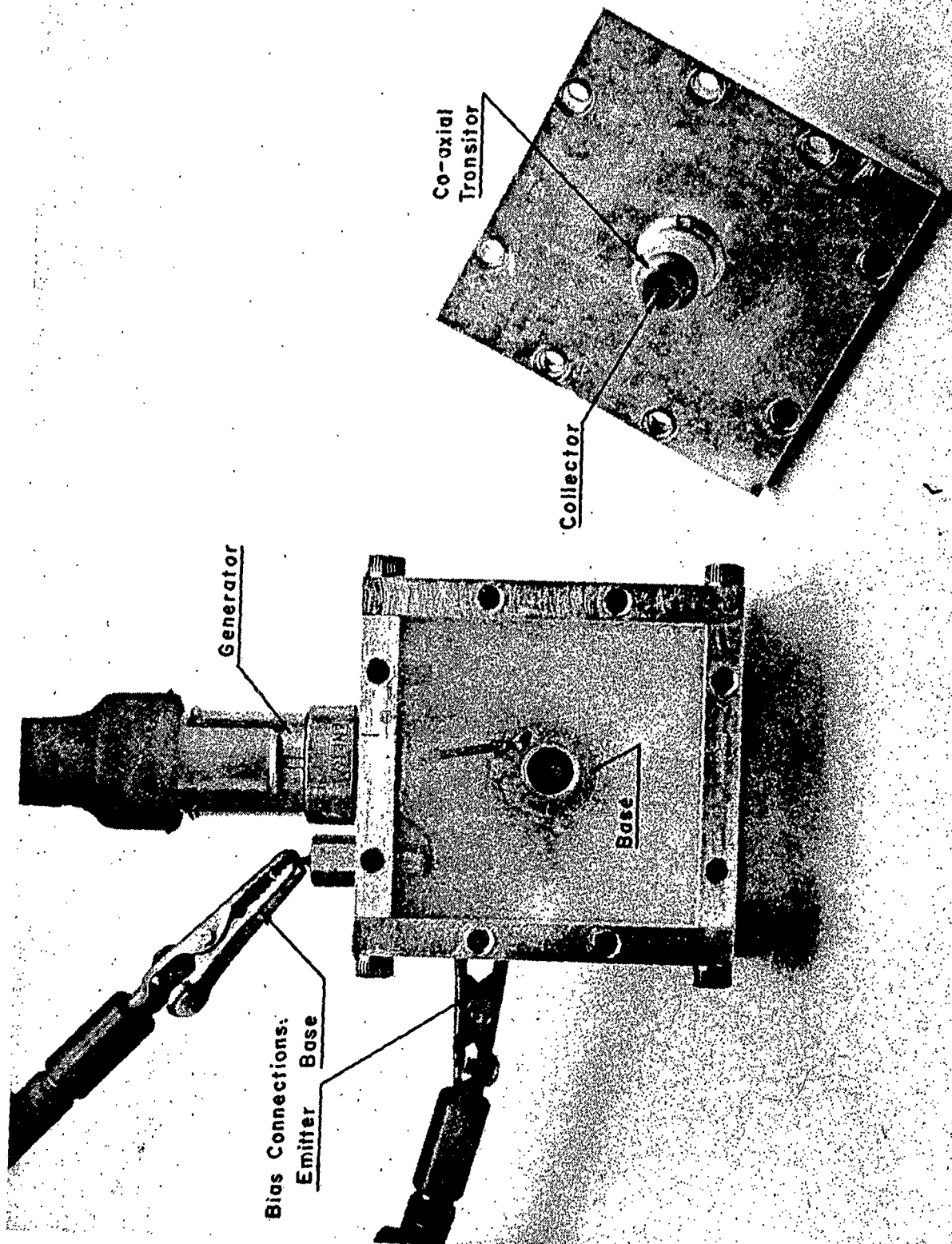


FIGURE 26 PHOTOGRAPH OF THE f_T JIG

6. NONLINEAR ELEMENTS IN TRANSISTORS FOR FREQUENCY CONVERSION

Mixing or converting of frequencies can be in general accomplished by a nonlinear, time varying element of resistive or reactive nature. The transistor in respect to resistive mixing has been treated in the literature⁽¹⁰⁾. For this type of mixing, detection takes place in the emitter diode and the conversion ability of the transistor is merely determined by the nonlinear resistance of the emitter which is described by

$$I_e = A \exp \left(\frac{q V_e}{kT} - 1 \right) \quad (29)$$

where

A	=	constant dependent on the semiconductor properties
q	=	electron charge
k	=	Boltzmann's constant
T	=	temperature in degree Kelvin
I_e	=	total current through the emitter junction
V_e	=	voltage across emitter junction

The local oscillator will vary the current flowing into the emitter. Experimentally it was found that for optimum operation it places a reverse voltage on the emitter junction only for a small fraction of its cycle. Since the emitter depletion layer capacitance is in shunt with the emitter differential resistance, r_e , it is apparent that the ultimate signal frequency limitation on the conversion ability of a transistor in this type of mixing operation is set by the reverse emitter shunting capacitance.

In the course of our investigation, we have established a reactive mixing operation of drift transistors. This occurs in the forward bias condition of the emitter diode, where the depletion layer capacitance of the emitter diode is not the limiting factor, but rather the essential parameter. A time variable reactance will be exhibited by the input impedance of the transistor which, under "current-tuning" can be used to produce a parametric mixing. The dominant nonlinear reactive component available for conversion can be derived from equation (21) under the assumption that the resistive term contained in the real part as a function of emitter current is negligible, e.g. small oscillator power and, therefore, small voltage swings. At a moderate forward bias of the emitter to base junction, the differential resistance varies little at the small current increments. From figure (19) it is obvious, that for small current variations around certain forward bias conditions, large reactance changes can be produced. The nonlinear reactance can be approximated by

$$X_{\text{reactive}} \approx -j \left\{ b(I_e) r_s' + \frac{r_e^2(I_e) \omega C_e}{1 + (\omega r_e(I_e) C_e)^2} \right\} \quad (30)$$

A theoretical investigation of equation (30) in function of emitter current, I_e , indeed reveals the general shape of the measurement in figure (19). The current dependent terms at a fixed frequency, ω , are implicitly in the imaginary part of the current amplification factor, $b(I_e)$ and in a higher order power in the second term from the variation of $r_e(I_e)$.

The a.c. power, e.g. oscillation, necessary for the conversion process can be either supplied from an external source, which leaves freedom

for biasing the transistor at certain d.c. operating points, or a self oscillation arrangement can be employed. In the self oscillating circuits one has the choice of a feedback or transit-time mode oscillator. The former type has the advantage of flexibility and one is able to vary the frequency over a wide range, whereas the latter type is restricted to certain frequency ranges, determined by the particular transistor used (9) (11). A self oscillating mixer in the transit-time mode has been described and analyzed in the second Interim Engineering Report. Employing a Hughes GXG4 transistor, a frequency range from 300 - 500 Mc can be covered. The circuit has been integrated with the Hughes coaxial transistor and the frequency range was extended into the microwave region. Electrical performances are reported in a previous section of the Third Interim Engineering Report. The unique arrangement of this type of oscillator without feedback, accomplishes a parametric interaction at ω_0 and $\omega_0/2$ by its tuning arrangements in the separated loops of the collector and emitter circuit.

Mixing in feedback oscillators and employing the nonlinear reactance type mixing of the input impedance have been reported in the literature, (12) (13).

Although no conclusive evidence has been obtained experimentally in our laboratory, another nonlinear reactance is present in drift transistors at high current densities. The nonlinearity should be capable of performing mixing. It arises from a reduction or swamping out of the drift field in the base region of a drift transistor under prevailing critical current densities. Appendix I gives the theoretical derivation and experimental results. For certain types and geometries of drift transistors, the critical current can be calculated and measured, e.g. a

plot of $1/f_T$ vs. $1/I_e$ departs from linearity. At the critical current densities a nonlinear change in the reduced base charge capacitance will occur. Measurements on a mixer at rather high currents have been reported in the literature⁽¹⁴⁾ and can be interpreted according to the theory. Additional measurements on the particular transistors used would be required to substantiate the statement.

APPENDIX I

Non-Linear Base-Charge Capacitance in Drift Transistors

The base-charge capacitance, C_b , was defined by Das and Boothroyd⁽³⁾ and can be written in terms of the total excess charge Q stored in the base region as

$$C_b = \frac{dQ}{dV_{eb}} = \left(\frac{dQ}{dI_e} \right) \left(\frac{dI_e}{dV_{eb}} \right) \quad (31)$$

In this definition, Q refers to the charge for the mean bias current, I_e and V_{eb} is the emitter-base voltage of the internal transistor.

The total charge in the transistor base is

$$Q = A_e q p_o W \int_0^1 p/p_o dX \quad (32)$$

where

$$p_o = \frac{I_e W}{q D_p A_e}$$

so that

$$Q = \frac{W I_e}{D_p} u \quad (33)$$

The variable u is current dependent and given by

$$u = \int_0^1 p/p_o dX \quad (34)$$

It is the area under the normalized charge distribution curve. The function p/p_0 vs. $X = x/W$ with normalized density. $\rho = I_e/I_0$ as parameter has been given in the literature for exponential impurity gradings^{(3) (15)} See also Figure 27. Differentiating (33) after the emitter current yields

$$\frac{dQ}{dI_e} = \frac{W^2}{D_p} \left[u + I_e \frac{du}{dI_e} \right] \quad (35)$$

and insertion into (31) results in

$$C_b = \frac{W^2}{D_p} \left[u + I_e \frac{du}{dI_e} \right] \frac{dI_e}{dV_{eb}} \quad (36)$$

Knowing u , $\frac{du}{dI_e}$ and $\frac{dI_e}{dV_{eb}} = g_e = \frac{1}{r_e}$

for a particular impurity distribution in the base of a transistor one can determine the capacitance behavior of any injection level, e.g. in function of the emitter current.

CASE A: Low Level Injection.

Under low-level injection, the charge distribution is independent of I_e , since $p_0 \ll N_E$ and, therefore,

$$\frac{du}{dI_e} = 0, \quad \frac{dI_e}{dV_{eb}} = g_e \approx \frac{q I_e}{kT} \quad (37)$$

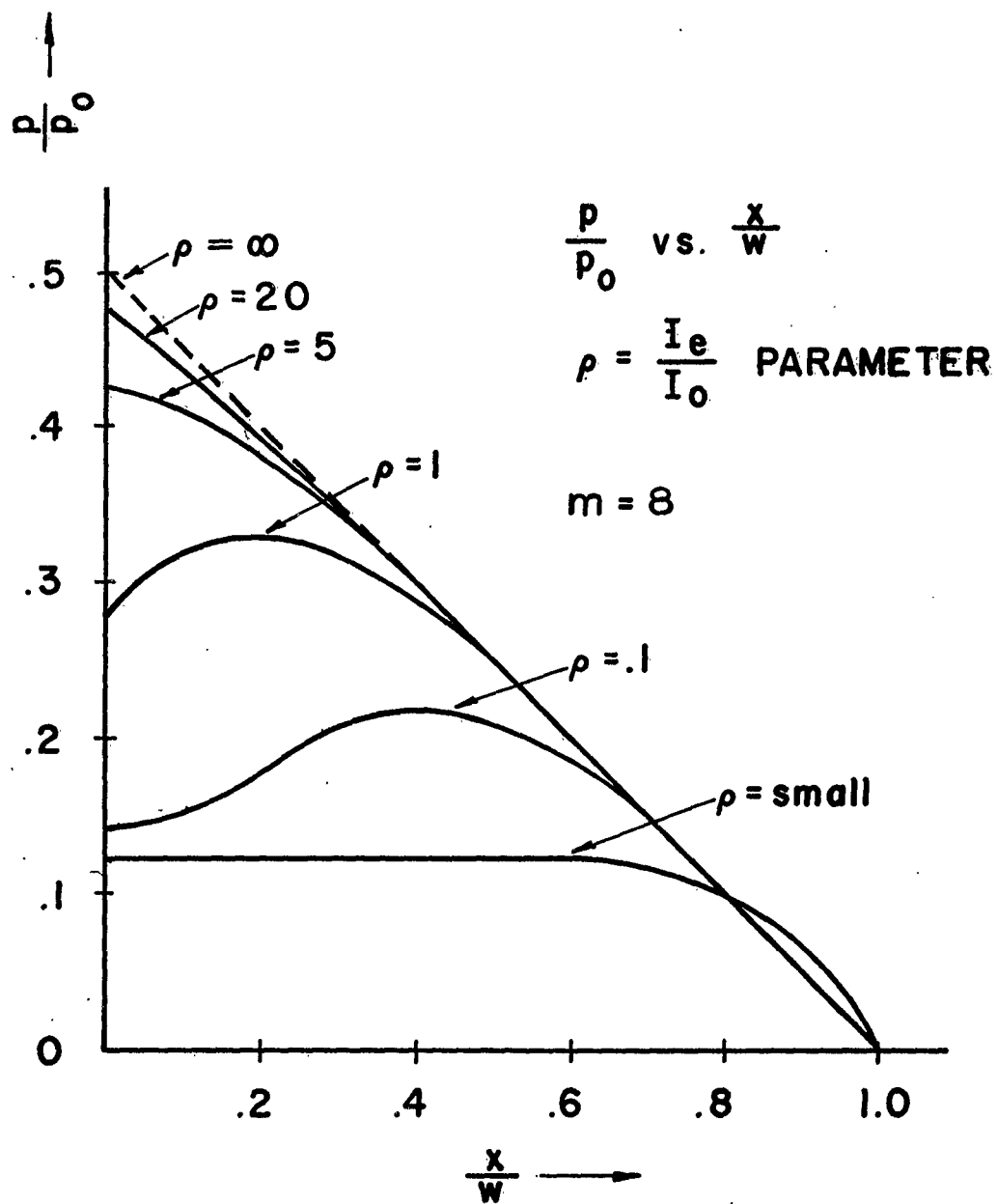


FIGURE 27

NORMALIZED EXCESS BASE CHARGE DISTRIBUTION, P/P_0 ,
 VS. NORMALIZED DISTANCE, x/x_0 , WITH REDUCED CURRENT
 DENSITY AS PARAMETER FOR A DRIFT TRANSISTOR.

Equation (36) now reads

$$C_b = \frac{W^2 I_e q}{D_p K T} u \quad (38)$$

For an exponential impurity gradient, u has been evaluated analytically^{(7), (18)} and is given by

$$u = \frac{m - 1 + e^{-m}}{m^2} \quad (39)$$

The drift field factor $m = \lg \left(\frac{N_E}{N_C} \right) = \frac{W}{x_o}$ and the impurity profile is

$$N(x) = N_E \exp \left(-\frac{x}{x_o} \right) \quad (x_o \text{ is the characteristic length, where}$$

$$\frac{N(x_o)}{N_E} = \frac{1}{e} \text{ .) For the exponential grading the field is constant in the}$$

base and given by

$$E_b = \frac{kT}{q x_o} \quad (40)$$

so that the built-in voltage is expressed as

$$V_b = \frac{kT}{q} \ln \left(\frac{N_E}{N_C} \right) \quad (41)$$

The maximum built-in voltage for germanium is about $8 kT/q$, e.g. $m = 8$ ⁽¹⁷⁾. The variable u for the low level injection is, therefore, numerically in accordance with equation (39):

m	0	1	2	3	4	5	6	7	8
μ	0.50	0.37	0.28	0.23	0.19	0.16	0.14	0.12	0.11

Diffusion Transistor ← → Drift Transistor

From the u function, one concludes that the higher the drift field, the lower will be the base charge capacitance, C_b . A plot of normalized capacitance versus normalized current is given in Figure 28. Thus under low level injection a linear relation of the base-charge (diffusion) capacitance, C_b , to the emitter current, I_e , can be expected for both types of transistors, i.e., the diffusion transistor with $m = 0$, and $u = 1/2$ and the drift transistor with $m > 0$. High level injection, however, will cause a deviation from this linear relation in both types of transistors and will introduce a non-linear behavior in specific current ranges. In most high frequency transistors this non-linear transition region is within moderate current levels. This is obvious from Figure 27 where in current ranges from approximately $0.1 \lesssim f \lesssim 1$ a diffusion current component exists towards the emitter.

CASE B. High Level Injection

a) Diffusion Transistor

In a diffusion transistor, where the minority carrier transport through the base region is merely caused by the diffusion gradient, the uniform doping results in $m = 0$ and one obtains $u = 1/2$. The base-charge capacitance or diffusion capacitance is then equal to

$$C_b = \frac{q I_e W^2}{2 D_p K T} \quad (42)$$

This relation will hold as long as the injected minority carrier charge density is small compared to the number of ionized impurity atoms in the base region. At high current densities, however, the injected minority carriers present, in combination with the majority carriers in the base region, which are necessary to meet the space-charge

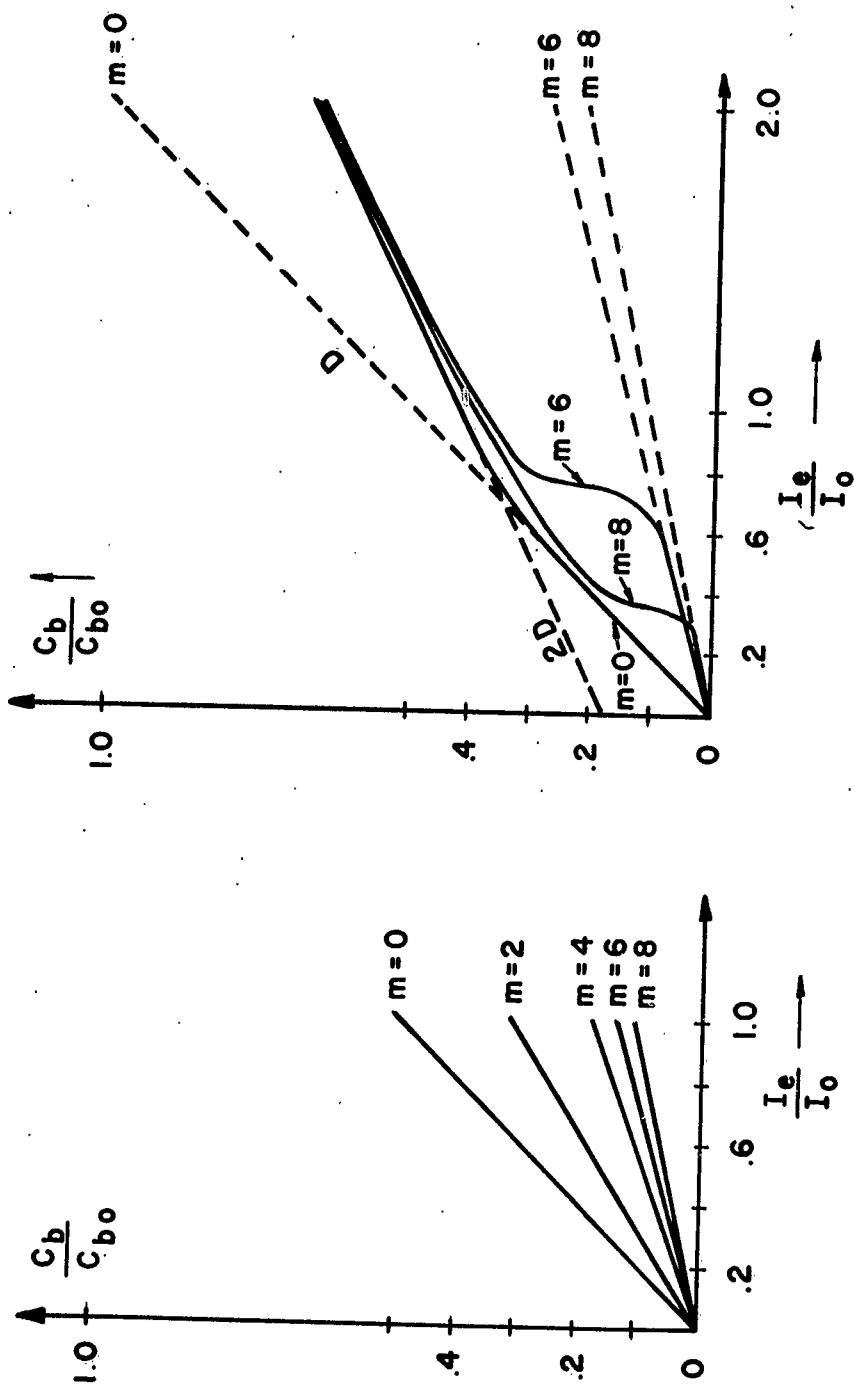


FIGURE 28

NORMALIZED BASE CHARGE CAPACITANCE, C_b/C_{b0} , VS.
 NORMALIZED EMITTER CURRENT, I_e/I_0 , FOR DIFFUSION
 AND DRIFT TRANSISTOR IN THE LOW LEVEL AND HIGH
 LEVEL INJECTION STATE.

neutrality condition, set up an electric field. This in turn tends to reduce the transit-time, or causes a virtual increase in the diffusion constant of minority carriers⁽¹⁸⁾. In a PNP transistor, the hole diffusion constant is effectively then

$$D_{p \text{ eff}} = D_p \left[1 + \frac{p}{p + N_D} \right] \xrightarrow{\text{for } p \gg N_D} 2 D_p \quad (43)$$

One would expect, therefore, a 2 : 1 slope change in the relation of C_b vs. I_e when going from low to high level injection. This has been evaluated theoretically for $m = 0$ and is given in a normalized graph in Figure 28. The experimental verification has been obtained with a micro-alloy transistor (uniform base) of Philco type 2N393 and the measurements are plotted in Figure 29A.

It shows the transition and non-linear region around a bias current of 3.5 mA. The emitter depletion layer capacitance, C_e , is of course additive and is in parallel with C_b .

b) Drift Transistor

The transition from the low level to the high level state in drift transistors can be portrayed by using equation (36). By integration of equation (34) by means of Figure 27, one would obtain u and $du/d I_e$. In addition, the change of $d I_e / d V_{eb}$ with injection level has to be taken into consideration. Combining both current-dependent variables, the base-charge capacitance, C_b , as a function of normalized current can be plotted. From data in reference⁽³⁾ and ⁽¹⁵⁾ the curves for $m = 6$ and $m = 8$ have been obtained (Figure 28). For $m = 6$ in a normalized current

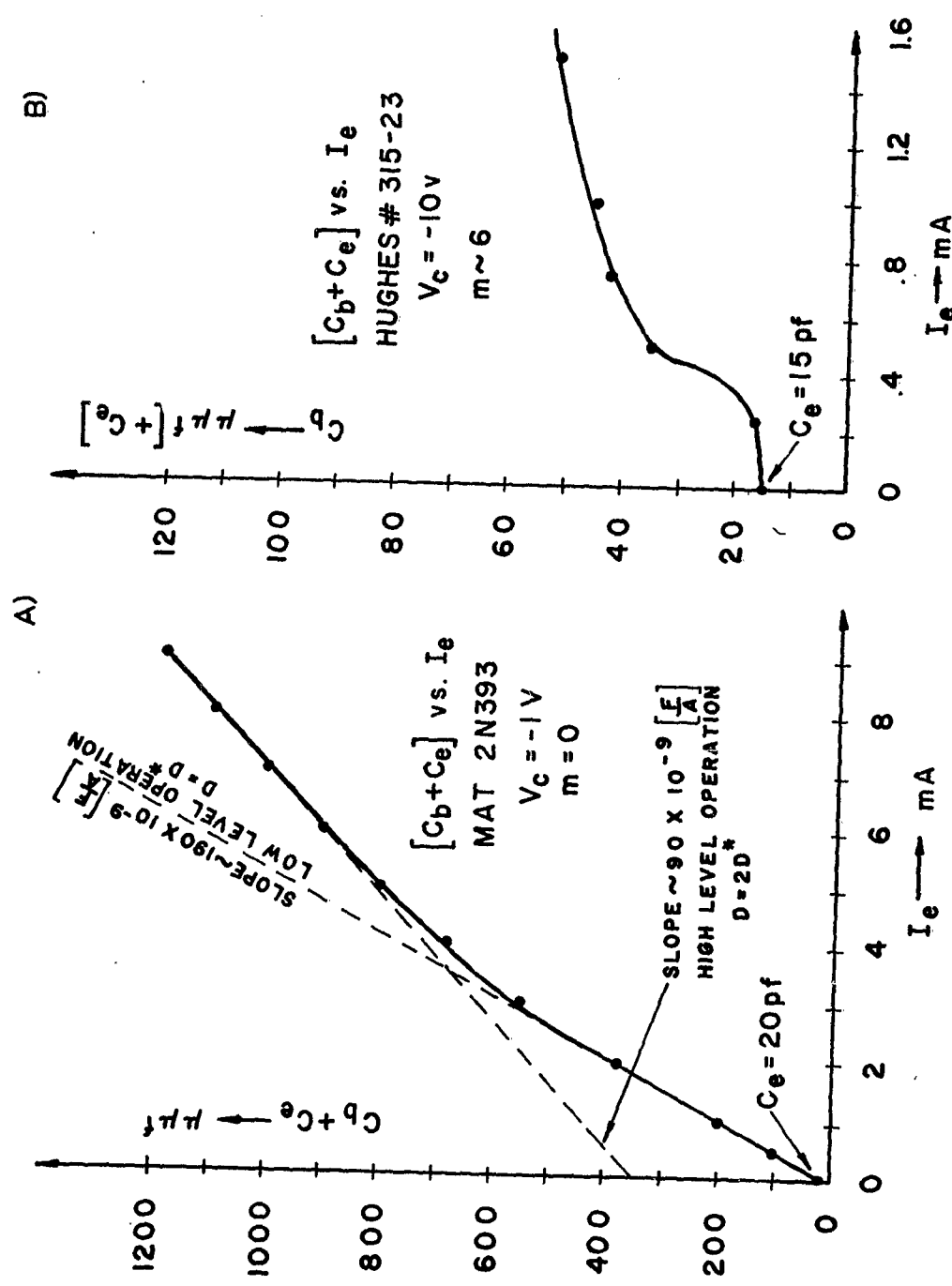


FIGURE 29 MEASUREMENTS OF BASE-CHARGE (=DIFFUSION) CAPACITANCE AS A FUNCTION OF EMITTER CURRENT
 A) FOR A DIFFUSION TRANSISTOR
 B) FOR A DRIFT TRANSISTOR

region of .7 - .8, a sharp non-linear transition will be present. Figure 29B verifies the theoretical curve of Figure 28 with an actual measurement on a Hughes experimental epitaxial mesa transistor No. 315-23 with $6 \leq m \leq 8$. According to reference ⁽³⁾ the normalized current density is

$$\rho = \frac{I_e W}{q D_p A_e N_E} \quad (44)$$

For transistor No. 315-23, the emitter area $A_e = 8 \times 10^{-5} \text{ cm}^2$, the base width $W = 1.5 \times 10^{-4} \text{ cm}$, and the doping at the emitter junction $N_E = 1 \times 10^{17} \text{ atoms/cm}^3$, so that with $D_p = 44 \text{ cm}^2/\text{sec}$ and $q = 1.6 \times 10^{-19} \text{ coulomb}$

$$\rho = 106 \times I_e \text{ (mA)} \quad (45)$$

Although a qualitative agreement of measurement with theory has been obtained, the quantitative normalization (equations 44 and 45) disagrees by one order of magnitude. This discrepancy can be resolved if we take into consideration:

- a) The diffusion constant is reduced for heavily doped materials, so that a constant D_p should not be used in evaluating equation (44).
- b) The effective emitter area is reduced at high current densities, because a transverse base current will bias the emitter periphery more forward than the inner section.

- c) The deviation from a one dimensional geometry to a two dimensional one under (b) may also be supported by non-uniform impurity distribution around and across the emitter area.

A better estimate, however, for the critical current in drift transistors at which non-linearities can be expected can be obtained from the following consideration (for a PNP transistor): To maintain space - charge neutrality in the base region, one must have

$$p + N_{D(x)} = p + N_E \exp\left(-\frac{x}{x_0}\right) = n \quad (46)$$

Differentiating (46) in respect to x yields

$$\frac{dp}{dx} - \frac{N_E}{x_0} \exp\left(-\frac{x}{x_0}\right) = \frac{dn}{dx} \quad (47)$$

The total hole current is

$$I_p = -q D_p \frac{dp}{dx} + \mu p q E_b \quad (48)$$

Assuming that in the transition region all the drift current is reduced to diffusion current, and that the critical current occurs at a condition where

$$\frac{dp}{dx} = \frac{d\left[N_{D(x)}\right]}{dx} = -\frac{N_E}{x_0} \exp\left(-\frac{x}{x_0}\right) \text{ then one obtains from}$$

(47) and (48)

$$I_p \approx I_{e \text{ critical}} = \frac{q D_p N_E}{x_o} \exp \left(- \frac{x}{x_o} \right) \quad (49)$$

which can be transformed by aid of equation (40) and (41) to

$$I_{e \text{ critical}} \approx \left[\frac{q D_p A_e N_E}{W} \right] \left[\frac{m}{\exp m} \right] \quad (50)$$

From equation (50) results the following critical current with values given in conjunction with equation (44) and assuming $m = 8$:

$$I_{e \text{ critical}} \approx 1.5 \text{ mA}$$

PART II

FINAL ENGINEERING REPORT ON
HIGH FREQUENCY TRANSISTOR STUDY

FOR

HUGHES PRODUCTS SEMICONDUCTOR DIVISION
NEWPORT BEACH, CALIFORNIA

BY

Mahmud Zareh-Farzian, Senior Engineer
Advanced Development Laboratory
Lenkurt Electric Co. Inc.,
San Carlos, California.

February 20, 1962.

SUMMARY

While conducting experiments on various circuits, V. W. Vodicka, the former manager of Lenkurt's Advanced Development Laboratory, discovered a new mode of transistor operation, referred to as the transit time mode, which extended the operating range of transistors significantly. At the same time, work was being conducted in the Hughes Semiconductor Division laboratories on transistors which were believed to have properties conducive to operation in the newly discovered transit time mode of operation. The Lenkurt Advanced Development Laboratory was, therefore, authorized by the Hughes Semiconductor Division to proceed with the design and construction of transistorized amplifier, oscillator, and mixer circuits which could operate with high stable gain and low noise at microwave frequencies.

When high frequency amplifier, oscillator, and mixer circuits containing various Philco transistors were constructed and tested, oscillation, amplification, and some mixing at microwave frequencies were obtained but no gain within these circuits could be demonstrated. When Hughes transistors were employed in these same circuits, however, frequency conversion at microwave frequencies was obtained with gains as high as 23 db in one mixer circuit.

From these experiments, it was concluded that by improving certain circuit components, particularly the coaxial transistor package, even greater gains could be obtained at microwave frequencies eventually extending transistor operation in the newly discovered transit time mode into frequency ranges as high as 4 to 10 Kmc.

TABLE OF CONTENTS

						<u>Page</u>
1.	INTRODUCTION	40
2.	DISCOVERIES AND DEVELOPMENT PRECEDING THIS INVESTIGATION	40
3.	DEVELOPMENT OF A CONVERTER CIRCUIT FOR HIGH FREQUENCY OPERATION	42
4.	RESULTS OF TESTS UPON A PROTOTYPE OF V. W. VODICKA'S CIRCUIT	44
	a) Results Obtained by Varying the Voltage of the Input Signal	
	b) Results Obtained by Varying the Output Load	
	c) Variation of Output Frequency with Varying Magnitude of Input Signals	
5.	DESIGN APPROACH AND PROBLEMS ENCOUNTERED IN THE DEVELOPMENT OF A HIGH FREQUENCY CONVERTER CIRCUIT	46
6.	IMPROVEMENT OF COAXIAL CAVITIES	49
	a) Results of Studies Conducted Upon a Circuit Proposed by R. Zuleeg	
	b) Results of Studies Conducted Upon a Circuit Proposed by J. F. Gibbons	
7.	RESULTS OF STUDIES UPON AMPLIFIER AND CONVERTER CIRCUITS CONTAINING HUGHES' TRANSISTORS	53
	a) Results of Tests Upon Amplifier Circuits	
	b) Results of Tests Upon Converter Circuits	
	c) Results of Tests Upon a Converter Circuit containing an HC-2 Transistor	
	d) Results of Tests Upon a Converter Circuit containing an HC-7 Transistor	
8.	CONCLUSIONS	56

LIST OF ILLUSTRATIONS

- | | |
|-----------|---|
| Figure 1 | Basic Grounded-Base Oscillator Showing Possible Feedback Path for High Frequency Oscillation. |
| Figure 2 | One Variation of the Vodicka Converter which has Provided Useful Gain at Frequencies Several Times the Transistor Alpha Cutoff Frequency. |
| Figure 3 | Circuit Arrangement. |
| Figure 4 | Input Voltage vs. Voltage Gain of the Converter and I-F Output Voltage. |
| Figure 5 | Output Frequency vs Magnitude of Input Signal. |
| Figure 6 | Coaxial Cavity I. |
| Figure 7 | Coaxial Cavity II. |
| Figure 8 | Amplifier Circuit. |
| Figure 9 | Output and Input Voltage Readings of the Amplifier Circuit. |
| Figure 10 | Amplification of the Transistor. |
| Figure 11 | Loss Factor of the Amplifier Circuit Excluding the Single Stub Tuner. |
| Figure 12 | Mechanical Drawing of Coaxial Cavity I. |
| Figure 13 | Insertion Losses of Coaxial Cavity I. |
| Figure 14 | Insertion Losses of Coaxial Cavity II. |
| Figure 15 | UHF Oscillator Circuit. |
| Figure 16 | Oscillator Circuit Designed by R. Zuleeg. |
| Figure 17 | UHF Frequency Converter. |
| Figure 18 | Voltage Gain of Frequency Converter vs. Input Voltage. |

High Frequency Transistor Study
Final Engineering Report

1. INTRODUCTION

This report describes the results of an investigation conducted on the properties of presently available transistors in circuits designed for operation in the microwave frequency range. In this study, the use of transistors in mixer and converter circuits was emphasized in order to determine the feasibility of developing an amplifier, mixer or harmonic generator operating with high stable gain and low noise in the 4 to 10 Kmc frequency range.

This report describes primarily the design of the circuits in which the transistors were used. The results obtained with these circuits were correlated with theoretical studies, and the interaction of devices within the complete circuits, as well as the interaction with one another, were calculated. Transistor parameters and the design and construction of the transistors employed are not described in this report.

The information presented in this report is based upon 10 months of research conducted in the Advanced Development Laboratory at Lenkurt Electric Co., Inc. This research was authorized by Hughes Aircraft, P.O. 1-877651-M11 for the Hughes Products Semiconductor Division, Newport Beach, California.

2. DISCOVERIES AND DEVELOPMENTS PRECEDING THIS INVESTIGATION

While working on various experimental microwave circuits, V. W. Vodicka the former director of Lenkurt's Advanced Development Laboratory,

discovered a new mode of transistor operation. On the basis of this discovery, he then designed and built a converter circuit which extended the range of transistor operation to frequencies much higher than their normal range.

At approximately the same time that V. W. Vodicka was working on the circuits in which the new mode of transistor operation was discovered, work was being conducted in the Hughes Semiconductor Division Laboratories on microwave transistors to be used in UHF circuits.

Since ordinary microalloy diffused transistors (MADT) had been used in the circuits invented by V. W. Vodicka, it was felt that the anticipated parameters of the Hughes' experimental transistors would prove even more suitable in high gain converter circuits designed for operation at microwave frequencies.

In view of these developments, Hughes Products authorized the Lenkurt Advanced Development Laboratory to conduct a study of transistor behavior at ultra-high frequencies. In particular, a study of converter circuits containing Hughes' experimental transistors or other comparable transistors was requested in order to determine the feasibility of developing a mixer circuit which could convert rf inputs ranging from 4 to 10 Kmc into an i-f output of 1 to 2 Mc.

Such a converter circuit would have numerous applications in television, radar, and other microwave receivers since the use of transistors, rather than expensive special purpose electron tubes, would make cheaper and more reliable microwave equipment readily available. It should also be noted that the primary advantage of this circuit, in contrast to conventional mixer circuits, is its high sensitivity. This sensitivity eliminates the need for a preamplifier in a receiving system thereby eliminating the major source of noise in such a system.

3. DEVELOPMENT OF A CONVERTER CIRCUIT FOR HIGH FREQUENCY OPERATION

In conventional UHF detector circuits using diode mixers, no gain is possible, signal loss always occurs, and noise is inherently high. In these circuits, a separate local oscillator is required, usually a special high-performance electron tube (such as a klystron or TWT) and even in the best previous transistorized mixer-oscillator circuits, little or no gain at low microwave frequencies could be obtained.

For example, in a basic grounded base transistor oscillator such as the one shown in Figure 1, oscillation may be difficult to obtain at high frequencies because of insufficient feedback from the collector to the emitter. The addition of a capacitor will increase this feedback but hampers the use of the circuit as a mixer because of the regeneration which may occur at the demodulated frequency.

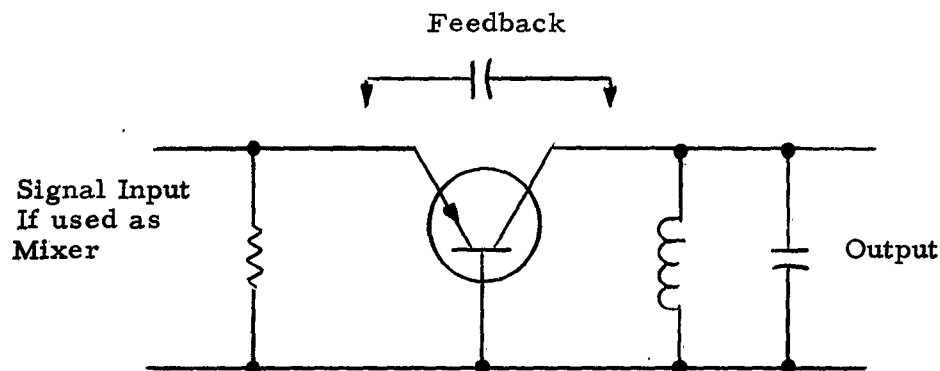


Figure 1. Basic Grounded-Base Oscillator Showing Possible Feedback Path for High Frequency Oscillation.

If the feedback capacitor is split and a high-Q tuned element, such as a cavity resonator, is substituted for the tank circuit connected to the

capacitors, as illustrated in Figure 2, it is possible to feed back harmonics of the input signal, harmonics of the frequency produced by internal oscillation, and a portion of the demodulated output signal, but little or none of the original input signal itself. Thus, the input applied to the transistor emitter may consist of the fundamental input signal and the second or higher harmonic of this signal. This harmonic signal then acts as a parametric "pump" frequency for the input signal and increases the amplification of the circuit.

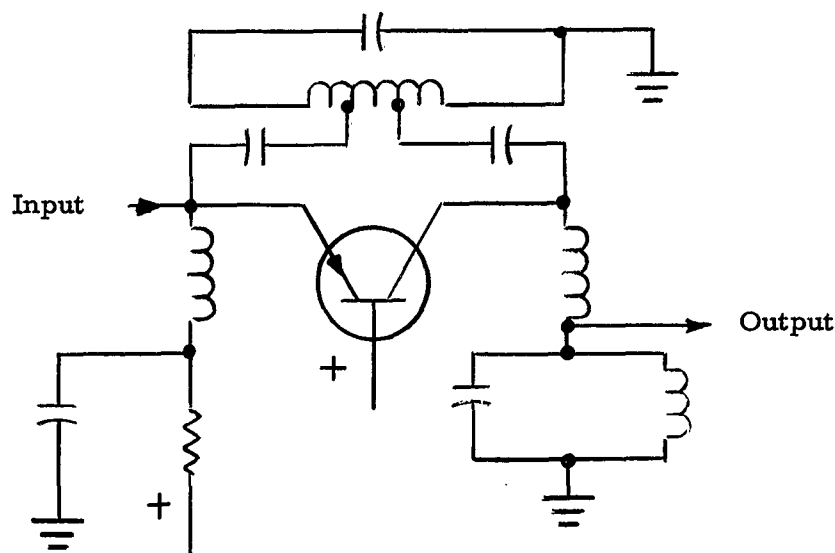


Figure 2. One Variation of the Vodicka Converter Which Has Provided Useful Gain at Frequencies Several Times the Transistor Alpha Cutoff Frequency.

If the input circuit is tuned to provide a high impedance to the demodulated signal, this demodulated frequency is amplified by the transistor. Efficiency is increased by tuning the collector to increase harmonic feedback.

Normally, a circuit of this type should not work because of a transistor's inability to produce harmonics at frequencies beyond its rated alpha cut-off frequency. However, because of the recently evolved transit time mode of operation, the frequency capability of a transistor may be extended significantly. In order to make use of this effect, the voltage and phase relations at the three terminals of a transistor must be correct and certain conditions of impedance and bias must be met. By modifying these variables, a transistor can be made to operate as a high gain, negative impedance converter without inherent limits upon the frequency at which conversion can be obtained.

Under laboratory conditions, for example, one converter configuration containing a parametric diode in addition to a single transistor obtained 96 db gain at 400 Mc with a bandwidth of 75 Kc. At 2 Mc bandwidth, 86 db gain was achieved and the signal-to-noise ratio for an input signal of 0.2 microvolt was better than 6 db.

4. RESULTS OF TESTS UPON A PROTOTYPE OF V. W. VODICKA'S CIRCUIT

To demonstrate a transistor's transit time mode of operation, a prototype of the original converter circuit designed by V. W. Vodicka was constructed during one phase of this investigation. This prototype circuit and the results of experiments conducted on it were then forwarded to the Electronic Parts and Warfare Branch of the Bureau of Ships in Washington, D. C. Since these results demonstrated the transistor properties which provided a basis for the studies described in this report, these results are discussed in detail in the following paragraphs.

a) Results Obtained by Varying the Voltage of the Input Signal

The circuits illustrated in Figure 3 were set up. After the emitter current had been adjusted to 1.5 milliamperes, V. W. Vodicka's

circuit operated as a mixer when the frequency of the injected signal was 352 Mc. While operating at these values of emitter current and input frequency, two maxima were observed around 352 Mc. These maxima were very close together and one was larger than the other.

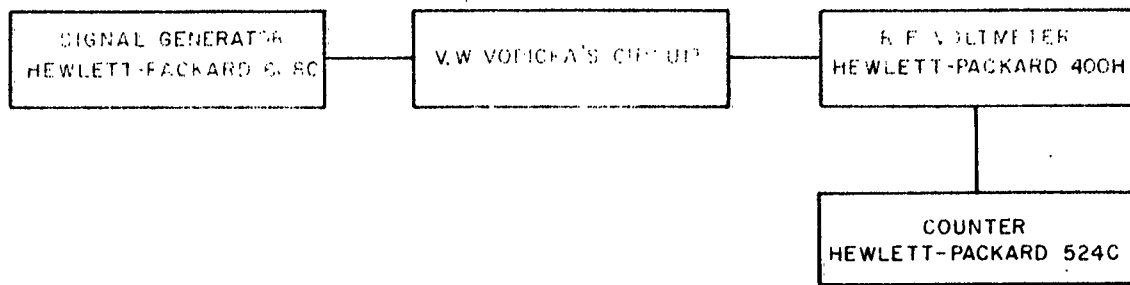
The magnitude of the input signal was then varied from 1 micro-volt to 500 millivolts while maintaining the input signal at a constant frequency of 352 Mc. As the voltage of the input signal was varied, the voltage gain of the output was measured; first, across a 10-megohm resistor at the input to the rf meter and then, across a 600-ohm resistor connected in parallel with the 10-megohm resistor. As shown in Figure 4, the drop in voltage gain indicated by these measurements, was approximately 35db. If the i-f resonant circuit had a Q equal to infinity, however, and the input impedance of the rf meter consisted of a pure resistance, the drop in voltage gain would have been:

$$10 \log \frac{10^7}{600} = 42 \text{ db}$$

b) Results Obtained by Varying the Output Load

When the output of the mixer circuit was loaded with a variable resistor, two facts were noted as the load was decreased (1) the power of the minimum detectable signal (MDS) increased and (2) the overload threshold of the mixer circuit decreased. This prototype of V. W. Vodicka's original circuit, therefore, operated as a "voltage" rather than a "power" circuit. In accordance with this characteristic, the maximum voltage gain of such a circuit may be obtained by employing a high impedance circuit at the input of the following stage.

A. Test Set Up



B. V. W. Vodicka's Circuit

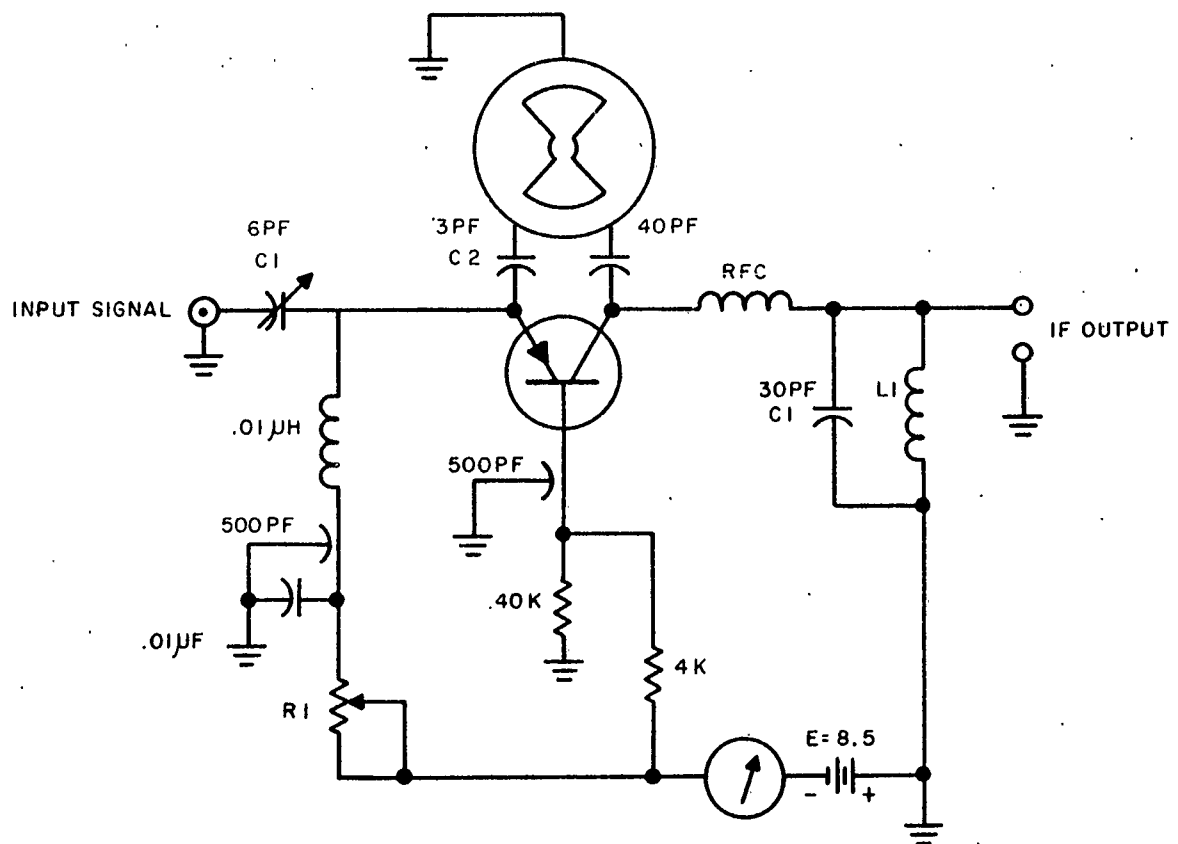


Figure 3. Circuit Arrangement

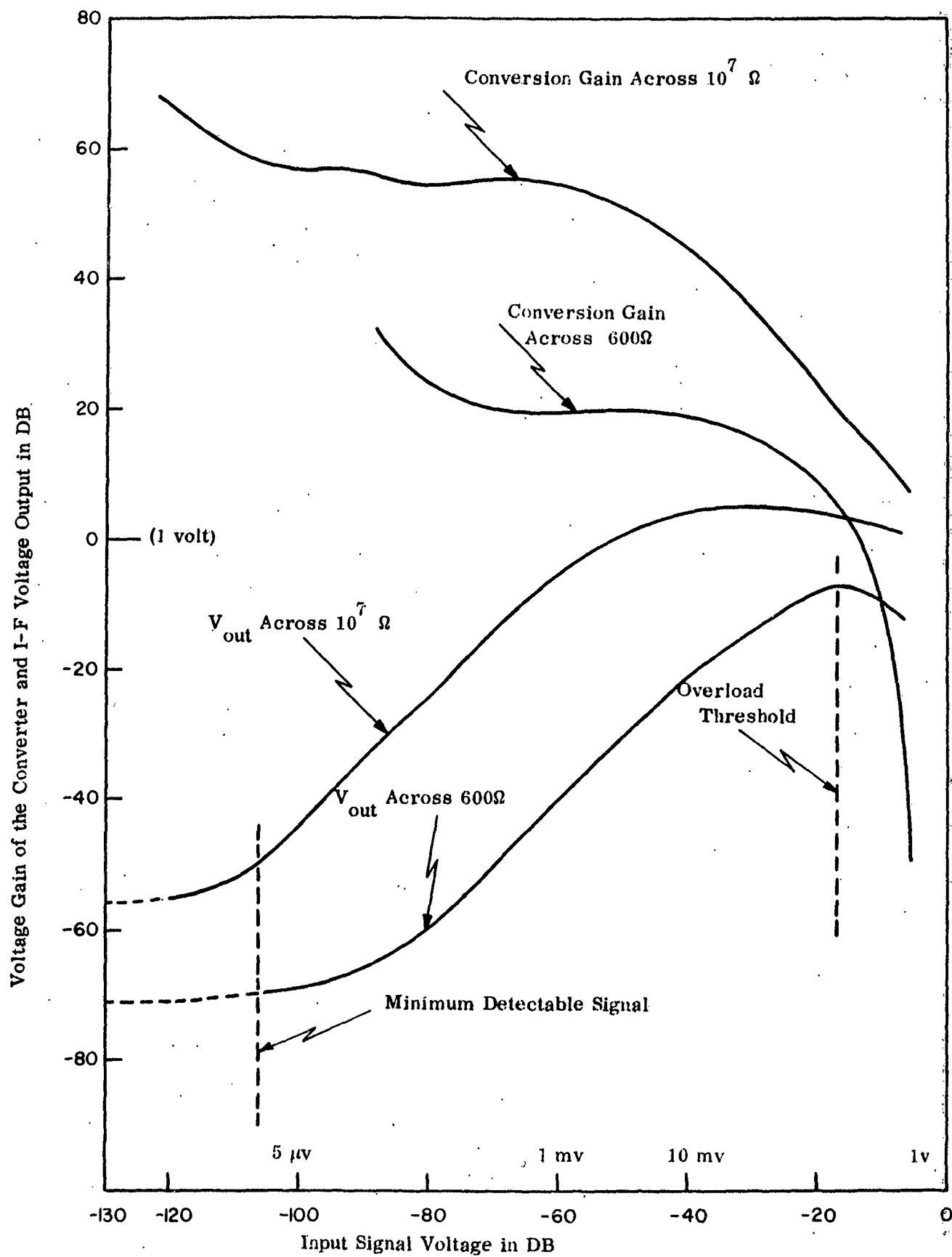


Figure 4. Input Voltage vs Voltage Gain of the Converter and I-F Output Voltage

c) Variation of Output Frequency with Varying Magnitude of Input Signals

As illustrated in Figure 5, the MDS voltage was 0.8 microvolts with a 10-megohm load. It was also noted that the frequency of the i-f output varied with the magnitude of the rf input signal. This probably resulted from the dependence of the capacitive elements of the resonant circuit upon the magnitude of the input signal. When the magnitude of the rf input signal was varied, it was also noted that a variation of the output frequency was produced, presumably by internal circuit oscillation at frequencies higher than that of the injected signal. In order to have this mixer circuit operate properly, however, the bandwidth of the rf input had to be very narrow, preferably less than 1 Mc.

5. DESIGN APPROACH AND PROBLEMS ENCOUNTERED IN THE DEVELOPMENT OF A HIGH FREQUENCY CONVERTER CIRCUIT

After an initial review of transistor behavior at high frequencies, particularly the behavior of drift transistors suitable for operation at microwave frequencies, modification of V. W. Vodicka's converter circuit began, to make it more suitable for operation in the microwave frequency range. Originally, this circuit had contained a butterfly resonator as the tuning element. Since this limited the effective range of operation to frequencies below 1 Kmc, the design of coaxial cavity resonators was undertaken to extend the useful range of operation of this circuit.

Two coaxial cavity resonators, illustrated in Figures 6 and 7, were designed and constructed; Coaxial Cavity I for operation in the 1 to 2 Kmc frequency range and Coaxial Cavity II for operation in the 2 to 4 Kmc frequency range. At first the work on this project was hampered because the priorities involved in purchasing military items delayed the delivery of the necessary coaxial transistors. During this time, as a matter of

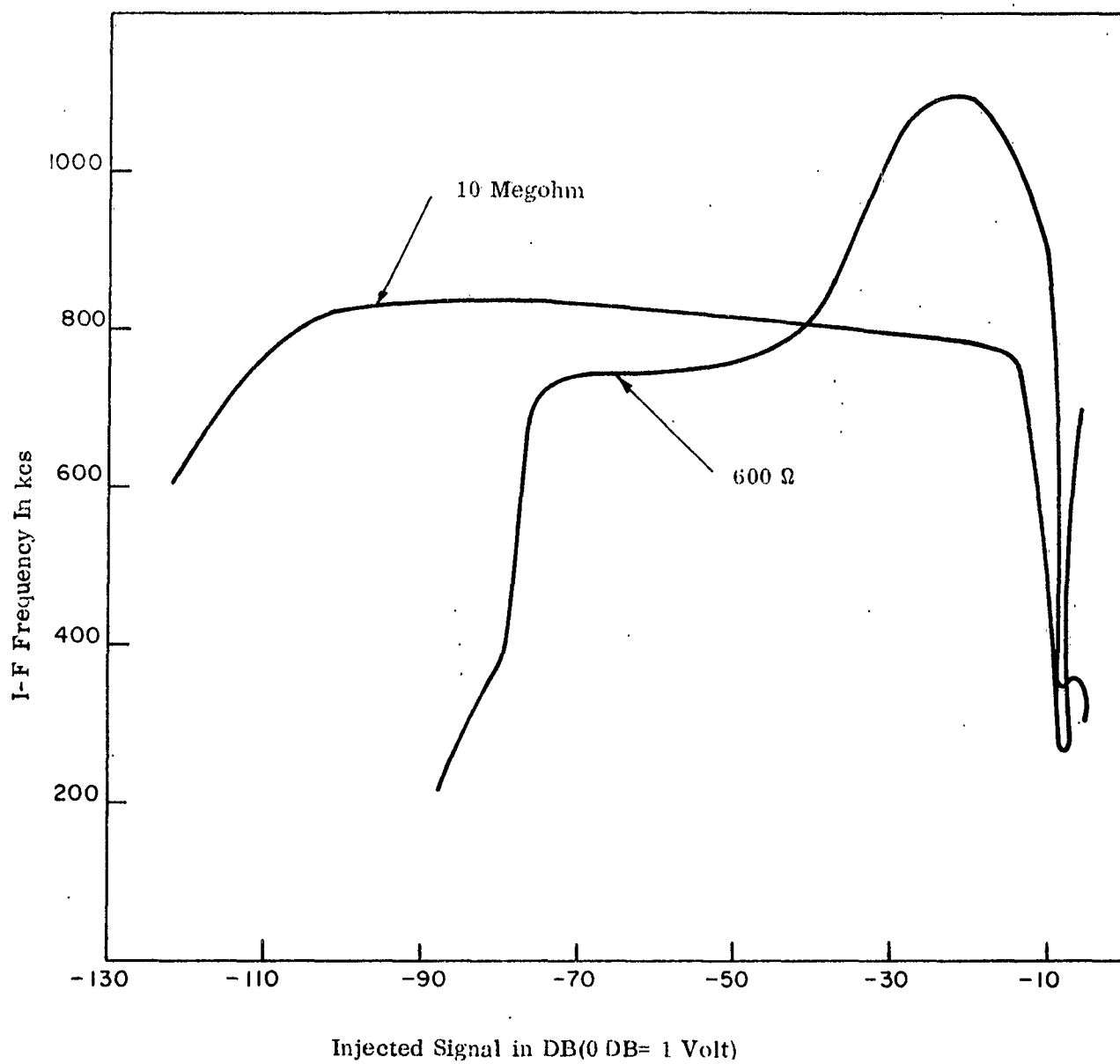


Figure 5. Output Frequency vs Magnitude of Input Signal

curiosity, a short was substituted for the coaxial transistor in Coaxial Cavity I to determine the various resonant modes of the cavity. (These modes changed when using the transistor because the capacitive loading of the end of the cavity became different). A blocking capacitor for the input of the coaxial transistor was also designed. This capacitor consisted of a 2 to 10 pf adjustable cylindrical trimmer inside a coaxial attenuator from which the resistive element had been removed. Although the adjustment of this capacitor was not critical, the trimmer could easily be reached when necessary by removing two screws.

As soon as it became available, a Philco coaxial transistor, L-5431, was used with both of these cavity resonators. Although no overall amplification of the signal between the signal generator and the output of either cavity was obtained at first, promising results were obtained with Coaxial Cavity I. The voltage gain of an amplifier circuit containing the transistor, illustrated in Figure 8, was determined by measuring the difference in the insertion losses of the system; first, with the power to the transistor on, and then, with the transistor power supply off. The input and output voltage readings obtained are shown in Figure 9. In this circuit, coaxial capacitor 3 acted as a variable blocking capacitor which prevented the dc bias of the emitter junction from reaching the signal generator. RF chokes 9 and 18 consisted of several turns of hook-up wire. These open wires, as well as the lead coming from T-section 4, were responsible for some of the overall losses within the system. Capacitors 10 and 19, each with a capacitance of approximately 1500 pf, served as rf bypass capacitors and also protected the transistor from converter switching transients. Potentiometers 11 (500 ohms) and 12 (10,000 ohms) were used for fine and coarse adjustments respectively of the emitter current. Fixed resistors 13 (200 ohms) and 17 (100 ohms) protected the transistor. In this amplifier circuit, the emitter currents ranged from 1 to 4 ma at points of resonance. Since the rf meter used for these measurements gave comparative voltage readings, the difference

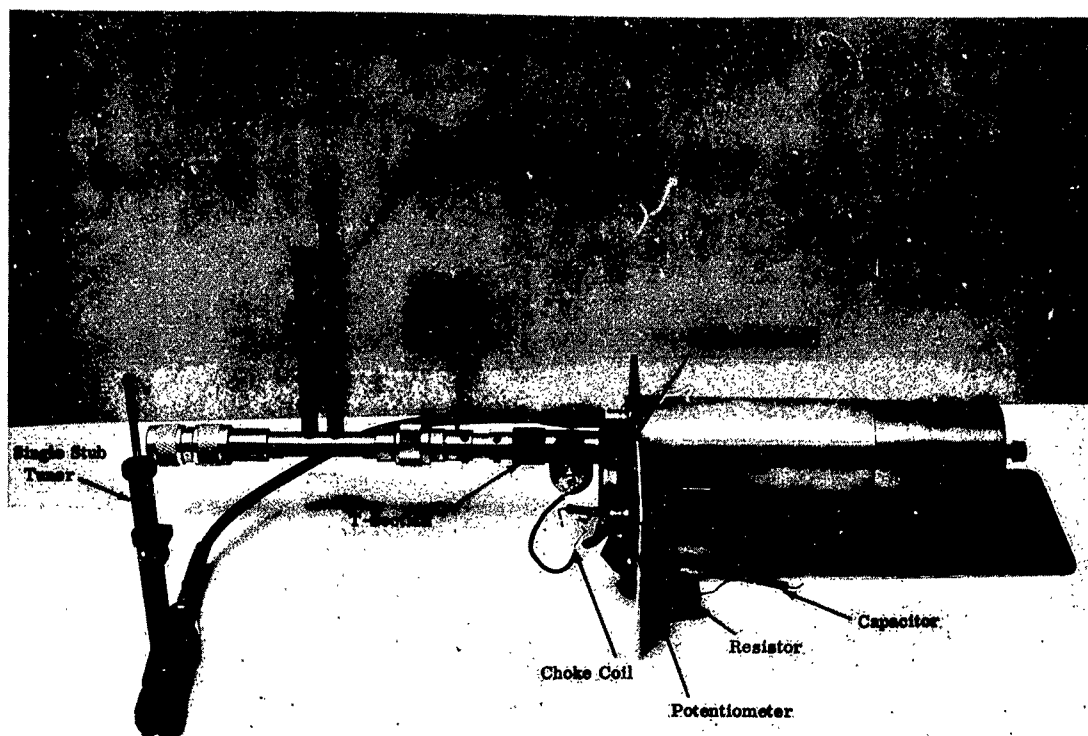


Figure 6. Coaxial Cavity I

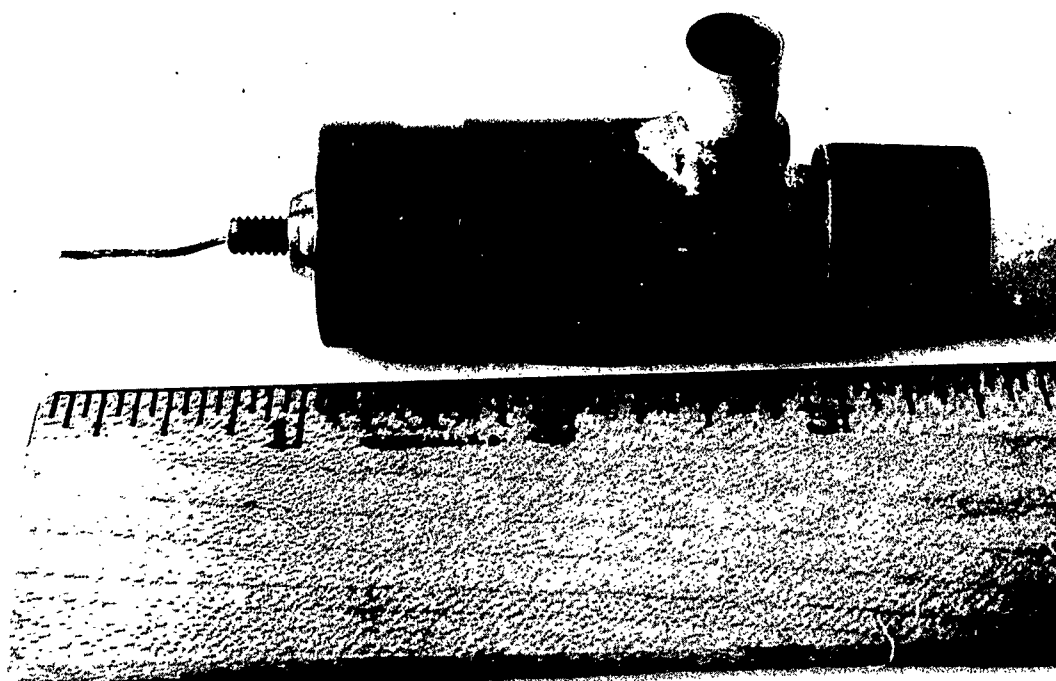
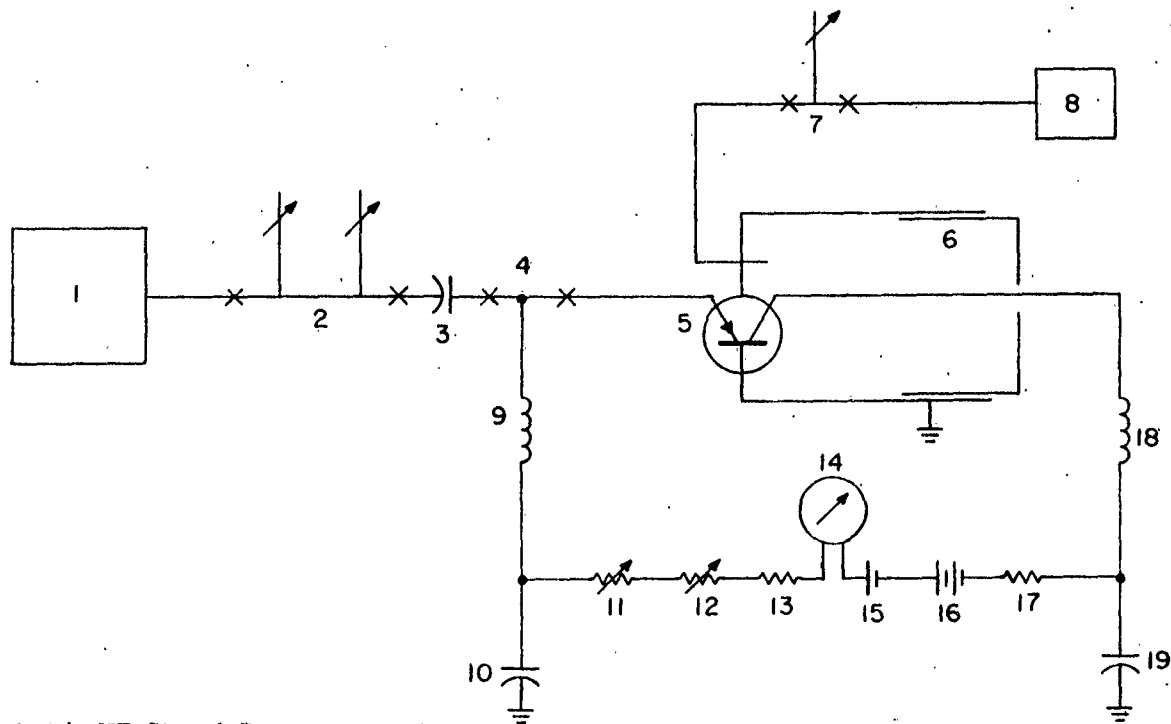


Figure 7. Coaxial Cavity II



1. 614A HP Signal Generator
2. Double Stub Tuner
3. Adjustable Coaxial Blocking Capacitor
4. T Junction
5. Coaxial Transistor (Philco L-5431)
6. Coaxial Cavity
7. Single Stub Tuner
8. 91CA Boonton RF Voltmeter
9. Choke Coil
10. Bypass Capacitor
11. Resistor Pot (Fine Adjustment)
12. Resistor Pot (Coarse Adjustment)
13. Resistor
14. Milliammeter
15. Emitter Bias Cell, 3 volts
16. Collector Bias Cell, 7.5 volts
17. Resistor
18. Choke Coil
19. Bypass Capacitor

Figure 8. Amplifier Circuit

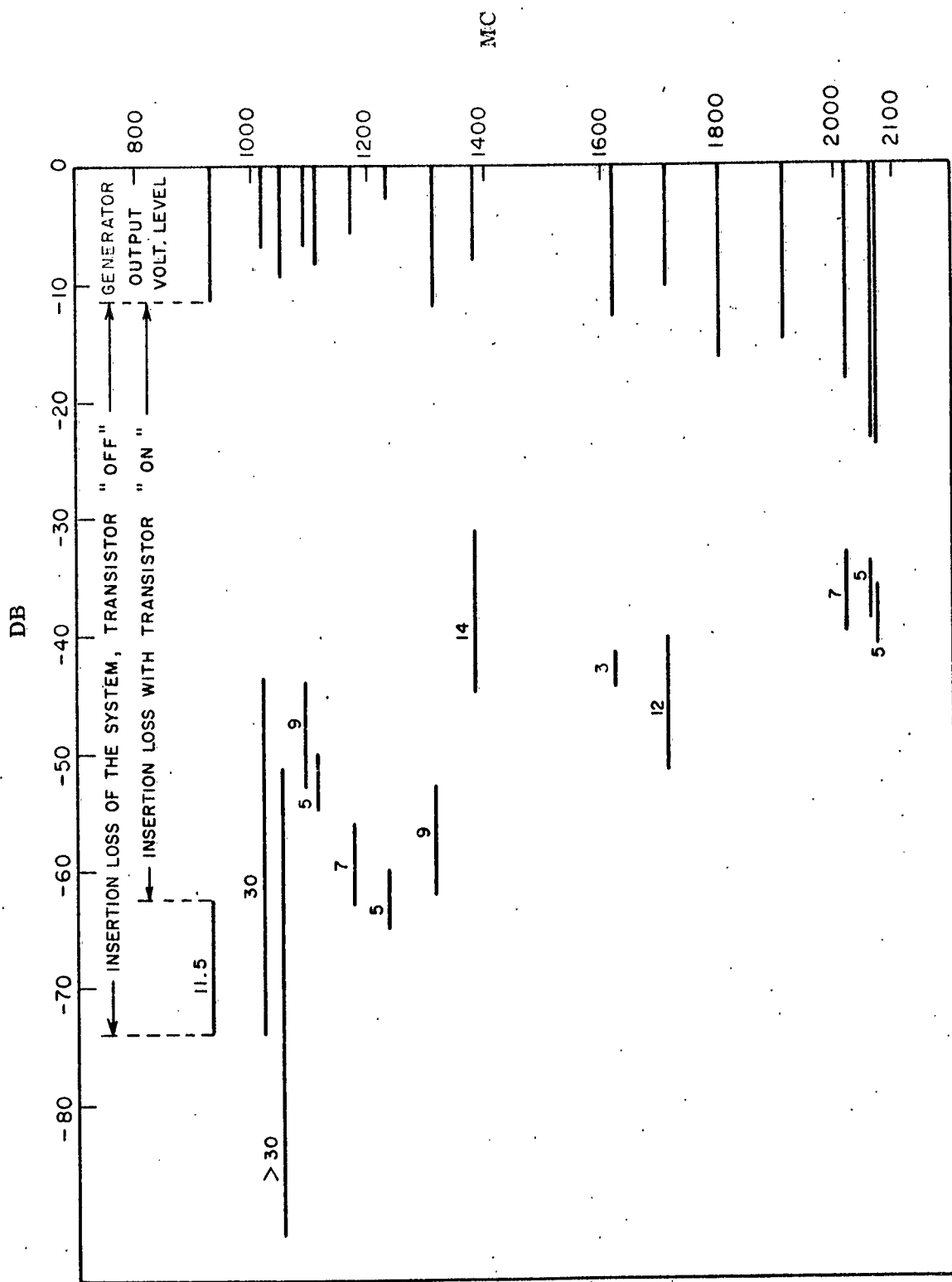


Figure 9. Output and Input Voltage Readings of the Amplifier Circuit

between the insertion losses of the circuit with the power to the transistor on and then off was a measure of the transistor amplification when the standing wave ratio (SWR) of the cavity resonator was 1.

As indicated in Figure 10, the amplification (voltage gain) of the transistor exceeded 30 db at 1.05 Kmc. This gain resulted from the change in impedance at a resonant condition (although the transistor was nearly unstable at a resonant condition) but then decreased to 7 db at a frequency of 2 Kmc. Coaxial Cavity I was also multi-resonant but since these resonances occurred after adjusting the length of the cavity and the emitter current, their presence was not objectionable.

The overall performance of Cavity I at this stage in its development is indicated in Figure 11. At this time, the cavity had a loaded Q of 122 at 1 Kmc and a loaded Q of 445 at 2 Kmc. These low values for the loaded Q's (Q_L) probably resulted from the "lossy" contact between the inner and outer tubes of the cavity as well as losses in the magnetic output pickup loop inserted into the front end of the cavity. (MIT RAD LAB Series, Vol. 11, page 322). The construction of Coaxial Cavity I is shown in Figure 12, which has been drawn on an approximate 1 : 1 scale.

In view of these results it was evident that optimum performance of Coaxial Cavity I occurred at 2 Kmc and that maximum transistor amplification occurred at 1 Kmc. Thus, it was believed that the amplification of the circuit could be improved by decreasing the insertion loss of the circuit components and increasing the Q of the coaxial cavity. This was done by:

- a) Replacing rf chokes 9 and 18 with coaxial chokes.
- b) Changing the magnetic pick up loop within the cavity resonator to a capacitive type of pick up loop.

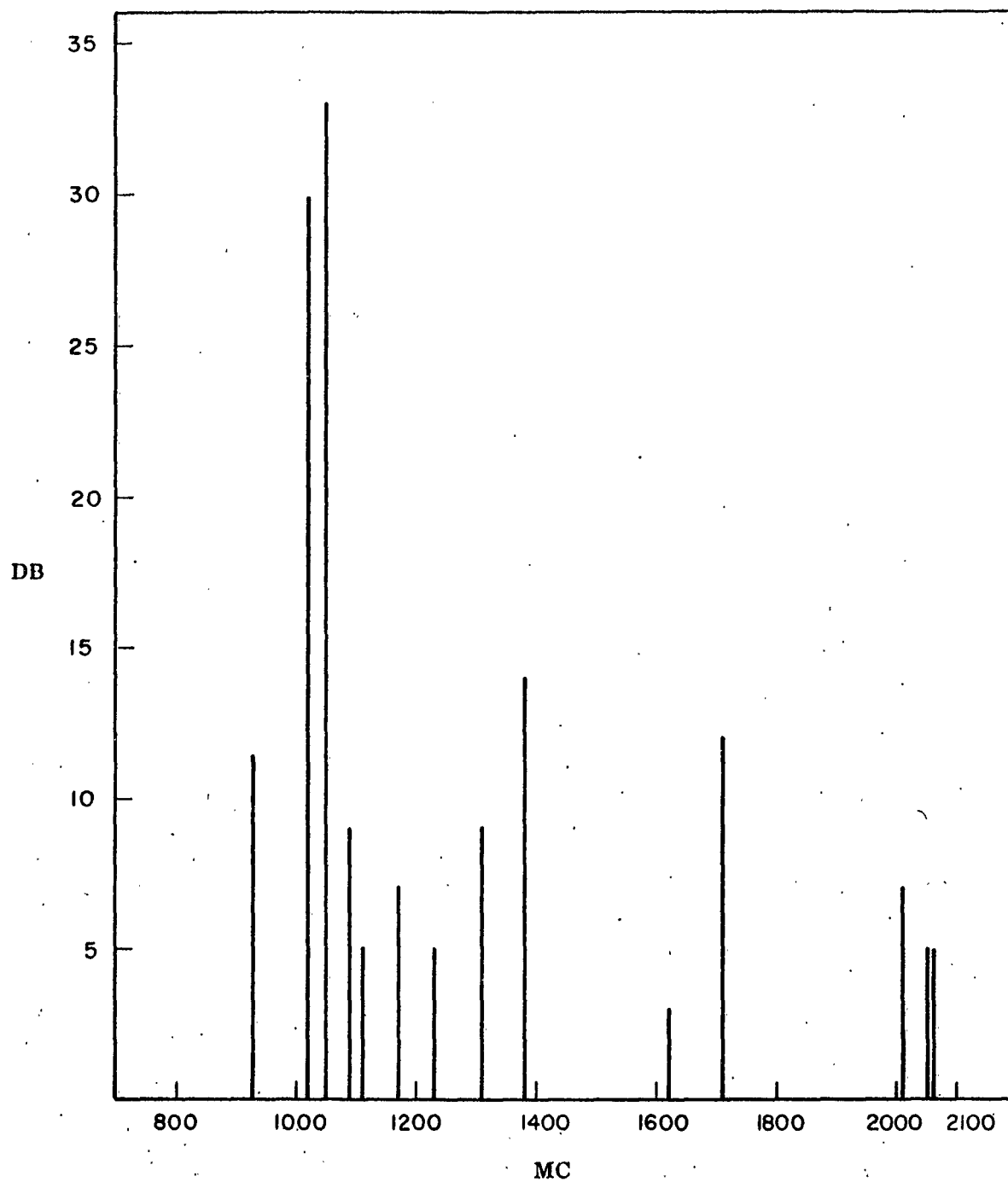


Figure 10. Amplification of the Transistor

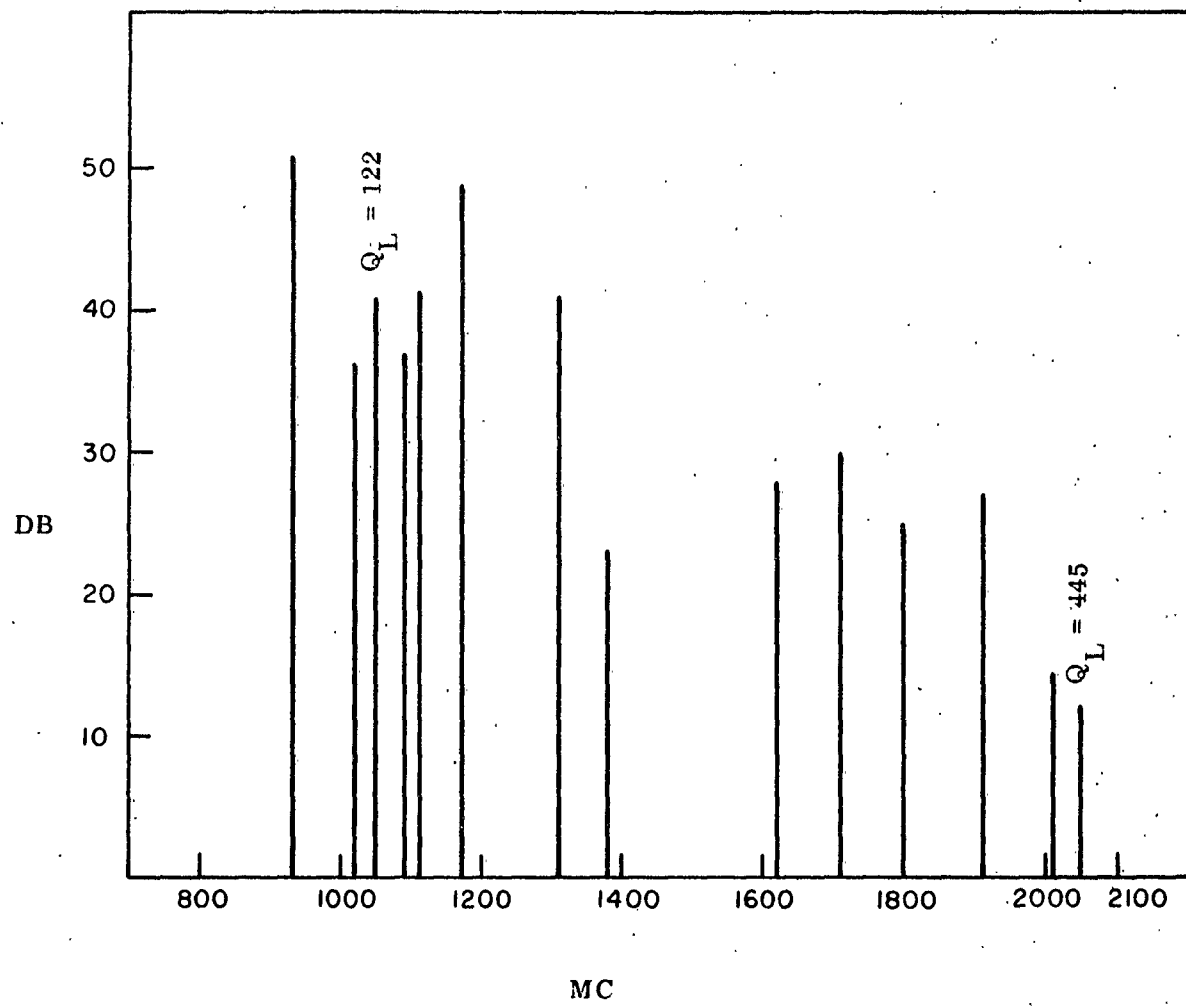
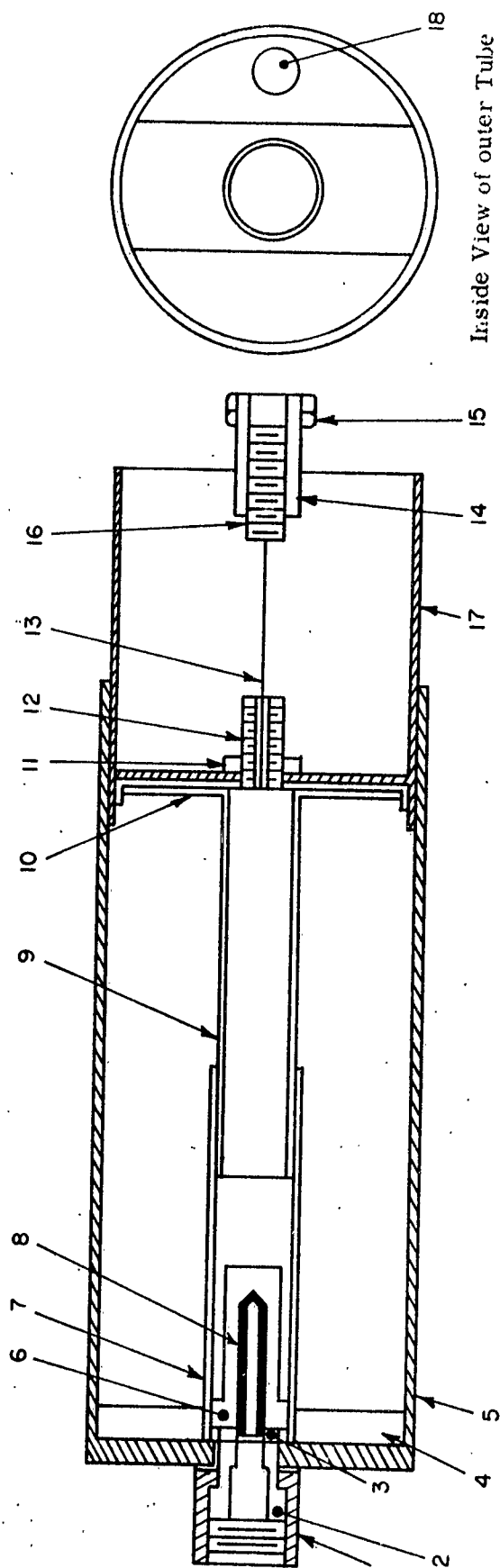


Figure 11. Loss Factor of the Amplifier Circuit Excluding the Single Stub Tuner



- | | |
|-----------------------------------|----------------------------|
| 1. Part of "N" Connector | 15. Bolt |
| 2. Bushing | 16. Screw |
| 3. Insulator | 17. Inner Tube |
| 4. Insulator | 18. Hole for Coupling Loop |
| 5. Outer Tube | |
| 6. Chuck Holder | |
| 7. Center Conductor of Outer Tube | |
| 8. Chuck | |
| 9. Center Conductor of Inner Tube | |
| 10. 1 mm mylar insulator | |
| 11. Bolt | |
| 12. Nylon Screw | |
| 13. Heavy Lead Wire | |
| 14. Nylon Bolt | |

Figure 12. Mechanical Drawing of Coaxial Cavity I

- c) Using cylindrical cavities (without center stubs) for amplification.

6. IMPROVEMENT OF COAXIAL CAVITIES

After changing from a magnetic to a capacitive type of output coupling loop, the insertion losses of Coaxial Cavity I were substantially improved. The results of this change are shown in Figure 13. This figure indicates the insertion losses of the cavity with the bias to the transistor on and off as well as the amplification obtained with the transistor. For purposes of comparison, the results obtained with the previous design of Coaxial Cavity I employing the magnetic coupling are also shown.

Although the transistor amplification curve drops at the rate of 10 db per octave in the 1 to 2 Kmc frequency range (rather than 6 db per octave as in most transistor amplification curves) this greater rate of decrease may be attributed to the variation with frequency of the insertion losses in the coaxial cavity and its associated circuits.

When Coaxial Cavity II was tested, the results obtained indicated that the amplification of the transistor was approximately 1 db around 4 Kmc, dropping to 0 db at 5.29 Kmc. These results as well as the insertion losses of Coaxial Cavity II are shown in Figure 14.

Both cavities at this point were used as oscillators by employing positive loop feedback. The output of Coaxial Cavity I, including the loss of the cavity, was approximately -33 dbm. Spectroscopic examination revealed that resonant frequencies occurred in this output at 1.118 and 1.75 Kmc. The output of Coaxial Cavity II was approximately -20 dbm and several resonant modes occurred at frequencies below 2 Kmc. The results obtained with both cavities at this time indicated the possibility of using

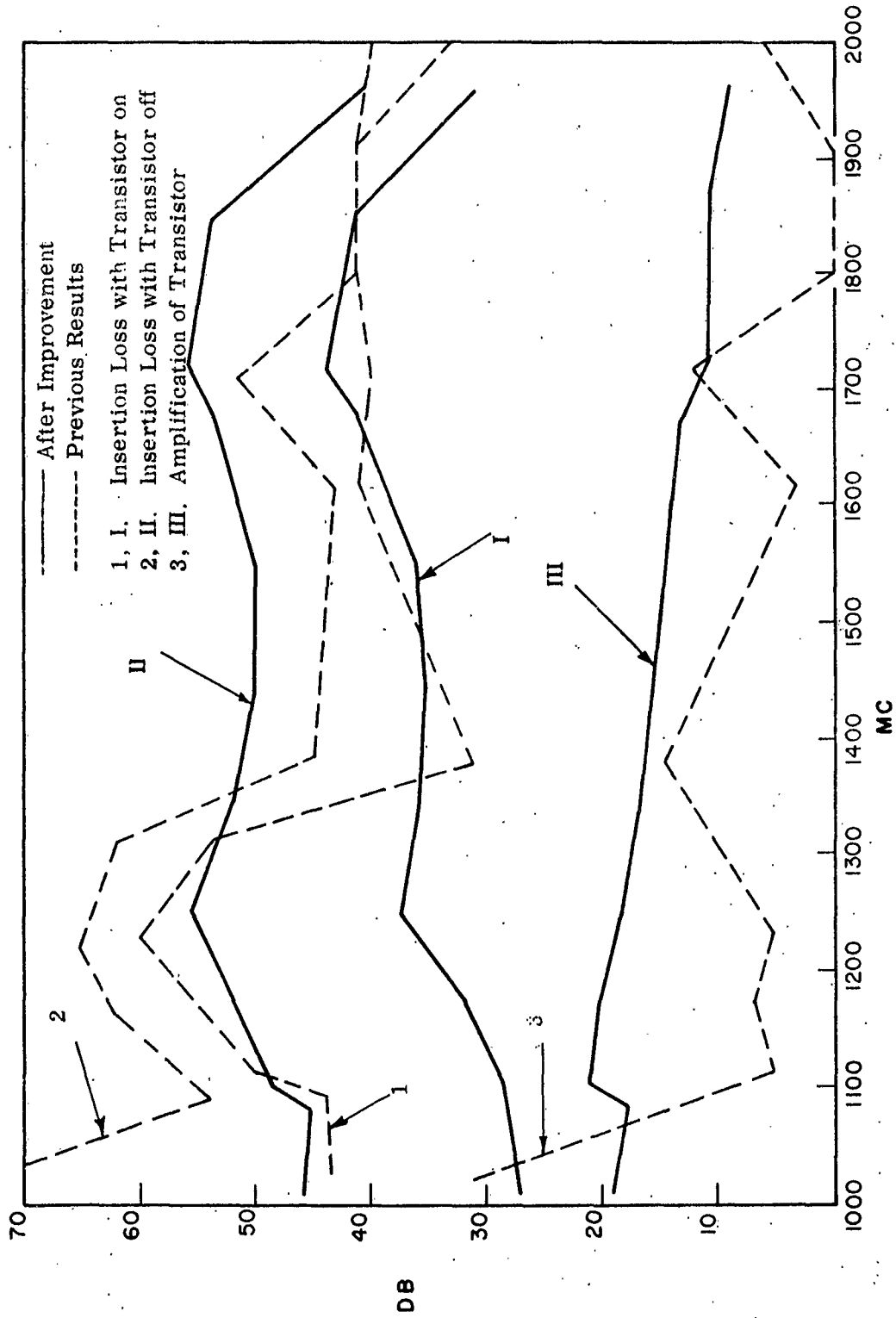


Figure 13. Insertion Losses of Coaxial Cavity I

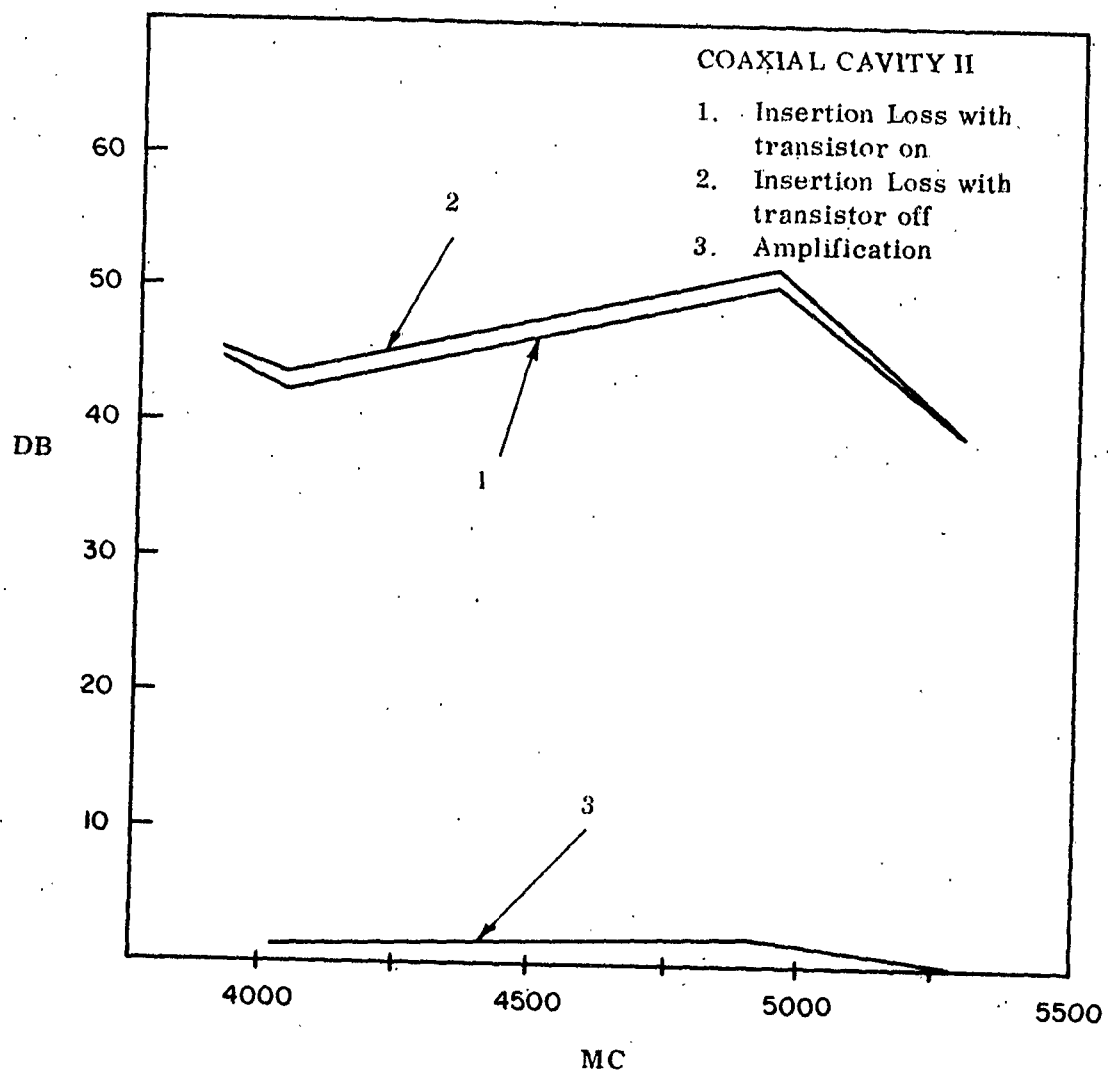
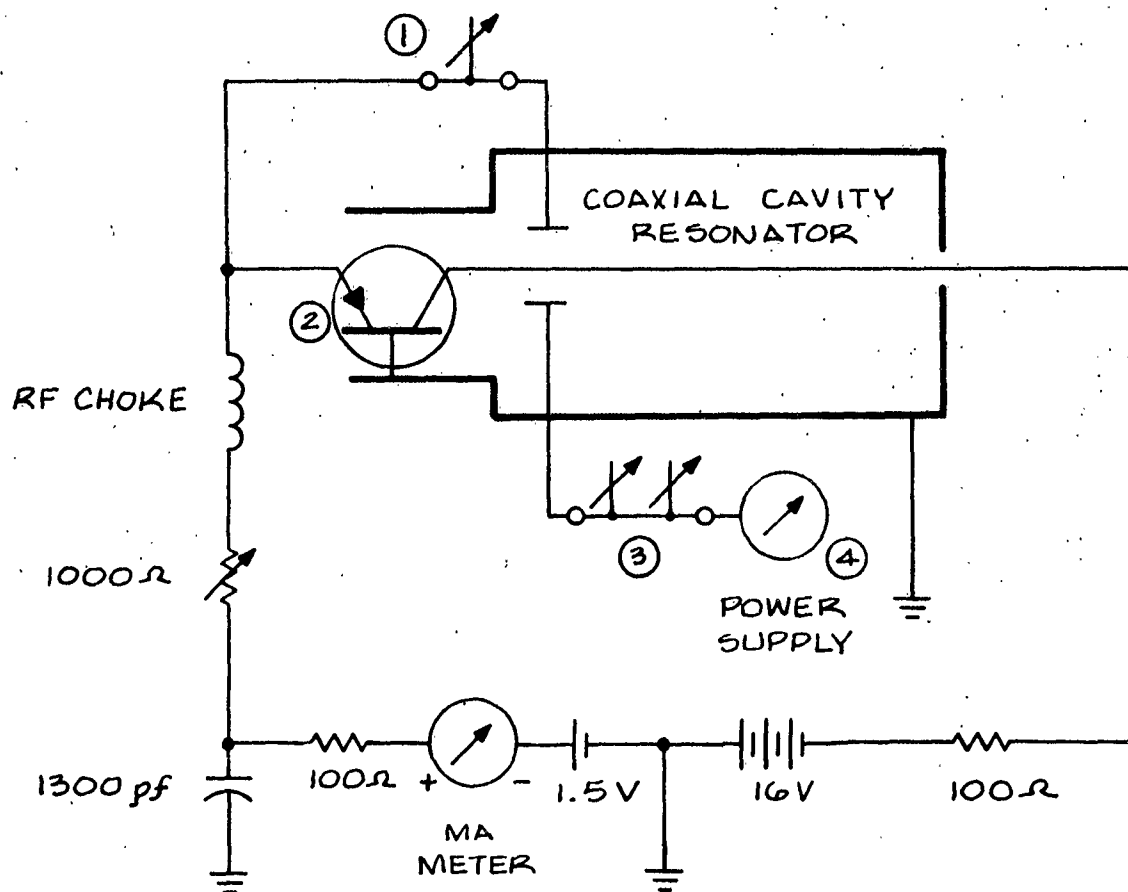


Figure 14. Insertion Losses of Coaxial Cavity II

a Philco L-5431 transistor in a mixer circuit capable of handling frequencies much higher than 1 Kmc.

Further improvements in Coaxial Cavity I, illustrated in Figure 15, consisting of changes in the coupling probes to the cavity, raised the output power of this cavity from the -33 dbm previously obtained to +3 dbm. In this transistorized UHF oscillator circuit, spectroscopic examination showed that these outputs appeared as complex waveforms whose complexity increased as the emitter current of the transistor was increased. The frequency of the output signals from Coaxial Cavity I extended from 1 to 2.55 Kmc. In addition, the output power of Coaxial Cavity II was raised to +6 dbm by increasing the emitter current to 8 ma. In Coaxial Cavity II, the number of modes within the 1 to 2.5 Kmc frequency range increased as the emitter current increased. The exact frequencies and relative amplitudes of these modes could not be determined at this time because a suitable cavity type frequency meter was not available.

Several phenomena of interest were observed during the improvement of Coaxial Cavity I. When the output impedance of the oscillator circuit was adjusted (using the double stub tuner), the dc voltage across the emitter decreased to zero and then became negative. This decrease in voltage and reversal of polarity, accompanied by a decrease in and reversal of polarity of the dc input resistance, was also observed when passing a frequency of 1200 Mc into the oscillator circuit and adjusting the emitter current to 2.4 ma or more. When the frequency of the input to the oscillator circuit was changed, however, these voltage variations did not occur. During these observations, it was also noted that loading of the oscillator circuit did not alter the voltage decrease produced by the increase of input power and emitter current. To check the theoretical behavior of transistors operating in oscillator circuits at high frequencies, several experiments were performed. These experiments and the results obtained were as follows:



- ① SINGLE STUB TUNER
- ② PHILCO COAXIAL TRANSISTOR
- ③ DOUBLE STUB TUNER
- ④ FXR POWER METER B 831 A

Figure 1. UHF Oscillator Circuit

a) Results of Studies Conducted Upon a Circuit Proposed by R. Zuleeg

(1) An oscillator circuit designed by R. Zuleeg of Hughes Semiconductor Division was constructed and the power output of this circuit was measured. This output was observed to be 0.5 milliwatts. Since this circuit, illustrated in Figure 16, was not carefully constructed for operation at high frequencies, even greater power outputs could presumably be obtained by improving the construction of the circuit. In addition, this circuit demonstrated a negative dc input resistance.

(2) In a later experiment with R. Zuleeg's circuit, although the position of the emitter bias voltage source in this circuit had been changed from the position originally proposed, this change seemed immaterial so far as circuit operation at high frequencies was concerned. This circuit operated nicely as an oscillator and frequencies as high as 790 Mc were obtained when the position of the shorting stub was such that $l_e = 11.5$ inches and $l_c = 1.25$ inches. During these measurements, the voltage output for the complex frequencies was 190 mv and the input resistance of the voltmeter was 50 ohms.

(3) Since the injected signal produced no observable effects upon the i-f output signal, however, it was assumed that this circuit could not operate as a converter using either the Philco 2N502A or T-1832 transistor.

(4) In further studies of the parametric properties of the circuit proposed by R. Zuleeg, oscillation frequencies up to 915 Mc (oscillations as high as the f_{max} of the transistor) were detected when Philco 502A or Hughes 315-25 transistors were used. However, operation of the circuit as a converter at i-f frequencies of 40, 10 and 2 Mc

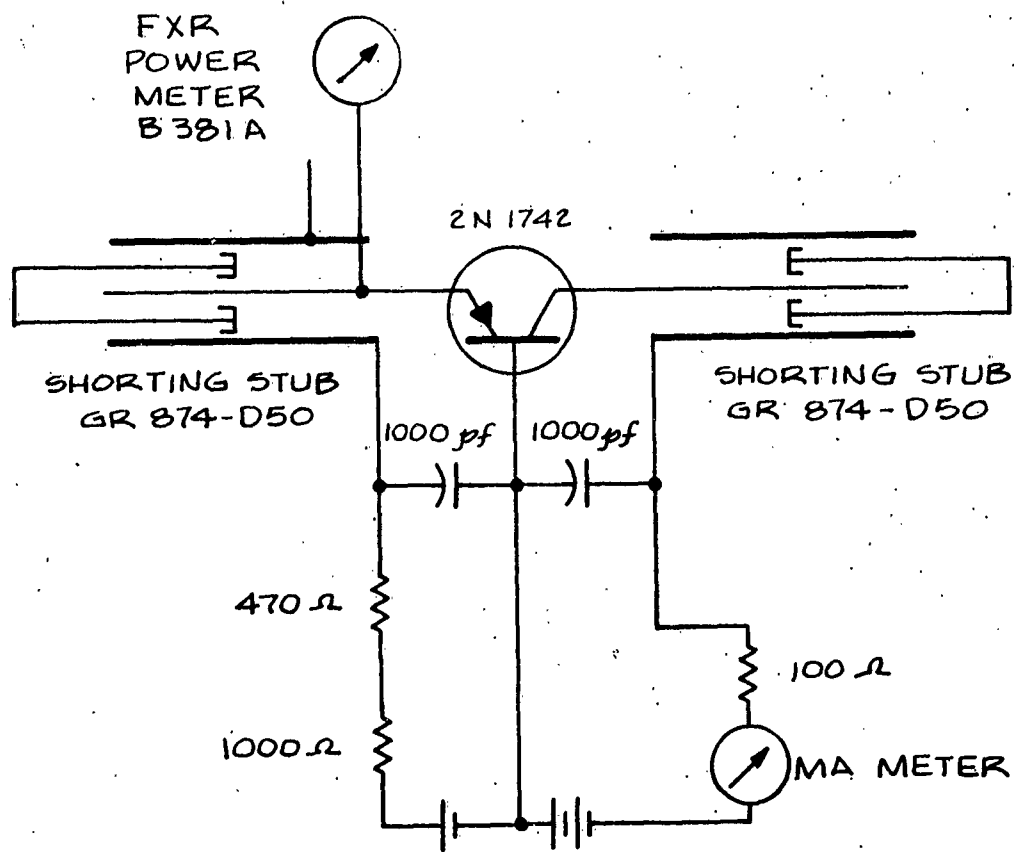


Figure 13. Oscillator Circuit Designed by L. Zuleeg

could not be demonstrated.

b) Results of Studies Conducted Upon a Circuit Proposed by
J. F. Gibbons:

(1) A variation of R. Zuleeg's oscillator circuit, suggested by J. F. Gibbons of Stanford University, was also constructed. In view of J. F. Gibbons' theories, it was believed that the maximum frequency limit imposed upon the operating frequency of transistors with a diffused base could be increased if the output and input impedances of an oscillator circuit favored transistor operation in the transit time mode. When a Philco 2N1742 transistor was employed in this variation of R. Zuleeg's oscillator circuit, however, satisfactory results were not obtained.

(2) In later experiments, J. F. Gibbons' circuit, containing a Philco 2N502A transistor rated at a typical f_{\max} of 800 Mc, was operated in the transit time mode and oscillations as high as 2.190 Kmc were obtained.

This circuit was then changed to a converter circuit by connecting a 40 -mc i-f tank circuit across its output terminals. When this was done, the i-f signal could be detected, but no frequency conversion was observed. In other words, the circuit merely oscillated at the i-f frequency.

(3) In further studies of the parametric properties of the circuit suggested by J. F. Gibbons, the circuit worked successfully as an oscillator and oscillations up to the maximum cutoff frequency of the Philco 502A transistor (1100 Mc) were observed. When the circuit was transformed into a converter circuit, normal frequency

conversion with loss was observed up to frequencies of 880 Mc but no parametric action could be detected.

7. RESULTS OF STUDIES UPON AMPLIFIER AND CONVERTER CIRCUITS CONTAINING HUGHES' TRANSISTORS

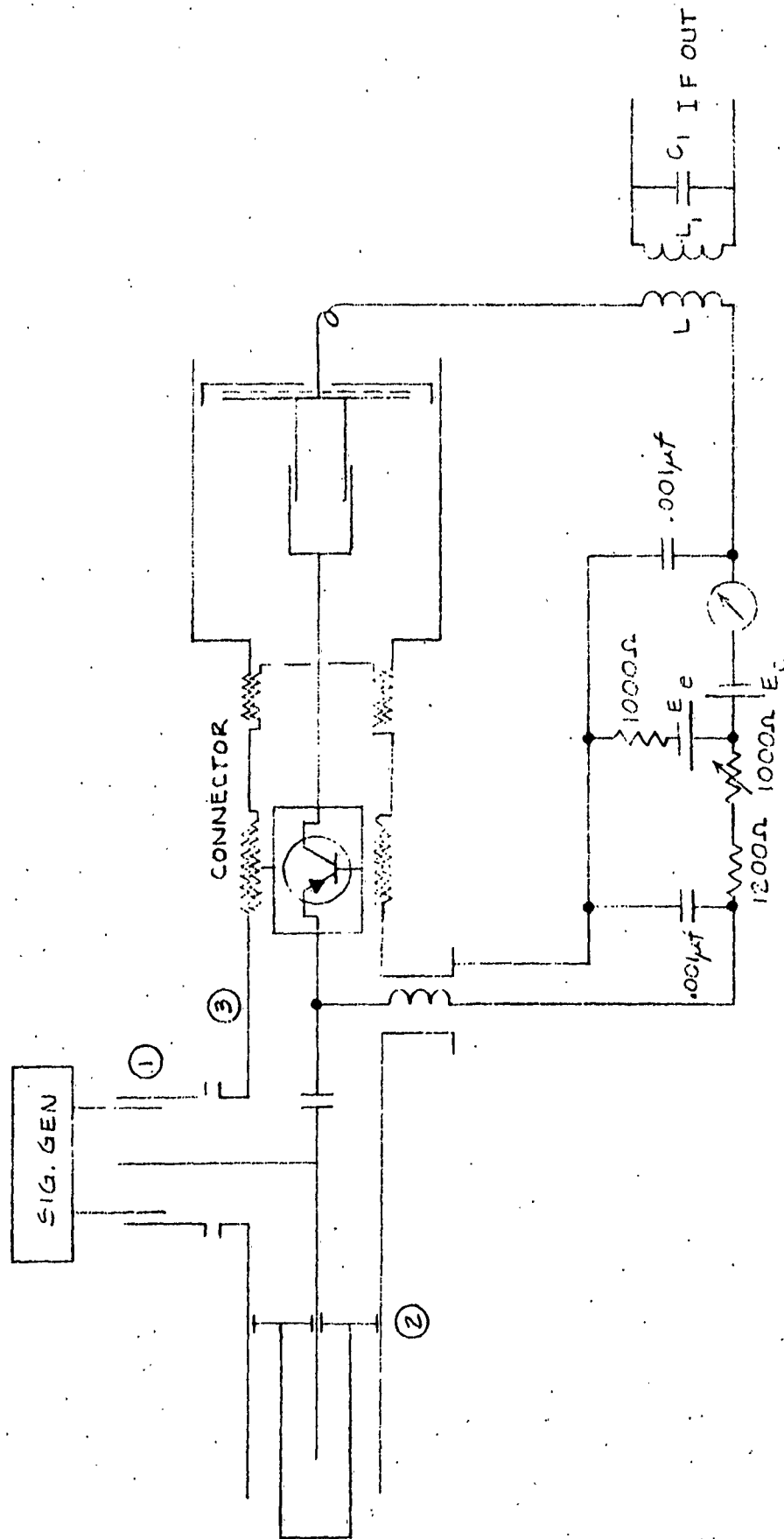
a) Results of Tests Upon Amplifier Circuits

Upon their arrival, Hughes HC-2 and HC-7 transistors were employed in the amplifier circuits developed during this study. Unfortunately, no amplification could be observed in the coaxial cavity resonators of these circuits at frequencies ranging from 450 to 1200 mcs.

b) Results of Tests Upon Converter Circuits

When Hughes' experimental transistors HC-2 and HC-7 were employed in the converter circuits developed during the study, the results obtained were more promising than the results obtained with the amplifier circuits. In one converter circuit, for example, a mode of operation similar to that obtained in the mixer circuit designed by V. W. Vodicka was observed at frequencies around 800 Mc. When the signal generator in this converter circuit, illustrated in Figure 17 was shut off, the circuit operated as an oscillator. When the signal generator was turned on (after the tuning units and injected frequency of the circuit had been properly adjusted), the self-oscillation of the converter circuit became locked in with the injected signal and the magnitude of the i-f output, varied with the magnitude of the input signal. This variation is shown graphically in Figure 18. Despite the similarity between the operation of this circuit and the circuit designed by V. W. Vodicka, the gain of this circuit was not as high as that of V. W. Vodicka's mixer circuit. This difference in gain may be accounted for by the following factors:

- 1) The operating frequency of the circuit developed in this study



1. GR 874-LK Adjustable Line
2. GR 874-D50 Adjustable Stub
3. Microlab HW 30N Monitor Tee

Figure 17. UHF Frequency Converter

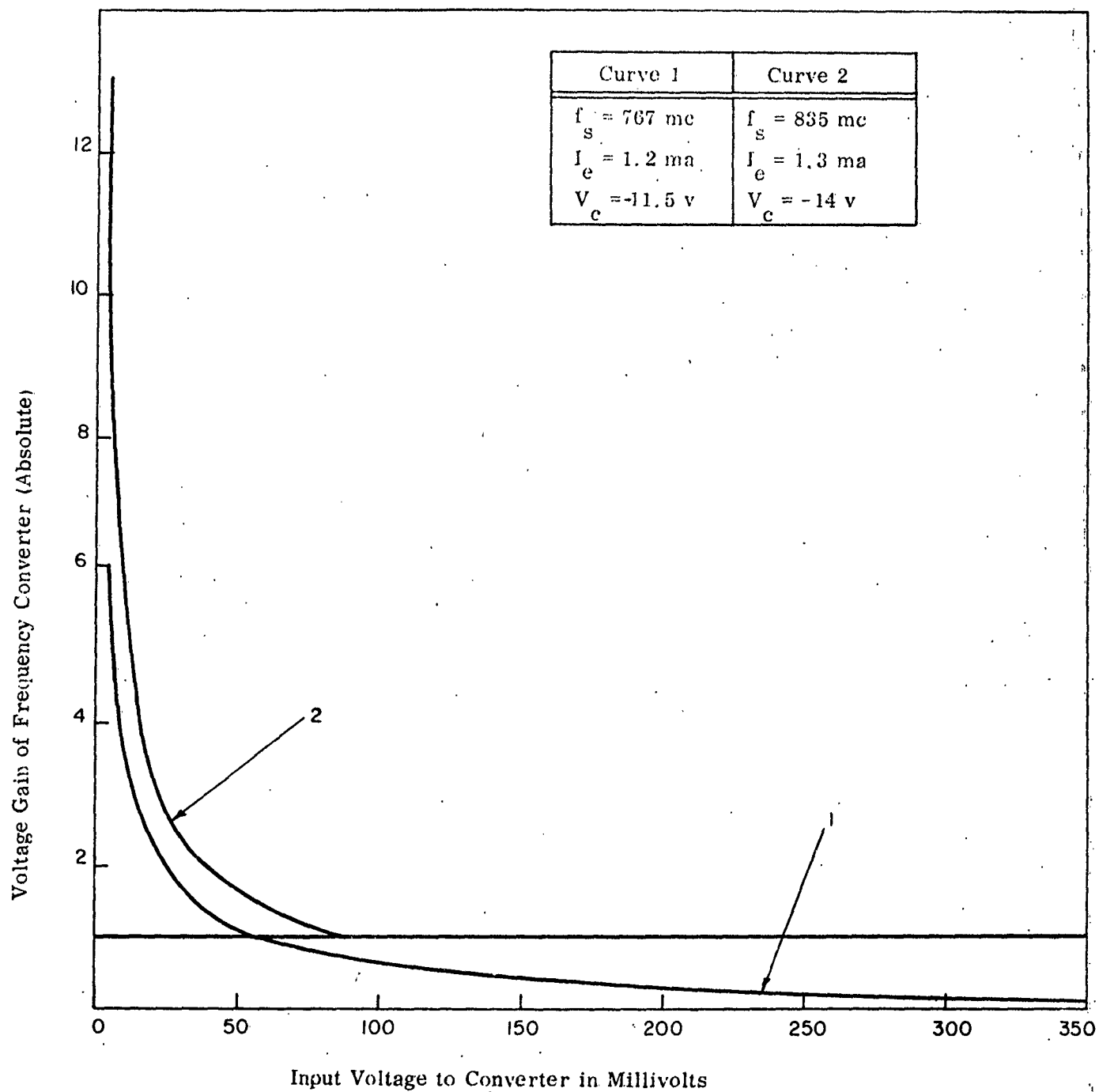


Figure 18. Voltage Gain of Frequency Converter vs Input Voltage

was more than twice as large as that of V. W. Vodicka's circuit whereas the maximum operating frequency (f_{\max}) of the transistors employed was about the same as that of the Philco 2N502A transistors employed in V. W. Vodicka's original circuit.

$$f_{\max} = \sqrt{\frac{f_T}{8\pi r_b C_c}} \simeq 1100 \text{ Mc}$$

(2) The gain of the converter circuit developed during this study was limited somewhat by the quality of the circuit components. Thus, the gain of this circuit could have been increased by improving certain units such as the coaxial cavity resonator or the transistor jig.

(3) Another reason that the gain of this circuit was relatively low was that the i-f tank circuit was not directly in the collector circuit but was magnetically coupled to it. This coupling is illustrated in Figure 17. Magnetic coupling was employed since no converting action could be observed when the tank was placed directly in the collector circuit. After using a large magnetic coupling, however, an increase of conversion gain with increased input voltage was observed. Several curves of the conversion gain with increased input voltage were obtained during tests on a converter circuit containing a Hughes' HC-2 transistor. Two of these curves, which almost coincide with one another, are shown in Figure 18.

o) Results of Tests Upon a Converter Circuit Containing an HC-2 Transistor

(1) The addition of 600 ohms resistance across the i-f output of

the circuit decreased the gain of the circuit slightly.

(2) Conversion gain within the circuit was obtained only within a very narrow range of emitter current, 0.9 to 1.3 ma. This narrow range of emitter current suggested that the gain occurred within the region of negative resistance of the transistor junction.

(3) The conversion gain increased in the same direction as that of the negative collector voltage.

(4) The i-f output waveform was distorted from its usual sinusoidal shape. The distortion was presumably caused by the double resonant frequency of the magnetic coupling employed in the collector circuit.

(5) It was possible to obtain frequency conversion, with losses, at frequencies ranging from 450 to 1200 Mc by setting the collector bias voltage at -3 volts. The results of experiments conducted at this collector bias voltage are not included in this report as they are not relevant to the objective of achieving frequency conversion with gain.

d) Results of Tests Upon a Converter Circuit Containing an HC-7 Transistor

No conversion gain was observed in converter circuits containing a Hughes' HC-7 experimental transistor.

8. CONCLUSIONS

On the basis of the investigations described in this report, the following conclusions have been reached:

- a) When Philco coaxial transistors were used in amplifier, oscillator, and mixer circuits operating within the 1 to 4 Kmc frequency range, both amplification and oscillation were observed but high gain frequency conversion could not be obtained. In other words, a parametric mode of operation, similar to that obtained by operating V. W. Vodicka's mixer circuit at 350 Mc, could not be demonstrated in circuits containing Philco transistors operating in the lower microwave regions. This absence of the parametric mode of operation may be explained by the assumption that a region of negative slope is not associated with the emitter characteristics (I_e vs V_{eb}) of Philco transistors operated at UHF frequencies.
- b) When Hughes' coaxial transistors were used in the same amplifier, oscillator and mixer circuits as those in which the Philco transistors were employed, conversion gains as high as 23 db were observed. Because of losses within the circuit, it is believed that these gains are not the highest which may be obtained with these transistors.
- c) On the basis of the results obtained during these experiments, the feasibility of developing an amplifier, mixer, or harmonic generator which can operate with high, stable gain and low noise in the 4 to 10 Kmc frequency range has not been excluded. However, many improvements in circuit design and circuit devices, particularly in the transistor package, will have to be made in order to reduce circuit losses and thus extend the practical range of transistor operation to frequencies higher than those which can presently be obtained.

PART III

FINAL ENGINEERING REPORT ON

HIGH FREQUENCY TRANSISTOR STUDY

INTRODUCTION

The present contract was a research and development program directed toward the investigation of transistor design parameters and circuit requirements which determine and/or influence transistor operation in the microwave frequency region. Extrapolation of these results should then determine the feasibility of developing an amplifier, mixer or harmonic generator operating with high stable gain and low noise at frequencies within the region of 4 to 10 Gc.

The work was divided up into the following areas:

- 1) Evaluate the Hughes experimental GXG 4 transistor design in a suitable microwave mounting for operation at 4 Gc and above.
- 2) Evaluate available high frequency transistors in circuits designed for operation at 4 Gc and above.
- 3) Correlate results with theoretical studies and calculate device and circuit interaction.
- 4) Design and fabricate experimental optimum device structures utilizing advanced techniques for fabrication such as epitaxial growth and oxide masking.
- 5) Design circuits for operation at 4 Gc and above.
- 6) Evaluate experimental transistors and package structures and determine the capabilities of these transistors for operation in the microwave region.
- 7) Determine feasibility of developing an amplifier, mixer or harmonic generator operating at 4 Gc or above.

Early development efforts at Lenkurt Electric Company, San Carlos, California, on transistor mixers produced interesting electrical performances with Philco 2N502 transistors in a special circuit when tuned with a butterfly LC circuit.

Since a butterfly has higher tuning modes with high Q's above the fundamental frequency, it was possible to produce conversion gain of the harmonics of the fundamental frequency of oscillation above the normal cut-off frequency of the transistor. In the fall of 1960, the Hughes experimental germanium PNP mesa drift transistor, GXG 4, was used by Lenkurt Electric in their circuit. The electrical performance data in the mixer exceeded those of the 2N502. The obvious reasons were a lower base resistance and a higher drift field. It was concluded, with this experimental verification, that enough evidence was presented to ascribe efficient conversion abilities to properly and specifically designed drift transistors. This prompted a "High Frequency Transistor Study" contract from the Navy Department, Bureau of Ships, Electronics Division. The contract was negotiated in November 1960 and started on March 10, 1961, for a period of 9 months, which was extended to 11 months at a later date.

1. ACCOMPLISHMENTS

a) Packaging of Transistor

The Hughes Design I coaxial package has been developed for microwave transistor encapsulation. It is terminated with approximately 50 ohm at the input and output and can be inserted into a 50 ohm standard line. The package comes in two parts and the mounting of the transistor structure is performed on the collector half portion. After the mounting operation the transistor is surface treated and tested before outbaking and surface stabilization. After outbake, the transistor is hermetically sealed in a dry atmosphere by aid of projection welding. The design is mechanically stable and practical for a pilot line production. The parasitic inductances have been reduced to less than 2 nH. This will assure interference free transistor high-frequency operation up to 2.5 Gc. The Hughes Design I package can be easily improved by minor changes to reach a frequency of operation around 5 Gc. An improved Design II is under consideration.

A germanium mesa PNP, 1 Gc, epitaxial transistor has been successfully fabricated in the Hughes Design I coaxial package and the electrical results have been reported in the enclosed Third Interim Engineering Report.

b) Development of Transistor

The Hughes non-epitaxial germanium PNP transistor (experimental model number GXG 4) has been optimized in respect to mixer performance and a report on the electrical performance in a novel mixer design is in the Second Interim Engineering Report. In the same report, the physical structure of the device was related to the electrical parameters. From

this correlation, a new transistor intended for operation in the frequency range from 1 to 2 Gc evolved by extrapolation and the incorporation of epitaxial material; this structure was then integrated into the coaxial package. The electrical evaluation of this design is presented in this Third Interim Engineering Report. Optimum performance of the coaxial transistor has not yet been experienced, and because of the time element involved in the feedback between design change and electrical evaluations, the following items are yet to be incorporated:

- i) Epitaxially grown P on P^+ material which has high resistivity with little or no impurity gradient has not been available. This would reduce the collector depletion capacitance, C_c .
- ii) The gold plating to the collector post in the new package is not satisfactory and the step of mounting the germanium die introduces a collector series resistance due to bad wetting. Improvement in the gold plating and several changes in the mounting procedure will remove this undesirable resistance to a remaining few ohms.
- iii) The gold alloying and evaporation for forming the base contact, together with optimized base diffusion can be adjusted to give very small spreading resistances, r_b , without impairing any other high frequency characteristic of the transistor.

With the present transistor structure under controlled and optimized fabrication conditions, the following electrical properties are guaranteed:

α	$>$.95
f_T	\sim	1 Gc
f_{ca}	\sim	1.7 Gc
r_b'	\sim	15 ohm
C_c	\sim	.3 pf ($V_c = -10v$)
C_E	\sim	4 pf at zero bias
f_{max}	\sim	3 Gc
BV_c	\sim	40 V
BV_E	\sim	.8 V
P_{max}	\sim	200 mW (in free air)

A slightly modified structure, including process changes, such as oxide masking and epitaxial growth, can lead to a transistor with the following electrical properties:

α	$>$.95
f_T	\sim	2 Gc
f_{ca}	\sim	3 Gc
r_b'	\sim	15 ohm
C_c	\sim	.2 pf ($V_c = -10V$)

$C_E \sim 2 \text{ pf at zero bias}$
 $f_{\text{max}} \sim 5 \text{ Gc}$
 $BV_C \sim 40 \text{ V}$
 $BV_E \sim 1 \text{ V}$
 $P_{\text{max}} \sim 200 \text{ mW (in free air)}$

c) Electrical Evaluation of Transistors and Packages

Electrical measurements in a frequency range from 200 - 1500 Mc have been performed with the General Radio Transfer Meter and Immittance Bridge. The measurements on the experimental Hughes transistors and the coaxial Philco MADT T-2351 are presented in the Engineering Reports. From these measurements, or separate measurements on passive parts, the parasitic elements of the package and the extrinsic and intrinsic electrical properties of the transistors have been obtained.

d) Instrumentation

A f_T - tester has been constructed, which will enable one to determine the gain-bandwidth product for a coaxially packaged transistor intended for grounded base operation with the outside shell as the ground reference. Circuitry will circumvent the grounded base configuration and simulate electrically a grounded emitter configuration necessary to accomplish the measurement.

e) Circuitry

Two basic forms of a transit-time, negative resistance, oscillator have been built and tested. The information is given in detail in the

First Engineering Report. Fundamental oscillations up to 1.5 Gc have been obtained. A mixer, with lumped coaxial elements and the transistor in the TO-5 package (Hughes GXG 4) has been constructed with the grounded base transit-time oscillator as basic unit. In this circuit arrangement, it is possible to obtain a parametric mixing by operating the oscillator at twice the signal frequency in the transit-time mode and using the nonlinear reactance of the transistor input impedance as conversion element. Electrical results are reported in the First Interim Engineering Report in the frequency range from 300 - 500 Mc. The same circuit has been integrated with the coaxial transistor and its frequency of operation extended into the lower microwave region. Measurements are reported in the Third Interim Engineering Report at a signal frequency of 750 Mc.

f) Theoretical Studies

The transit-time effects of minority carriers in the drift transistor have been analyzed in respect to unilateral gain properties. From these results, negative resistances have been predicted in certain frequency bands, which lie in a range where the current gain has a phase shift larger than 180° and smaller than 360° . Oscillator circuits, using the negative resistance, resulting from the transit-time mode will operate above the normal cutoff frequency of the transistor.

The intrinsic current amplification factor, α_i , has been expressed in a convenient form, which was confirmed experimentally. The influences of parasitic package elements such as inductances and stray capacitances, as well as the extrinsic elements of the transistor, such as base resistance and collector and emitter depletion layer capacitances, have been computed as functions of frequency.

A modified equation for the input impedance of a drift transistor, h_{ib} , including the emitter depletion layer capacitance, has been derived and can qualitatively reproduce the nonlinear reactive components. General agreement exists with the experimental data given in the Third Interim Engineering Report. The bias setting for maximum conversion efficiency agrees also with the bias setting found in the mixer circuit when adjusted for optimum operation.

The stored base-charge (diffusion) capacitance, C_b , of a drift and diffusion transistor as the limiting case, has been used to derive the nonlinear behavior resulting from emitter current variations. In diffusion transistors, having no drift field in the base over a critical current range, the diffusion constant will change by a factor of two and thus introduce a departure from linearity in C_b vs. I_e .

In drift transistors with drift fields greater than $4KT/q$, in a critical current range, the effect of injected carriers in the high current density range of operation reduces the drift field and the drift transistor then operates essentially as a diffusion transistor.

Strong nonlinearities in capacitance are predicted in this critical current range of C_b vs I_e and have been computed in a normalized form for specific cases.

CONCLUSIONS

In this conclusion, we refer to the seven objective areas listed in the introduction by numbers.

- 1) The Hughes Design I coaxial package will operate up to 2.5 Gc in combination with the epitaxial germanium mesa PNP drift transistor. Modification of the package and the transistor will achieve operation above 4 Gc.
- 2) The only high frequency transistor available was the Philco MADT-T-2351 and operation above 1.5 Gc has been found impaired by a resonance condition owing to the rather large parasitic inductances, of the order of 5- 7 nH, contained in the package.
- 3) Circuit performance of all transistor types investigated have been correlated by measurements of electrical parameters of the device with the theoretical prediction of extended semiconductor theory.
- 4) During the course of the program, we have scaled down the Hughes GXG 4 transistor with the incorporation of epitaxial material and coaxial packaging, and improved the frequency response to 2.5 Gc. Further improvements can be expected when utilizing advanced techniques, such as oxide masking, and an ultimate frequency range, at least with germanium, of 5 Gc should be possible.
- 5) A coaxial mixer has been designed and built which will operate in a frequency range up to 3 Gc. The same design can be used as an amplifier. Experiments showed that operation above 3 Gc is limited by the Hughes Design I coaxial package. A new package will extend the frequency limit up to 5 Gc.

- 6) The Philco coaxial transistor and the Hughes experimental unit have been tested. The low inductance in the Hughes Design I package permits operation up to 2.5 Gc. Effective parametric mixing is possible at 2 points where the input impedance changes from an inductance to a capacitive reactance and vice versa. This is not possible with the Philco transistor because of the high package inductance.
- 7) A mixer, which can be tuned up to 3 Gc, has been operated with Hughes coaxial transistors. This particular design unit can be built for operation above 3 Gc if suitable coaxial microwave transistors are available.

An amplifier is also possible in this frequency range if a suitable package is available. In respect to harmonic generation, neither transistors nor circuits have been tested.